Charles University
Faculty of Science

Study programme: Biology
Branch of study: Cell and Developmental Biology - Developmental Biology

Bc. Petr Nickl

Mutagenesis in *Danio rerio* using CRISPR technology

Mutageneze v *Danio rerio* pomocí CRISPR technologie

Diploma thesis

Supervisor: RNDr. Ondřej Machoň, Ph.D.

Prague, 2019

ABSTRAKT

CRISPR/Cas9 systém je nástroj genového inženýrství umožňující sekvenčně specifické editace genomu. Tato technologie byla využita za účelem studia funkce transkripčních faktorů s DNA vazebnou TALE homeodoménou (TALE - three amino acids loop extension) v průběhu vývoje buněk neurální lišty a její derivátů. Hlavními proteiny zájmu této práce jsou *Meis1* transkripční faktory, které se v genomu *Dania* vyskytují v podobě dvou paralogních genů *meis1a* a *meis1b*. Funkce jednotlivých proteinů byla analyzována prostřednictvím mutageneze TALE homeodomény za účelem narušení schopnosti transkripčního faktoru vázat DNA a tím narušit regulaci podřízených genů. Tvorba a následná analýza fenotypu mutantních ryby by mohla odhalit potenciální roli *Meis1* proteinů v regulaci vývoje buněk neurální lišty, popřípadě poukázat na důležitost homeodomény v regulační funkci těchto proteinů. Současně byl proveden *knock-down* experiment pomocí morpholino oligonucleotidů k předběžné analýze funkce jednotlivých *meis1* genů a odhadu vzájemné funkční komplementarity. Předběžné výsledky poukazují na důležitost *Meis1b* proteinu v regulaci vývoje buněk neurální lišty a funkční důležitost jeho DNA vazebné domény. Snížení exprese *Meis1a* ukázalo, že i tento protein má podíl na regulaci kraniofaciálního vývoje, přičemž detailní popis jeho funkce bude určen až po analýze genetických mutantů metodou CRISPR/Cas9.

KLÍČOVÁ SLOVA

CRISPR/Cas9, transkripční faktor, neurální lišta, *Danio rerio*, Meis, mutageneze, vývoj

ABSTRACT

CRISPR/Cas9 technology is currently one of the most important tools of genome engineering. This technology allows a precise site-specific gene editing and such ability was applied to study the role of TALE (TALE - three amino acids loop extension) homeodomain transcription factors during neural crest cells development. The main genes of interest, belonging to sub-family of TALE proteins, are *Meis1* transcription factors that are present in the zebrafish genome as two paralogous genes, *meis1a* and *meis1b*. Their function was assessed by mutating their DNA-binding domain – homeodomain to abrogate the ability of transcription factor to bind DNA and by that disturb regulatory network, in which *Meis1* proteins operate in. Phenotype analysis of mutant fish would reveal a potential role of *Meis1* proteins in regulation of neural crest cells development and outline the functional significance of the homeodomain in regulatory operations. To determine the regulatory relationship between *meis1a* and *meis1b* genes morpholino-based knock-down of the genes was performed. Preliminary results suggest a dominant role of Meis1b in neural crest cells regulation and importance of its homeodomain. Furthermore, knock-down of *Meis1a* indicates its contribution to regulation of craniofacial development. However, a detailed description of factors will be completed after thorough analysis of genetic mutants generated by CRISPR/Cas9 system.

KEY WORDS

CRISPR/Cas9, transcription factor, neural crest, *Danio rerio,* Meis, mutagenesis, development

PROHLÁŠENÍ

Prohlašuji, že jsem závěrečnou práci zpracoval samostatně a že jsem uvedl všechny použité informační zdroje a literaturu. Tato práce ani její podstatná část nebyla předložena k získání jiného nebo stejného akademického titulu.

V Praze, 26.4. 2019 Bc. Petr Nickl

PODĚKOVÁNÍ

Tato diplomová práce vznikala v letech 2017-2019 na Ústavu experimentální medicíny Akademie věd České republiky na Oddělení vývojové biologie a za podpory Oddělení transkripční regulace Zbyňka Kozmika a Oddělení buněčné diferenciace Petra Bartůňka z Ústavu molekulární genetiky. Rád bych tímto chtěl poděkovat všem členům laboratoří, ve kterých jsem po dobu vypracování této práce působil. Zvláště pak mému školiteli RNDr. Ondřeji Machoňovi, Ph.D. za vedení práce, cenné rady a trpělivost, a Jiřímu Pergnerovi, Ph.D. za cenné rady do života.

CONTENT

1 LIST OF ABBREVIATIONS

aa - amino acid
AAV – adeno-associated virus
ABS – Alcian Blue staining
AP – anteroposterior
BMP – bone morphogenic protein
Cas – CRISPR associated protein
CRISPR - clustered regularly interspaced short palindromic repeats
crRNA - CRISPR RNA
dCas9 – dead Cas9
DSB – double strand break
dsDNA – double stranded DNA
DV - dorsoventral
Exd – Extradenticle
FGF – fibroblast growth factor
FS – frame shift
GFP – green fluorescent protein
HD – homeodomain
HDR – homology directed repair
HMA – heteroduplex mobility assay
hpf – hours post fertilization
hpf –hours post fertilization
Hth – Homothorax
IHC – immunohistochemical staining
indel – insertion/deletion
IVF – *in vitro* fertilization
KD – knock down
KO – knock out
MEIS – myeloid ecotropic interation site
MO – morpholinos
mpf – months post fertilization
NC – neural crest
NCC – neural crest cells
NHEJ – non-homologous ends joining
NUC – nuclease lobe
PAM – protospacer adjacent motif
PI – PAM interacting domain
RA – retinoic acid
RBP – RNA binding protein
RE - restriction endonuclease
REC - recognition lobe
RNAi – RNA interference
RT-PCR – reverse transcription PCR
RVD – repeat-variable residue
sgRNA/gRNA – single guide RNA/guide RNA
SpCas9 – streptococcus pyogenes Cas9 protein
ssDNA – single stranded DNA
SSN – site-specific nuclease
ssRNA – single stranded RNA
TALE – three amino acids loop extension
TALE – transcription activator-like effector
TALEN – transcription activator-like effector nuclease
TF – transcription factor
tracrRNA – trans-activating RNA
WISH – whole-mount *in situ* RNA hybridization
ZFN – zinc finger nuclease

2 THESIS INTRODUCTION

This diploma thesis is focused on application of CRISPR technology to elucidate developmental essence of TALE homeodomain (TALE - three amino acids loop extension) in context of neural crest.

The neural crest represents transiently occurring population of multipotent cells. Those cells migrate during development and settle down in their target destination, where differentiate into a wide range of cell types. The neural crest give rise to craniofacial bones, cartilage and neurons, melanocytes, enteric ganglia and contribute to septation of heart (Simoes-Costa *et* Bronner, 2015). Any disruption of neural crest development can have pathological consequences, such as neuroblastoma (Colon *et* Chung, 2011), intestinal agangliosis (Sullivan 1996), neurofibromatosis (Choe *et* Crump, 2014), cleft palate (Louw *et al*. 2015) or truncus arteriosus (impaired septation of pulmonary outflow; Machon *et al*. 2015; Lin *et al*. 2012).

TALE homeodomain transcription factors are sub-family of protein participating in processes involving hindbrain development (Stedman *et al*. 2009), haematopoiesis (Cvejic *et al*. 2011) or tumorigenesis (Dardaei, Longobardi *et* Blasi, 2014). This sub-family includes proteins, such as Prep, Pbx and Meis. This work focuses on proteins within Meis proteins group, because it has been reported that TALE homeodomain transcription factors, such as Meis2 may play a role in regulatory network during neural crest cells development (Machon *et al*. 2015). Furthermore, other publications imply connection of Meis1 proteins to neural crest development (Maeda *et al*. 2001) . Therefore, this work studies the function of Meis1 proteins, specifically zebrafish orthologues, *Meis1a* and *Meis1b*, during neural crest cells development.

The experimental part of the work aims for generation of *meia1* and *meis1b* mutant zebrafish lines and determine the contribution of those genes in neural crest cells regulation. Mutant lines were generated by introducing frame shifting mutation in homeobox region of *meis1* genes to abrogate the ability of the protein to bind DNA. Furthermore, morpholino mediated knock-down was performed to determine the contribution of each *meis1* gene. Preliminary data analysis suggests that *meis1b* contributes more to neural crest cells development and that homeodomain is an important part of the gene product while the function of *meis1a* in the process remains unclear.

3 THEORETICAL INTRODUCTION

3.1 Genetic studies in the zebrafish model

The zebrafish (*Danio rerio*) is widely used model organism due to its rapid development, short generation time, high fecundity, embryo transparency, genetics and small size in adulthood. Those are key features for research in developmental biology and its branches, such as embryology, neurobiology, cardiology or regenerative medicine. Mentioned disciplines benefit from an emerging tool for research of gene function, CRISPR/Cas9 system. A new technology capable of editing a fish genome by introducing a mutation in specific locus. The mutation could lead to a change of gene function or complete loss of the function. The loss usually sheds a light on a role of the gene in the organism.

3.1.1 General properties of the zebrafish model

The zebrafish is tropical fresh water bonefish that belongs to the *Cyprinidae* family. In nature, the species can be found in waters of Indian rivers, Ganga and Brahmaputra. General visual characteristics of the fish are small size (4-5 cm), distinct blue and black striped pattern (Spence *et al*. 2007), and sexual dimorphism: males are slender and have golden bright stripes on body and fins. Adult females are rounded and silvery in the ventral part. The most apparent sexual dimorphism is in the period of spawning. In the wild, a single female can spawn every 2-3 days and a single spawning usually contains dozens of eggs (Gerlai *et al*. 2000).

The embryogenesis in zebrafish is analogous to the early development in higher vertebrates including humans. The main developmental difference, between higher vertebrates and the fish, is external fertilization as well as development. Moreover, the egg and embryo themselves are transparent first couple of days after fertilization (Wixon 2000). Development of zebrafish embryo after fertilization is very fast. In the first 24 hours all essential organs are developed and the third day the fish hatches. The fry grows rapidly and reaches sexual maturity in 3-4 months (Fig.1; Stern and Zon 2003).

In 2013, after the first zebrafish genome sequences were published, Howe and colleagues compared human and zebrafish genomes. Surprisingly, the results showed more pronounced complexity in the fish genome compared to the human, 70% of human genes have at least one specific orthologue in zebrafish genome (Howe *et al*. 2013). Even though the zebrafish genome is smaller than the human genome. The complexity was generated by genome duplication that occurred approximately 300 million years ago (Fig.2). An additional genome duplication had initiated evolution of almost 25 000 Teleostei fish species that were specified by genome transforming processes, such as gene loss, sub-functionalization and neo-functionalization of genes. Gene loss led to elimination of redundant duplicated genes, sub-functionalization contributed to complementary functional separation and specification, and the process of neo-functionalization generated

new properties and functionally separated duplicated genes (Fig.3; Furutani-Seiki *et* Wittbrodt, 2004).

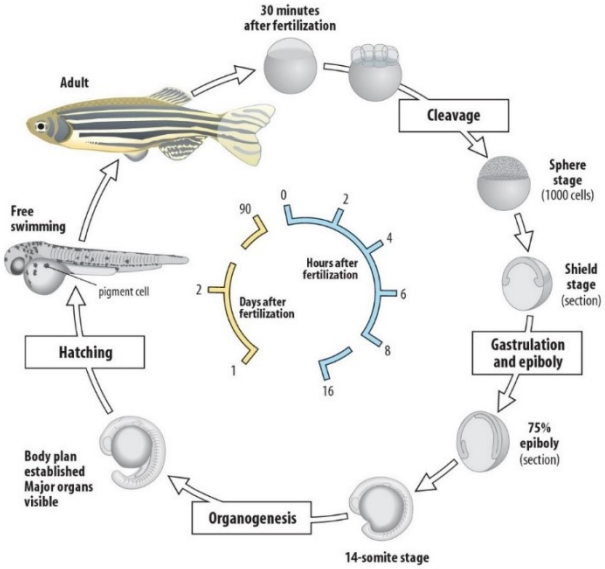

Figure 1: Scheme of zebrafish development from the moment of fertilization to adulthood. The first cell cleavage occurs within 30 minutes after fertilization. The multiple cell cleavage is followed by cell migration culminating into gastrulation and organogenesis. Body plan and all major organs are developed during the first 24 hours. Following day, a larva continues to develop, grow, and gains a pigment in the eyes and skin. On the second day, larvae hatch and become free swimming. The zebrafish reaches adulthood in 90 days (adapted from Pennonen et Leinonen, 2017).

A range of physiological structures is similar to human, such as central nervous system, muscles, cardiovascular system, skeletal system and hematopoietic cells (Lieschke *et* Currie, 2007). Furthermore, the similarities between genomes and molecular processes allow study of human diseases in the zebrafish model. The injection of the zebrafish with the gene causing disease in human, can lead to development of the same disease in the fish. That is one of the reasons why the species has been widely used in research of genetic disorders, such as schizophrenia, Alzheimer's disease, Parkinson's disease (Best *et al*derton, 2008), and muscular dystrophy (Bassett *et* Currie, 2003).

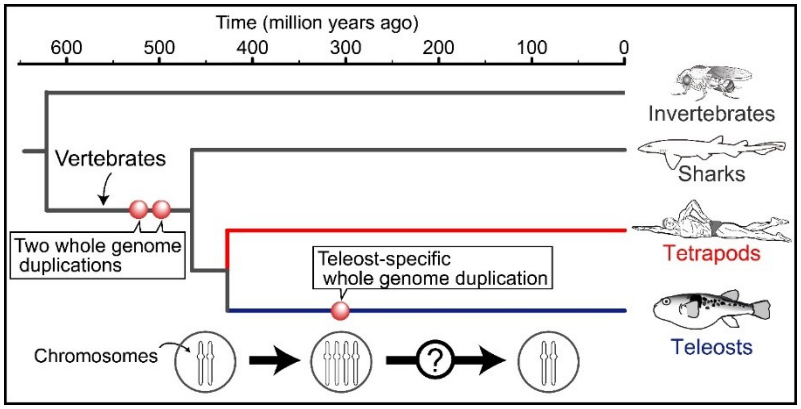

Figure 2: Evolutionary relationship between four organism lineages and three hypothetical genome duplications events (red dots). While, the last one occurred in Teleost lineage 300 million years ago (adapted from Inoue et al., 2015).

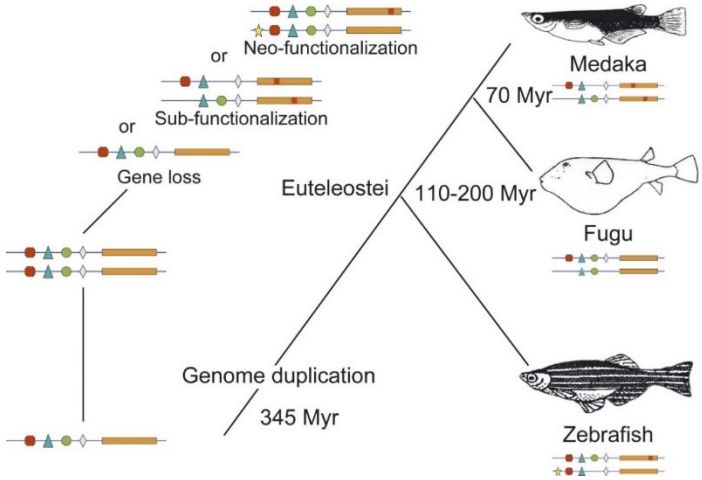

Figure 3: Cladogram showing evolutionary relationship between teleost fish zebrafish, fugu fish, and medaka that are frequently used as model systems. Figure demonstrates hypothetical consequences of genome duplication after the point of species division. On the left side is depicted how the duplication of a gene or a whole genome can lead to gene loss, sub-functionalization or neo-functionalization of a new paralogous gene. Processes of sub- and neo-functionalization does not occur only in non-coding regions (coloured symbols), but they can affect the coding region (orange line, differences in red). The schematic gene representation suggests that the duplication at the basis of teleost species radiation led to different gene functions throughout teleost model organisms (adapted from Furutani-Seiki et Wittbrodt, 2004).

3.1.2. Gene function analysis methods in zebrafish model system

In the pre-genomic era, "forward genetics" experiments were based on random mutagenesis induced by ionizing radiation or mutagenic chemicals, e.g. N-ethyl N-nitrosourea. Generated phenotypes were then evaluated and the gene responsible for such phenotype was found by cytogenetic techniques, cloning into plasmid and backcrossing. Forward genetics approaches have been done in larger scale and it has been very time-consuming and financially demanding process. Nowadays, in the post-genomic era, life science offers cheaper and more precise techniques for studying gene function, such as gene knock-down methods or site-specific nucleases.

3.1.2.1 Morpholinos

Morpholino is one of the gene knocking-down techniques based on artificial single-stranded uncharged thermostable DNA, resistant to nucleases (Fig.3). Morpholino oligonucleotides (MO) bind target mRNA by Watson-Crick base pairing and prevent the mRNA from being translated into a protein. The gene expression inhibition is achieved by an injection of a zebrafish egg with morpholino complementary to ribosome recognition sequence or exon-intron boundary region of target mRNA (Fig.4). Interactions in these regions cause disruption of mRNA processing mechanisms, such as intron splicing, or the mRNA is not recognized by ribosome, therefore is not translated. Impaired intron splicing leads to production of non-functional protein, while the blockage of ribosome binding site prevents production of the protein (Fig.4). Due to the effect on the gene expression, morpholino can mediate generation of a specific phenotype at the early stages of zebrafish development (Corey *et* Abrams, 2001).

Morpholino based knock-down approach offers fast and inexpensive functional analysis of gene expression. However, the reliability of this technique has been questioned. Kok and collective have pointed out a discrepancy between phenotypes of morphants (MO treated organisms) and mutants (Kok *et al*. 2015). One reason of false phenotype might be non-specific interaction with other mRNAs, which is more severe on the level of RNA than off-target activity of site-specific nuclease on the level of DNA. Mutant phenotype can be compensated by second non-mutated allele and be milder due to the compensation (Rossi *et al*. 2015). Off-target effects can be prevented by using at least two morpholinos, a translation blocker and a splice-inhibitor (Fig.4). At first, both mentioned MOs ought to be tested separately and then simultaneously to verify their ability to generate similar phenotype (*Eisen et* Smith, 2008).

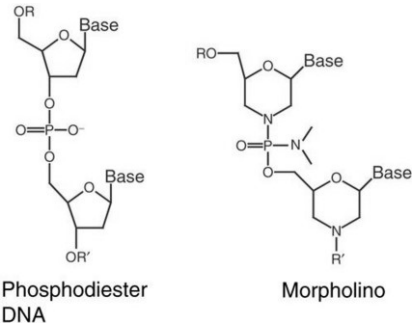

Figure 3: Structure of DNA (left) and morpholino (right) oligomers. Morpholino is single-stranded usually 25-bases long oligonucleotide, analogous to DNA. Its chemical structure is built of bases bound to methylenemorpholino rings. The rings are connected to each other by fosfodiamidate linkages and all together form a backbone of the oligomer. MO binds ssRNA or ssDNA, i.j. mRNA according to Watson-Crick base pairing. MO is synthetic compound with no charge, thus it is not recognized by any type of nuclease or other proteins. R and R' mark continuation of oligomers (adapted from Koller et al., 2000).

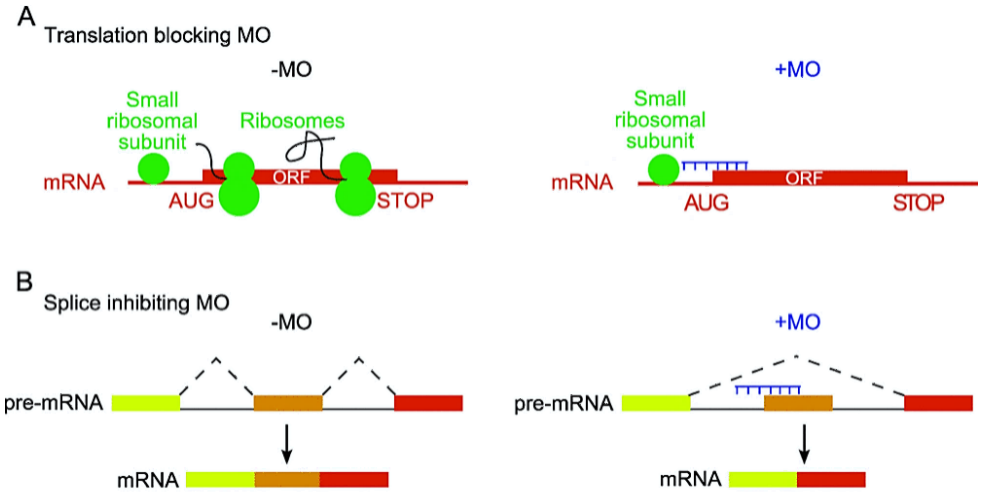

Figure 4: Morpholino oligonucleotides interacting with mRNA and inhibiting the mRNA processing. (A) Translation blocking. Natural process of translation in the absence of a MO (left) and translation initiation blocked by a MO (right). MO blockage prevents the small ribosomal subunit from scanning the 5'UTR, thus the large ribosomal subunit can't be recruited and assembled with the small ribosomal subunit at the start codon (AUG), and translation does not occur. (B) Splice inhibition. Normal pre-mRNA splicing (left). The hybridization of the MO causes skipping of the exon (orange) in the splicing process because it is not recognized (adapted from Hardy et al., 2010).

The other reason for phenotype differences is presence of maternal mRNA in mutant embryo. This maternal mRNA enables partial gene expression rescue in comparison to morphant embryo where maternal mRNA expression is blocked by MO. Furthermore,

morpholino oligonucleotides mediate only transient gene knock-down. Injected MOs are diluted during embryo's development by cell proliferation and mRNA production, therefore they are less and less potent in time. At the end, morphant phenotype is caused by transient gene expression inhibition at early stages of development. Later, the proper gene expression is resumed. The time of resumption is dependent on the concentration of injected MOs and the mRNA turnover. To avoid misinterpretation of the results from MO experiments, it is important to analyse generated phenotypes by additional experiments proving the specificity of used morpholino oligonucleotides.

The issues of the non-specific effects of MOs can be solved by following approaches. If an animal with mutated gene of interest is available, it is possible to compare phenotypes of a mutated and a knock-down fish. In case no mutant fish has been generate yet, following alternative experiments can determine and improve MO specificity. Loss of protein can be examined by *in situ* antibody staining or by Western blot. Incorrectly spliced pre-mRNA might be verified by RT-PCR (reverse transcription PCR) with consecutive electrophoresis or sequencing. Other relevant experiment would be whole-mount mRNA *in situ* hybridization to determine whether the mRNA is detained in the nucleus or not. Also, the important part of morpholino experiments must be the use of controls. Possible controls may be morpholinos, affecting the gene that is not expressed in the cells of interest, mismatched MO or inverted MO. Most suitable are five-base mismatch MOs due to their similarity to experimental MOs (Eisen *et* Smith, 2008).

Alternative control experiment can be RNA rescue, consisting of co-injection of MOs and mRNA of targeted gene that is not interacting with MOs. The endogenous mRNA is affected by MOs and co-injected mRNA shall rescue the expression, therefore any possible off-target effects are identified by such experiment (Eisen *et* Smith, 2008).

In the past, random mutagenesis experiments allowed generation of mutations in wide range of genes, but the process of such approach was un-cheap and very time consuming. Nowadays, emerging methods of site-specific mutagenesis enable relatively cheap generation of concrete mutants. Those methods are discovering biological functions of genes and uncover false-positive phenotypes that were generated by MO-based approaches.

3.1.2.2. Site-specific nucleases

Targeted gene disruption using site-specific nucleases (SSNs) is an emerging approach of deciphering a gene function. A toolkit of genome engineering involves SSN, such as zinc finger nuclease (ZFN), transcription activator-like effector nuclease (TALEN) or CRISPR/Cas9 system (Clustered Regulatory Interspaced Short Palindromic Repeats/CRISPR associated protein 9). SSNs are artificially generated proteins (ZFN and TALEN) or modified ribonucleoprotein complexes (Cas9) designed to cut DNA in a sequence specific manner (Govindan *et* Ramalingam, 2016). The first nuclease of the group is ZFN which is an artificial

restriction enzyme composed of zinc finger transcription factor DNA binding domains and DNA cleavage domain of bacterial restriction endonuclease (RE) *Fok*I (Fig.5; Kim, Cha *et* Chandrasegaran, 1996). TALEN was generated equivalently. It is also a fusion of DNA cleavage domain derived from *Fok*I RE and DNA binding domain (Fig.5). In the case of TALEN, transcription activator-like effector proteins (TALE) are used as a part of DNA binding domain. It is a common protein in *Xanthomonas* bacteria ensuring initiation of an infection by regulation of gene expression in host plant cells (Christian *et al*. 2010).

CRISPR/Cas9 system has been established on significantly different basis. The system comprises of Cas9 protein, responsible for DNA cleavage, and single guide RNA, navigating the Cas9 to target sequence where the protein binds and cleaves (Fig.5; Gasiunas *et al.*, 2012; Jinek *et al.*, 2012).

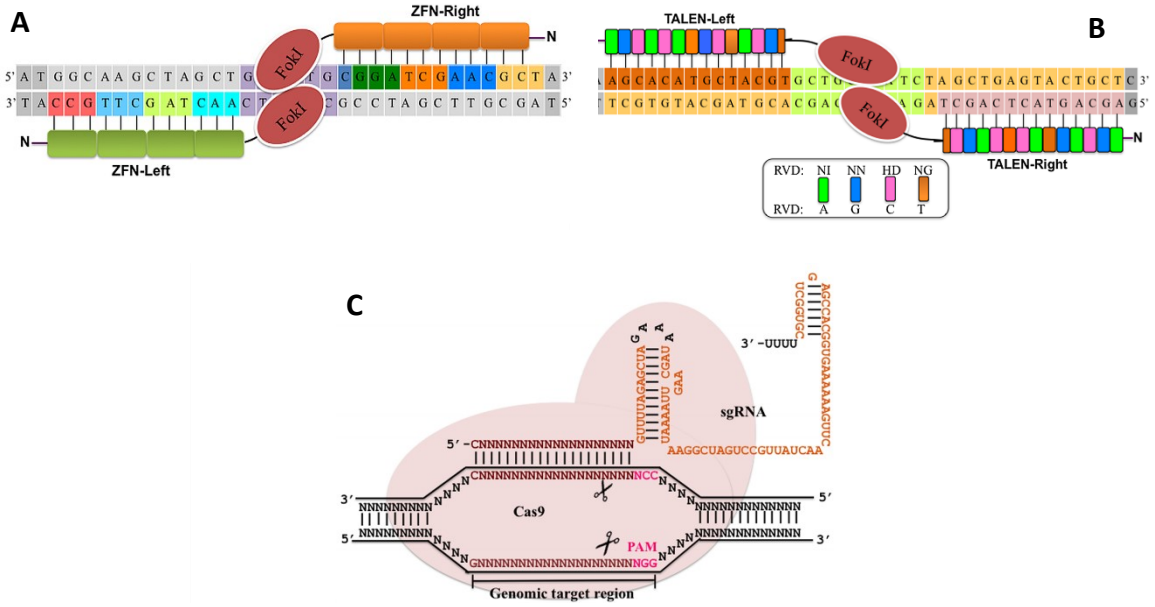

Figure 5: The structure of site-specific nucleases interacting with specific DNA sequence. (A) Zinc finger nucleases are fused zinc finger proteins ZFP to the cleavage domain of FokI restriction enzyme. Each ZFP has a ZF motif which recognizes specific triplet (3 bp) and interacts with DNA by introducing the α-helix into the major groove of dsDNA. DSB is then mediated by two ZFN monomers facing each other and forming active catalytic site for FokI domains. (B) TALENs are fused TALEs to the cleavage domain of FokI restriction enzyme. TALEs have a central DNA-binding motif of 13 to 28 monomers, consisting of 34 aa. Each monomer is formed by highly conserved aa sequence, except for two hypervariable residues at position 12 and 13. These hypervariable residues are also called repeat-variable residues (RVDs), because each repeat can have a different pair of amino acids in these positions. The pair determines a specificity and affinity of repeat to the nucleotide. (C) CRISPR/Cas9 system functions as an RNA-protein complex using sgRNA to bind a specific DNA sequence via Watson-Crick base pairing. As soon as the sgRNA/Cas9 complex binds PAM (protospacer adjacent motif, NGG) and recognizes the target, Cas9 cleaves DNA (adapted from Govindan et Ramalingam, 2016).

SSNs have been widely used to generate a variety of genomic alterations including small deletions or insertions (Hwang *et al*. 2013), correction of deleterious mutations (Howden *et al*. 2016) and insertion of exogenous DNA molecules (Hisano *et al*. 2015). Such alterations can be achieved by SSN-mediated DSB within a target sequence. The break can initiate DNA reparation via non-homologous end joining, which often leads to introduction

of insertion or deletion (indels), and within a coding sequence can cause reading frame shift (Fig.6). Also, indels can disrupt integrity of gene regulatory elements, such as enhancer, promoter or intron splicing signal that can affect gene expression. However, SSN have been also used for gene correction that often occurs in presence of donor dsDNA (Hisano *et al*. 2015) or ssDNA molecule (Yoshimi *et al*. 2016) with partial or full homology to the site where DSB was generated. Therefore, a correct form of the gene can be inserted through homology directed repair (HDR) and restore its function (Fig.6.). Furthermore, a transgene (e.g. GFP, Cre, LacZ, etc.) with exogenous regulatory elements (promoter, terminator, enhancer) and appropriate homology arms, flanking the transgene, can be also inserted in a site-specific manner into the genome (Fig.6; Kimura *et al.*, 2014).

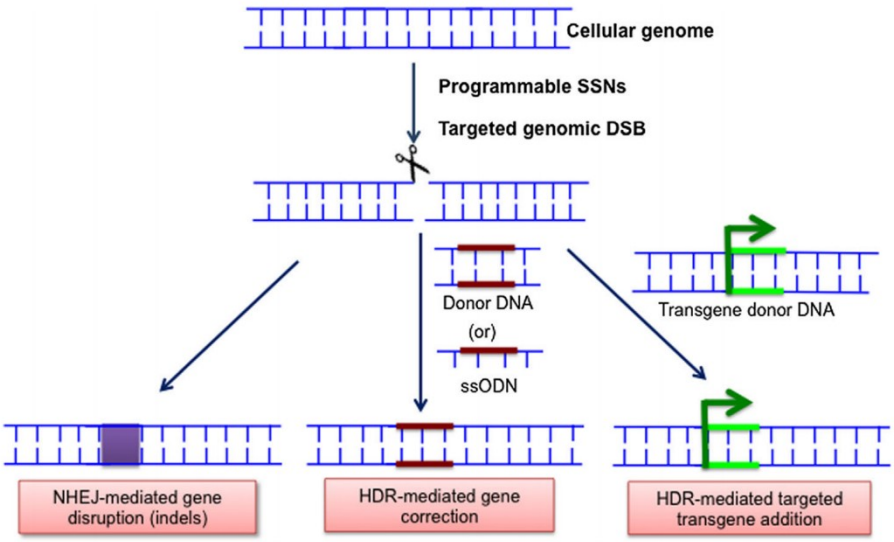

Figure 6: Sequence specific genome editing using programmable SSNs*. NHEJ: Non-homologous end joining repair (left) is error-prone mechanism of DNA damage reparation that often results in indels. HDR: Homology directed repair (in the middle) requires dsDNA or ssDNA donor molecule to use it as a template for reparation. Homology directed insertion of transgene (right), a donor molecule contains a transgene, flanked by homology arms that mediate an insertion to the locus of interest (adopted from Govindan and Ramalingam, 2016).*

To edit genomic sequence, nucleases must be delivered into the nucleus of the host cell. Nucleases are delivered in form of a protein or expression vector. Additional HDR donor is co-delivered as a circular or linearized molecule. Delivery can be performed via non-viral or viral approaches, where common non-viral approach includes cationic lipid-mediated transfection, electroporation, hydrodynamic injection and microinjection. The last option is most common in the zebrafish model. The most broadly used viral vectors are adenoviruses, lentiviruses and adeno-associated viruses (AAV). However, the obstacle for direct *in vivo* applications is the inability to deliver nuclease in cell or tissue-specific manner (Liu *et* Shui, 2016).

The application of site-specific editing systems is not flawless and has potential off-target effects. The reduction of non-specific cleavage of ZFN includes a design of *Fok*I domains with opposite charges that only dimerize while correct pairing of ZFNs occurs (Doyon *et al.*, 2011; Miller *et al.*, 2007) or delivery of ZFN as proteins to shorten the time of

exposure of nuclease to the genome (Gaj *et al*. 2012; Liu *et al*. 2015). Modularity of ZFN and TALEN enables intuitive design and synthesis. However, ZFP interactions with DNA are dependent on the modular context within a molecule and that is limiting factor in the process of ZFN assembly (Gersbach, Gaj *et* Barbas, 2014). Therefore, it sometimes requires optimization to find a functional ZFN. In case of TALEN, the approach of modular assembly appears to be more effective in gene targeting, thus extensive engineering and optimization is not required. Furthermore, TALEN have been proven to be more specific and less cytotoxic than ZFN (Mussolino *et al*. 2014).

In comparison to ZFN and TALEN, CRISPR/Cas9 system functions differently. It recognizes the target sequence via RNA-DNA interaction based on Watson-Crick base pairing. The system requires two components, an invariant Cas9 protein and programmable single guide RNA. The only Cas9 nuclease limitation is a requirement of conserved protospacer-adjacent motif (PAM) which is crucial for DNA-protein interaction. Although, this limitation appears to be overcome by modification of the Cas9 PAM interacting domain (Kleinstiver *et al.*, 2015). Alternatively, it is possible to use Cas9 orthologues from different bacterial species with distinct PAM pattern recognition (Hou *et al*. 2013; Ran *et al.* 2015a). In spite of the seemingly high specificity given by base-pairing and DNA-protein interaction, off-target cleavages have been reported even during application of this system (Fu *et al.* 2014). However, CRISPR technology is flexible enough to address this issue, for instance the use of Cas9 orthologues with more complex PAM requirements. Other possibility is to use Cas9/sgRNA complex in a limited amount (Hsu *et al*. 2013) or to use short-lived Cas9 protein (S. Kim *et al*. 2014), inducible Cas9 expression system (Zetsche, Volz *et* Zhang, 2015), two Cas9 nickases (Mali *et al*. 2013), inactive Cas9 fused to *Fok*I cleavage domain (Guilinger, Thompson *et* Liu, 2014) or Cas9 fused to DNA-binding domain (Bolukbasi *et al*. 2015). The robustness of CRISPR technology, programmability and a direct usage make the technology the most flexible genome editing tool at the moment.

3.1.2.3 CRISPR/Cas9 system

CRISPR is a locus in prokaryotic genome containing DNA fragments derived from viruses or invasive plasmids. The fragments were incorporated into bacterial genome during infection. Bacteria keeps the viral genetic information and builds simple prokaryotic immune system to prevent subsequent viral infection (Barrangou, 2015). An essential part of the immunity are Cas proteins which play an important role in capture and incorporation of a viral fragment to the genome. Also, they contribute to primary transcript processing where the result is crRNA. At the final stage, processed crRNA interacts with tracrRNA and Cas9 protein and together they form ribonucleoprotein complex which is able to recognize exogenous DNA (Fig. 7; Marraffini, 2015). Described CRISPR system is specific for *Streptococcus pyogenes*. All bacterial CRISPR systems are not the same and their composition is species-specific.

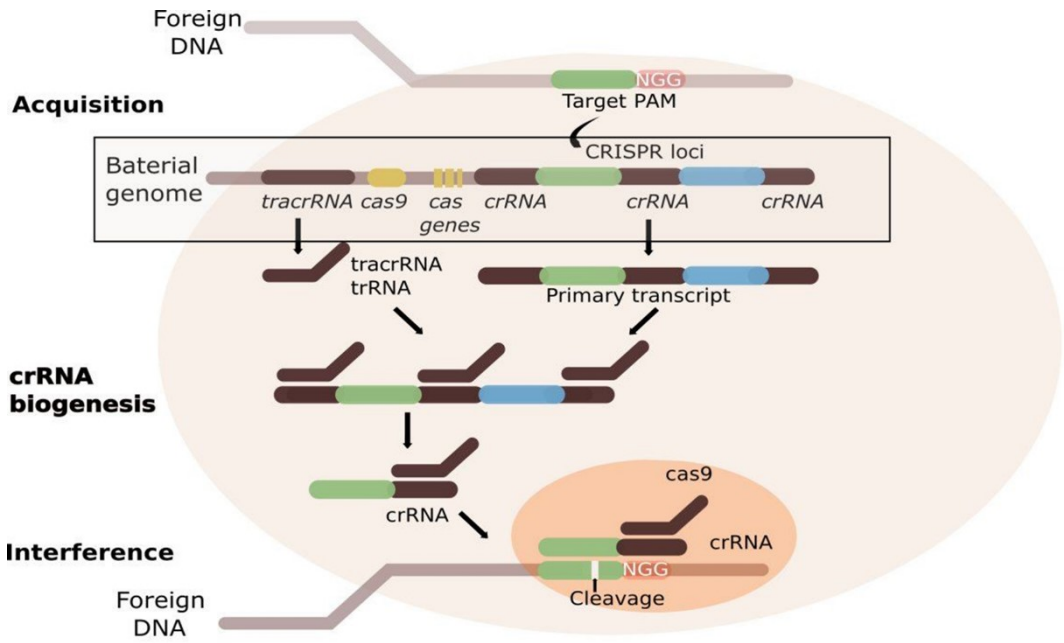

Figure 7: The stages of CRISPR prokaryotic antiviral defence mechanism. Acquisition stage is characteristic for recognition of invading DNA by Cas proteins, its cleavage and integration as a protospacer into the prokaryotic genome. crRNA biogenesis is initiated during infection by a virus that has been already recognized and adapted as an DNA fragment in CRISPR locus. A long primary transcript is transcribed and processed by Cas proteins to produce crRNAs, then crRNAs and tracrRNA form dsRNA secondary structure which is further processed by Cas9 and RNaseIII. crRNA-tracrRNA duplex molecule activates Cas9 and navigates it to the target sequence. After PAM recognition by the Cas9, the RNA-DNA interaction based on base pairing is made and that leads to cleavage and degradation of invading DNA (adapted from Pampel, 2016).

The genome editing tool, programmable nuclease Cas9, was derived from the prokaryotic immune system (Fig.7). The understanding of a crRNA-tracrRNA function in wild type Cas9/RNA complex led to production of chimeric sgRNA, which was essential step towards programmability of Cas9 (Fig.8). The sgRNA is a crucial component, mediating specific navigation of the Cas9 within the genome. Currently, the field of genome engineering provides a wide range of sgRNA designing tools such as CRISPOR, CCTop, ChopChop, CRISPR Design etc. Those tools are open-access programs predicting potential targets for sgRNA and Cas9, or Cas9 orthologues recognizing different PAM pattern (Nowak *et al*. 2016).

The sgRNA is functionally and structurally flexible element. It contains several secondary structures essential for its function, such as the nexus, stem loop, tetraloop, bulge and 3´end hairpins. It has been reported that the bulge and nexus (Fig.8) are the most sensitive structures and play an important part in the DNA cleavage. Surprisingly, large deletion mutations in the upper stem of sgRNA (Fig.8) do not abolish Cas9 cleavage activity (Nishimasu *et al*. 2014; Briner *et al*. 2014; Jinek *et al*. 2012). Alternations of upper stem structures and alternatively extensions of the stem loop (Fig.8) can even increase sgRNA stability and enhanced complexation with dSpCas9 (dead SpCas9, catalytically inactive SpCas9; Chen *et al.*, 2013; Ma *et al.*, 2016; Shao *et al.*, 2016). Activity and off-target cleavage of the SpCas9/sgRNA complex depends on factors such as sgRNA design (Yang *et*

al. 2013), chromatin accessibility (Wu *et al*. 2014), nucleotide composition (Doench *et al*. 2014) or length of the sgRNA (Moreno-Mateos *et al*. 2015).

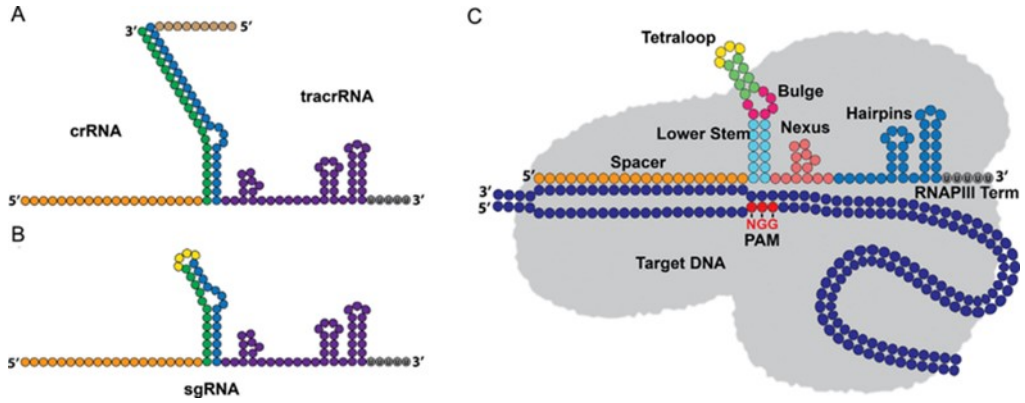

Figure 8: Secondary structure of RNA in complex with SpCas9 (Streptococcus pyogenes Cas9 protein).(A) Endogenous and wild type crRNA, comprised of 20 nucleotides long spacer (target recognizing sequence; orange) and 22 nucleotides long repeat (green), interacts with complementary region of tracrRNA (blue). The tracrRNA 3´ region (purple) forms a functionally significant structure that is essential for recognition by SpCas9. (B/C) The synthetic sgRNA was produced by fusion of tracrRNA and crRNA via tetraloop (yellow). (C) Anatomy of the sgRNA molecule. The spacer sequence (orange) navigates SpCas9 to the target locus. The lower stem (cyan) is formed by hybridization of CRISPR repeat sequence of crRNA and complementary region of the 5´end of tracrRNA. The protein interacts with lower stem (cyan) and upper stem (green) regardless of their sequence. In contrast, interaction with bulge (dark pink) is sequence dependent. The nexus (pink) is a central part of the sgRNA that has sequential and structural properties important for DNA cleavage. The nexus is essential for formation of a junction between the sgRNA, SpCas9 and DNA. The terminal hairpins enable stabilization of the sgRNA and formation of sgRNA/SpCas9 complex. Hairpins are flexible structures and despite large deleterious mutations in the region the Cas9/sgRNA complex, it is still able to cleave DNA (adapted from Nowak et al., 2016).

Indeed, sgRNA engineering proved that deletions introduced into its sequence can be beneficial in terms of stabilization or decrease of off-target effects. It has been shown that truncation of the 5´end of the sgRNA to 17 or 18 nucleotides long spacer decreases potential off-target cleavage (Fu *et al*. 2014). Larger truncations, down to 15 nucleotides, abrogate SpCas9 ability to cleave DNA but the complex is still able to target complementary sequence. The truncated sgRNAs are useful in complex with catalytically active Cas9 fused to transactivating domain, because Cas9 with truncated sgRNA (≤16 nt) has similar properties as a dCas9. It binds DNA without cleavage (Dahlman *et al*. 2015; Fu *et al*. 2014). Therefore, the complex with truncated sgRNA might be used for the same purposes as the dCas9 (Kiani *et al*. 2015). Moreover, the SpCas9/truncated sgRNA complex can be utilized for genomic imaging (Chen *et al*. 2013; Ma *et al*. 2016).

Additionally, more advanced modifications of sgRNA have been invented. Modifications such as an incorporation of functional secondary RNA structures known as RNA aptamers that can be recognized and bound by RNA binding proteins (Peabody, 1993; Bertrand *et al*. 1998). Adapter-recognizing proteins can be fused to transcription activators, repressors or epigenetic modifiers (Esvelt *et al*. 2013; Kiani *et al*. 2014; Konermann *et al*. 2015; Zalatan *et al*. 2015; Xu *et al*. 2016; Nishimasu *et al*. 2014; Mali *et al*. 2013; Dahlman

et al. 2015) or fluorescent proteins (Ma *et al*. 2016) which allows to study a gene function or genome topology not only by sequence-specific cleavage.

The CRISPRainbow system is multiplex labelling approach based on RNA aptamers within the sgRNA in complex with dCas9, where a set of multiple fluorescent proteins is attached to distinct RNA aptamer-binding protein. RNA aptamers are incorporated into sgRNA secondary structures such as tetraloop, the first hairpin or the 3´ end. The CRISPRainbow system allows to perform a multiplex imaging of genomic loci with up to seven different sgRNA molecules (Ma *et al*. 2016). As has been already noted, advanced secondary structure engineering opens new possibilities for CRISPR technology applications (Chavez *et al*. 2015).

The SpCas9 endonuclease is a key element of prokaryotic adaptive immune system. It was adapted to function in eukaryotic organisms and now it is broadly used as a genome engineering tool (Jinek *et al.*, 2012). In general, the protein is activated by interaction with crRNA-tracrRA duplex or sgRNA that leads to stochastic search for target DNA by scanning DNA molecules for PAM sequence. As soon as PAM is found, SpCas9/RNA complex forms an interaction with target sequence via sgRNA-DNA base pairing and upon formation of interaction, it induces a DSB in target locus (Sternberg *et al*. 2014).

The process of Cas9 activation and cleavage is tightly linked with conformational changes (Fig.9). The Cas9 protein consists of six domains, REC I, REC II, Bridge Helix, PAM Interacting Domain (PI), HNH and RuvC, which altogether form two lobes, REC (recognition lobe) and NUC (nuclease lobe). The REC lobe contains the largest domain REC I, domain responsible for binding the guide RNA, and REC II domain that is also involved in binding the guide RNA, but the mechanism is not properly described. The bridge helix is arginine-rich structure, important for initiation of DNA cleavage. The NUC lobe consists of the PI domain that determines PAM specificity of the Cas9. Its function is to initiate binding to target sequence. The HNH and RuvC are nuclease domains where each of them cleaves ssDNA (Fig.9; Nishimasu *et al.*, 2014).

The REC I domain is responsible for Cas9 activity because of its stabilization of repeat/anti-repeat stem loop (Fig. 8A). The PI and RuvC domains bind the nexus and 3´ end hairpins. The activation is followed by a conformation change upon binding of sgRNA (Nishimasu *et al*. 2014). The recognition of target sequence by Cas9/sgRNA is mediated by the initial binding of Cas9 to PAM. The protein stochastically scans a DNA molecule until it finds PAM to interact with. When PAM is detected, the protein tests a complementarity of potential target to its sgRNA by unwinding the remaining target DNA. If the tested sequence is complementary to sgRNA, the Cas9 reaches a conformational state that allows the nuclease domains to cleave DNA (Sternberg *et al*., 2014).

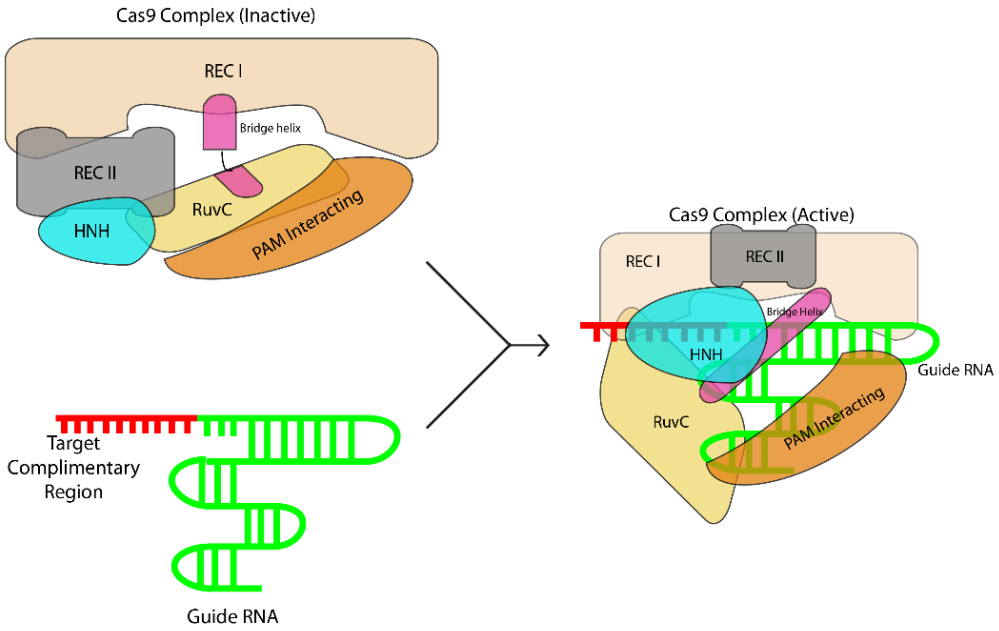

Figure 9: Schematic picture conformational change of Cas9 protein during formation of sgRNA/Cas9 complex (adapted from Jinek et al., 2014).

The DNA strand complementary to sgRNA is cleaved by the HNH domain. This domain is inactivated in Cas9 nickase or dCas9 by H840A mutation. Histidine-840 is essential for activation of water molecule. A consecutive electrophilic attack of water molecule is coordinated by magnesium ion and results in cleavage of 3´-5´ phosphate bond. The other strand, not complementary to the sgRNA, is cleaved by RuvC nuclease domain. The RuvC catalysed ssDNA cleavage in the manner similar to the two-metal cleavage mechanism of RuvC Holiday junction resolvase (Górecka, Komorowska *et* Nowotny, 2013; Nishimasu *et al.*, 2014). Mutations in one of the major catalytic residues His983, Asp986, Asp10 and Glu762 causes a total inhibition of nuclease activity, thus production of Cas9 nickase or dCas9, in case of functional disruption of both nuclease domains (Nishimasu *et al*. 2014).

The CRISPR/Cas9 system is a versatile genome editing tool due to its programmability and flexibility of usage at many levels of gene expression. The field of genome engineering expands its toolkit by discovering new Cas9 orthologues (Friedland *et al*. 2015; Hou *et al*. 2013; Ran *et al*. 2015b) but also by the re-engineered Cas9 (Kleinstiver *et al.*, 2015). All that has been done in order to reduce the size of Cas9, increase Cas9 specificity and expand the number of targets (Kleinstiver *et al.*, 2015). The size of naturally occurring Cas9 is a limiting factor in the process of packaging and delivering into cells via viral systems, hence there has been attempts to reduce Cas9, but it had a limited outcome. In contrast, the targeting scope was broadened by the discovery (Esvelt *et al*. 2013) and engineering of new Cas9 protein variants with less complex demand for PAM (Hirano *et al*. 2016). Besides, the specificity Cas/sgRNA complex is dependent on PAM recognition patter, the more complex PAM is, more specifically the Cas9 protein interacts with DNA (E. Kim *et al*. 2017). The field of genome engineering faces a difficult challenge to produce an ideal

Cas9 protein. It has been shown that smaller orthologues of Cas9 often requires more complex PAM, which means a higher fidelity of the protein and reduction of potential off-targets, but also narrowing of the targeting range (Friedland *et al.*, 2015; Ran *et al.*, 2015; Kim *et al.*, 2017). However, this obstacle is overcome by modified versions of Cas9 protein or sgRNA (Hirano *et al*. 2016).

The wild-type SpCas9 and engineered sgRNA provide a solid base for advanced modifications. Apart from mentioned sgRNA secondary structure, engineering the Cas9 protein can be also adjusted for a wide range of purposes. At first, the Cas9 protein was used as easily programmable nuclease introducing DSB likewise ZFN or TALEN (Jinek *et al.*, 2012). But, its versality gave a rise to a new tool used for more than changing a DNA sequence. The variety of applications is shown in Fig. 10 and Fig. 11, demonstrating what is possible to study by using this tool and how significant role CRISPR/Cas9 system plays in current genome research.

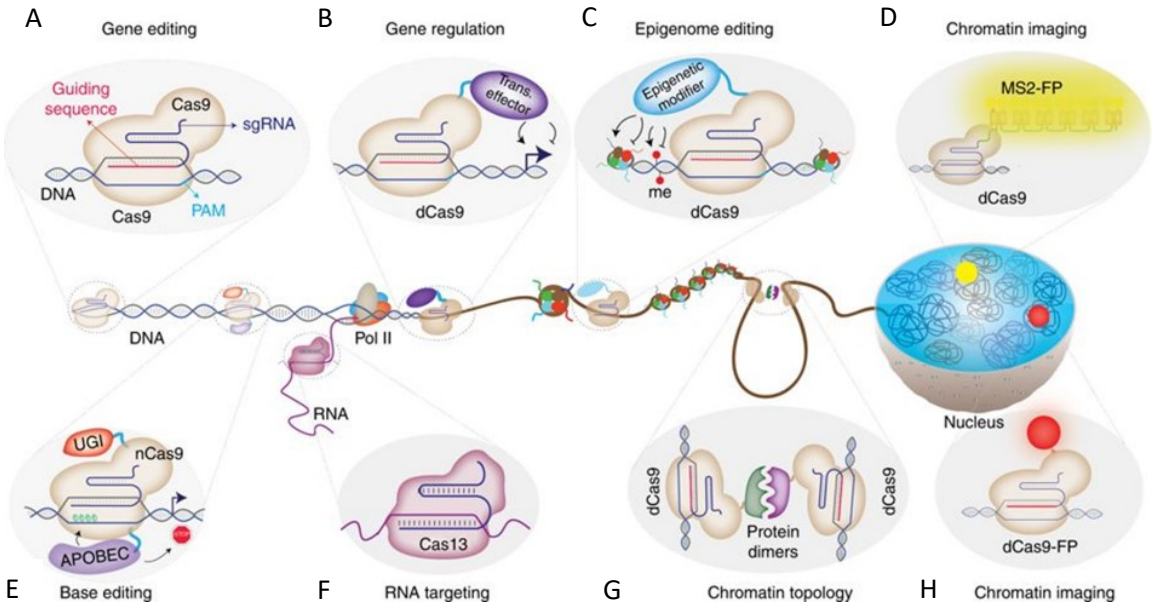

Figure 10: Advanced modification and applications of CRISPR technology (adapted from Adli 2018). Apart from genome editing with wild-type Cas9 by introduction of DSB (A), here several modifications of the technology are presented. For instance, (B) the Cas9 fused to trans-effector to regulate a promoter activity (Thakore *et al*. 2015)*; (C) the Cas9 fused to epigenetic modulator to modify histones or DNA* (Groner *et al*. 2010)*; (D) the Cas9 activated by sgRNA with aptamers binding MS2 proteins labelled with fluorescent protein* (Qin *et al*. 2017)*; (E) base editing performed with nickase Cas9 fused to ABOBEC1 (deaminase enzyme) and Uracyl Glycosylase inhibitor (UGI),)the protein multicomplex is able to convert cytosine into thymine* (Komor *et al*. 2016)*; (F) CRISPR technology enables RNA targeting by using Cas13* (Abudayyeh *et al*. 2017)*; (G)Chromatin topology approach can change proximity of enhancer and promoter and can pull the enhancer from silent region of chromatin to active chromatin* (Morgan *et al*. 2017)*; (H) technique of chromatin imaging is based on dCas9 fused to fluorescent protein and it is used to label the location of target loci* (Shao *et al*. 2016)*.*

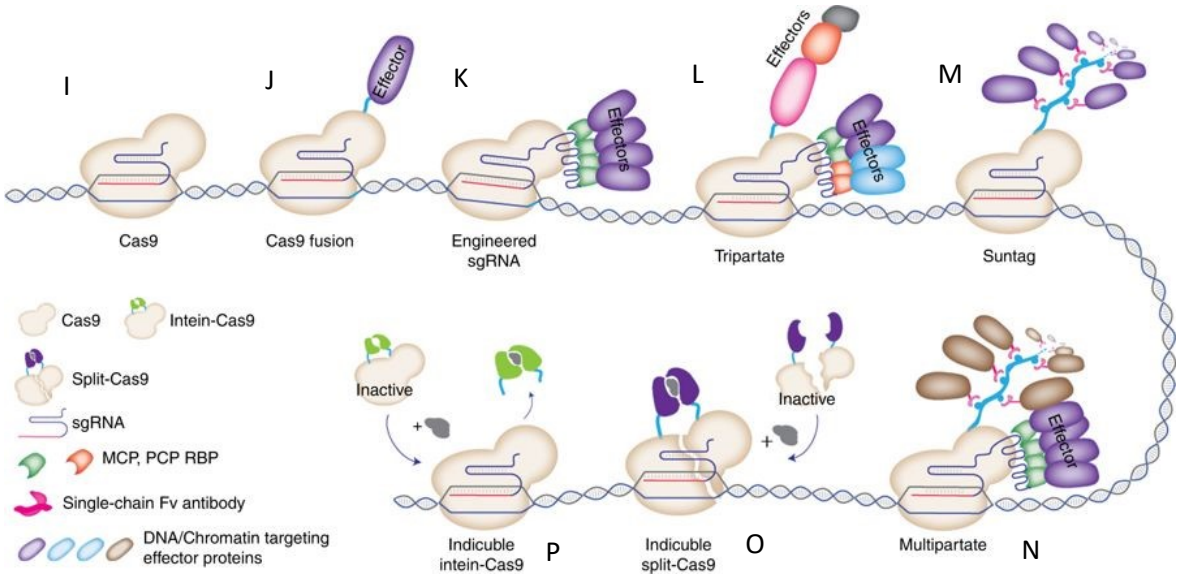

Figure 11: Advanced modifications and applications using sgRNA scaffold or fused proteins (adapted from Adli 2018). This figure shows a targeting capacity of Cas9 and its modularity in terms of additional components such as fusion to effector protein via peptide linker (J), connecting effector and Cas9, or via sgRNA scaffold which is sgRNA with functional aptamers that interact with RNA binding proteins (RBP; K). Effector protein can be fused to RBP and assemble to a multiprotein complex localized in the genome in the sequence-specific manner (K). (L) Tripartate approach is based on recruitment of multiple different effectors attached to dCas9 through peptide linker and sgRNA scaffold (Chavez *et al*. 2015). *(M) Suntag strategy uses a repeating peptide chain as a scaffold linked to dCas9, to bind an array of antibody-fused effector proteins* (Tanenbaum *et al*. 2014). *Due to a different fashion of attachment to the Cas9/sgRNA complex, Tipartate and Suntag strategies can be combined to produce Multipartate (N; Adli, 2018). The Cas9 activity can be chemically inducible to enable the control of the Cas9 activity in time. Here are depicted two approaches (O,P): Inducible intein-Cas9 system is activated by a chemical which ensures detachment of Cas9 inhibiting molecules (P; intein; Lu et al., 2017). The second system uses Cas9 protein split in halves, where each half has chemical-dependent assembly domain. The Cas9 is brought together in the presence of the chemical connecting assembled domains (O; Zetsche, Volz et Zhang, 2015).*

3.2 The role of Meis transcription factors during neural crest cells development

The thesis is focused on mutagenesis of meis1 genes in the zebrafish to study their impact on development of neural crest cells (NCCs). This chapter explains what are Meis transcription factors and neural crest cells and what is the role of Meis transcription factors in context of development.

3.2.1 Neural crest cells

Neural crest cells are population of migratory multipotent embryonic cells that are formed transiently to give rise to a vast variety of structures, including craniofacial cartilage and bone, melanocytes, glia and peripheral and enteric neurons (Bronner *et* LeDouarin, 2012; Dupin *et* Sommer, 2012).

The neural crest is temporarily formed structure, unique for vertebrates. In early stages of its development, after gastrulation, it specifies as a structure called the neural

plate border, localized between the neural plate and the non-neural ectoderm (Fig.12B). Subsequently, during neurulation, neural plate borders converge along the neural plate and connect at the dorsal midline to build the neural tube (Fig.12C-D). After the neural tube is formed, neural crest cells undergo and an epithelial to mesenchymal transition. They delaminate and migrate from neuroepithelium to the periphery, differentiating into distinct cell types (Fig.12E; Huang *et* Saint-Jeannet, 2004).

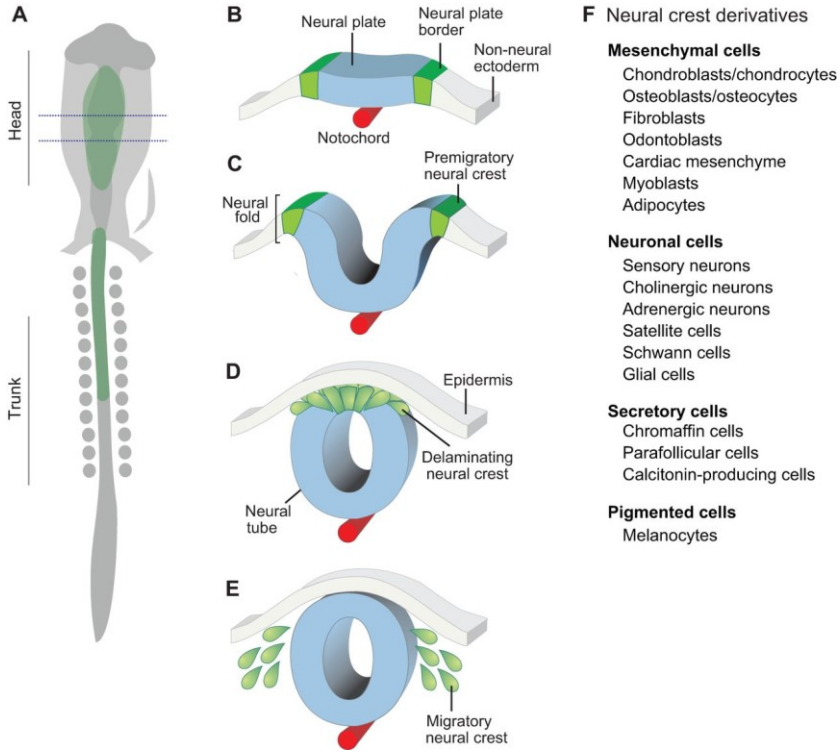

Figure 12: The early stages of neural crest development and list of NCCs derivatives. (A) Scheme of a 10-somite chick embryo from dorsal view with highlighted neural crest (green) and lines showing location of cross-sections B-E. (B) The specification of NCC in the neural plate border. (C) The closure of neural tube and the specification of neural crest progenitors in neural folds. (D) Epithelial to mesenchymal transition and delamination of neural crest cells. (E) The migration of NCC to diverse destinations to generate distinct derivatives. (F) The list of cell types derived from NCC (adapted from Simoes-Costa et Bronner, 2015).

The NCCs differentiation is largely dependent on their migration and their final destination. Four populations of neural crest cells (NCCs) are distinguished along the anterior-posterior axis with respect to their differentiation. The cranial (cephalic) neural crest, the trunk neural crest, the vagal and sacral neural crest and cardiac neural crest (Gilbert 2000).

The cranial neural crest involves cells that migrate dorsolaterally to produce craniofacial mesenchyme that differentiates into craniofacial cartilage, bone, neurons, glia and connective tissue. Also, these cells differentiate into thymic cells, odontoblasts of the tooth primordia, the bones of middle ear and jaw (Gilbert 2000).

The trunk neural crest cells take two major pathways. One of them leads dorsolaterally to give rise to pigment-synthetizing melanocytes that continue migrating towards the ventral midline of the belly. The second pathway navigates the trunk NCCs

ventrolaterally through sclerotomes. Some NCC remain in sclerotome and form the dorsal root ganglia that integrate the sensory neurons. The NCC that do not remain in sclerotomes follow the pathway more ventrally and contribute to formation of sympathetic ganglia, the adrenal medulla and the nerve clusters surrounding the aorta (Gilbert 2000).

The vagal and sacral neural crest differentiate into the parasympathetic (enteric) ganglia of the gut (Le Douarin *et* Teillet, 1974; Pomeranz, Rothman *et* Gershon, 1991). The vagal (neck) neural crest is situated near somite 1-7 and the sacral neural crest is located posteriorly from somite 28 (Fig.13; Gilbert, 2000).

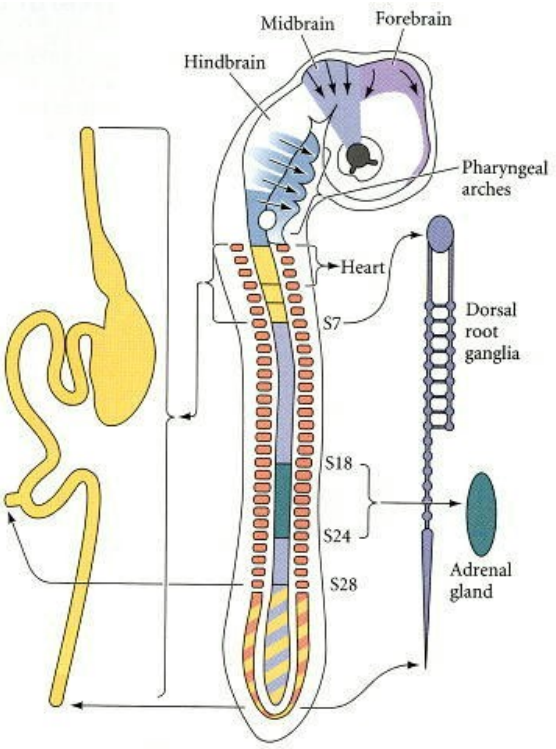

Figure 13: Schematic description of the neural crest of chick embryo. The cranial crest cells migrate into pharyngeal arches and the head to build up the bones and cartilage of the neck and face. The cranial NC also differentiates into melanocytes and forms cranial nerves. The vagal NC (region of somites 1-7) and the sacral NC (posterior region to somite 28) gave rise to the gut parasympathetic nerves. The cardiac NC is formed from NCC in the region somite 1-3; they are essential for separation of the aorta and the pulmonary artery. The trunk NCC localize in regions of somite 6 through the tail and form sympathetic neurons. The region of somite 18-24 contains NCCs, forming the medulla portion of the adrenal gland (adapted from Le Douarin et Teillet, 1974).

The cardiac neural crest is positioned between the cranial and trunk neural crest. Those cells occupy the region of somite 1-3 thus overlying the region occupied by the vagal neural crest (Kirby *et* Waldo, 1990; Kirby *et* Hutson, 2010). This type of neural crest can differentiate into melanocytes, neurons, cartilage and connective tissue of pharyngeal arches 3, 4 and 6. Furthermore, the cardiac neural crest generates the arterial musculoconnective tissue and partially builds up the septum, separating the pulmonary outflow from the aorta (Le Lièvre *et* Le Douarin, 1975).

The NCCs are a transient population of cells, therefore they cannot be observed in adult vertebrates. The only evidence of their presence are cell types that were differentiated from them. Any disruption of specification, migration or differentiation of NCCs can lead to impaired developmental of those derivatives, and furthermore to developmental defects, such as cleft lip or palate (Trainor 2010), absence of peristaltic movement of bowels, truncus arteriosus (Machon *et al*. 2015) or ocular anomalies (Williams *et* Bohnsack, 2015).

3.2.2 MEIS proteins

The Meis proteins belong to the class of TALE (three amino acids loop extension) homeodomain transcription factors (TFs), involving Meis, Prep and Pbx proteins. It has been shown that TALE transcription factors are important regulatory elements in processes of development and adult physiology maintainance. Therefore, their disruption can lead to development of various pathological defects.

MEIS is the acronym for myeloid ecotropic interation site. This acronym was stated after the discovery of connection between myeloid leukemia and mutations in these genes (Moskow *et al*. 1995). There are three *MEIS* genes (*MEIS1*, *MEIS2*, *MEIS3*) in mouse and human but in the zebrafish, five *meis* genes are present (*meis1a*, *meis1b, meis2a, meis2b* and *meis3*). It is due to the genome duplication the species went through during evolution (Fig.2; Furutani-Seiki *et* Wittbrodt, 2004). However, the difference in the biological function of *meis1a* and *meis1b* has not been fully understood yet.

It has been reported that proteins among the class of TALE transcription factors are often a part of regulatory multimer. Their structure allows them to interact with each other, but also, with other transcription factors. TALE transcription factors have two domains mediating those interactions. In case of Pbx, such domains are PBC-A and PBC-B. Prep and Meis proteins have MEIS-A and MEIS-B domains. TALE TFs share highly conserved homeodomain (HD) which is essential for DNA binding and transport to the nucleus due to localization of NLS within the domain (Fig.14). Additionally, HD is important for dimerization with HOX proteins (Longobardi *et al*. 2014).

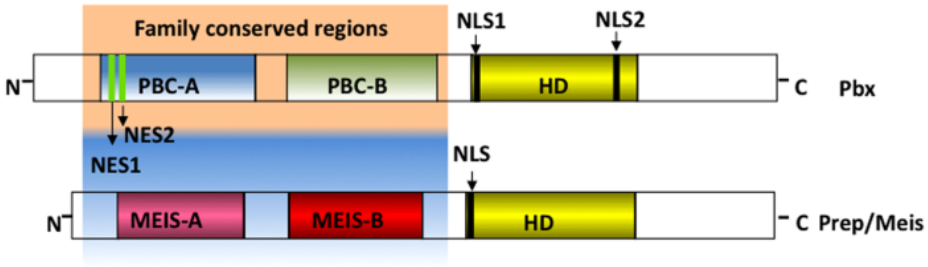

Figure 14: Scheme of the TALE proteins anatomy. The homeodomain (HD) is conserve throughout the TALE proteins class. PBC-A/B are interacting domains found only in the PBX family. On the N-terminal of the Pbx are located nuclear export signals (NES1, NES2) and within HD and nuclear localization signals (NLS1, NLS2). The Prep/Meis sub-families proteins contain MEIS-A and MEIS-B interacting domains and HD with NLS (adapted from Longobardi et al., 2014).

The TALE transcription factors can interact with each other but also with a vast variety of other transcription factors to prevent tumorigenesis (Dardaei, Longobardi *et* Blasi, 2013) HOX proteins to regulate quiescence of hematopoietic stem cells or the cell cycle of cardiomyocytes (Yuan *et* Braun, 2013).

3.2.3 Regulation of neural crest cells development

The specification of NC is orchestrated by signals coming from the future neural and non-neural ectoderm. This process is coupled with signal molecules, such as Wnt, bone morphogenic protein (BMP) or fibroblast growth factor (FGF). These molecules stimulate signalling pathways, regulating the specification of the neural plate border, and induce expression of early specifiers Msx1, Msx2, Pax7 and Zic1. Transcription factors Pax7 and Zic7 are controlled by Wnt and FGF pathways and operate synergistically to turn up expression of NC specific genes, involving Snail, FoxD3 and SoxE transcription factors in emerging neural folds (Sauka-Spengler *et* Bronner-Fraser, 2008). The key element in processes of cell cycle control and multipotency maintenance is expression of c-Myc, which functions as a switch between those processes (Bellmeyer *et al*. 2003). The segregation of NCCs from dorsal neuroepithelium is then controlled by Sox9 that upregulates Snail, an anti-apoptotic factor, preventing apoptosis of the trunk NCC (Cheung *et al*. 2005).

At the beginning of the stage of epithelial to mesenchymal transition (EMT), the NC specifiers, such as Sox9, Snail and c-Myc, regulate cell proliferation and delamination (Cheung *et al.*, 2005; Sauka-Spengler *et* Bronner-Fraser, 2008). Moreover, the FoxD3 and Sox10 remain to be expressed in delaminating and migrating NCCs and influence expression of their subordinate effector genes, involving cadherin type II, cadherin-7, matrix metalloproteases, integrins, neuropilins, Eph and other receptors (Fig. 15; Nakagawa *et* Takeichi, 1995, 1998; Hadeball, Borchers *et* Wedlich, 1998; Cheung *et al.*, 2005)

After migration of NCCs to the target destination, the process of differentiation begins. Differentiation is controlled by small regulatory modules, often dependent on expression of NC specifiers. Major determinants are SoxE transcription factors. These TFs, together with other TFs, control differentiation of NCCs into distinct cell types and derivatives by regulating their downstream effector genes. Moreover, expression of SoxE genes remains active in the specific derivatives, where they play an important role in terminal differentiation (Lefebvre *et al*. 1997; Kelsh 2006).

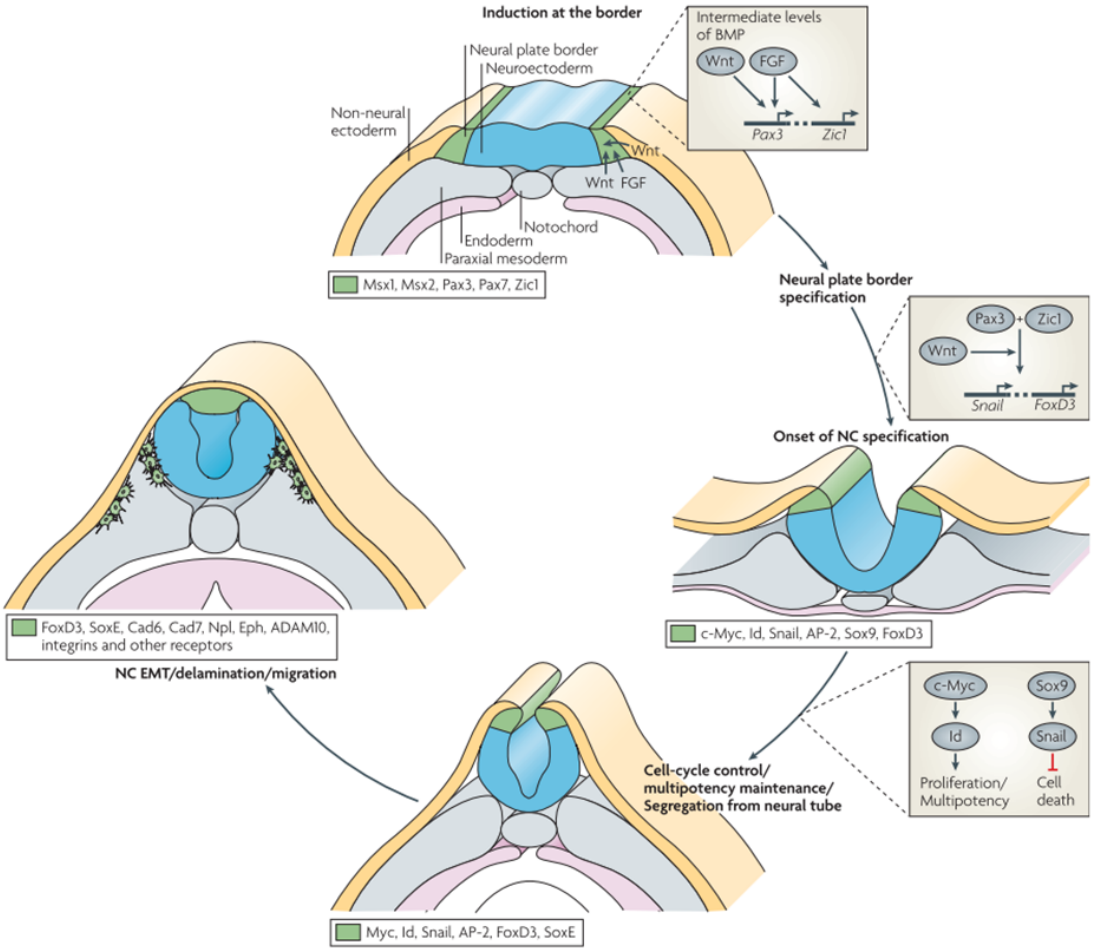

Figure 15: Regulatory machinery of the neural crest development. The NC specification starts at the neural plate border. It is induced by fibroblast grow factor (FGF) and Wnt signalling molecules from underlying paraxial mesoderm (grey) and the surrounding non-neural ectoderm (yellow). Both or only one signal can positively influence the expression of NC specifiers (Pax3, Zic1). In this case, the FGF and Wnt signalling is dependent on the level of bone morphogenic protein (BMP). Pax3 and Zic1 activate expression of downstream effector genes, other NC specifiers Snail and FoxD3, in the neural fold and dorsal neural tube. The c-Myc and Id (Inhibitor of DNA binding/differentiation) proteins function as a switch controlling the cell-fate decision by proofreading cell cycle and, at the same time, maintain the NC progenitors in a multipotent state. Sox9 is essential for survival of trunk NCC. It upregulates expression of Snail, an anti-apoptotic factor. Expression of the early NC specifiers controls cell behaviour, specifically cell proliferation, delamination and migration during EMT (adapted from Sauka-Spengler et Bronner-Fraser, 2008).

Development of neural tube is followed by its segmentation alongside anteroposterior (AP) axis. This segmentation is dependent on expression of homeodomain transcription factors (Hox) genes. Early Hox expression is initiated in the neural tube and is coordinated by gradients of molecules, for instance retinoic acid (RA), FGFs and Wnt proteins (Dupé *et* Lumsden, 2001; Kiecker *et* Niehrs, 2001; Paige *et al.*, 2012). Members of Hox gene family are responsible for specification of AP identity of progenitor compartments known as rhombomeres (R1-R7; Lumsden *et* Krumlauf, 1996; Rijli, Gavalas *et* Chambon, 1998; Schneider-Maunoury, Gilardi-Hebenstreit *et* Charnay, 1998). Localized expression of homeodomain transcription factors along the AP and dorsoventral (DV) axes characterizes developmental programme of progenitor cells. Equivalently, the cranial NCCs, migrating to pharyngeal arches, are responsive to signals determining spatial

information and therefore their fate. In general, the cranial NC development is dependent on the expression of Hox genes (Lumsden, Sprawson *et* Graham, 1991; Serbedzija, Bronner-Fraser *et* Fraser, 1992; Sechrist *et al.*, 1993). However, it has been reported that in context of the NCCs, Hox proteins form multimeric complexes with other co-factors to regulate expression of downstream effector genes. One of the major co-factor classes are TALE homeodomain transcription factors, including Meis, Prep and Pbx proteins (Choe, Vlachakis *et* Sagerström, 2001).

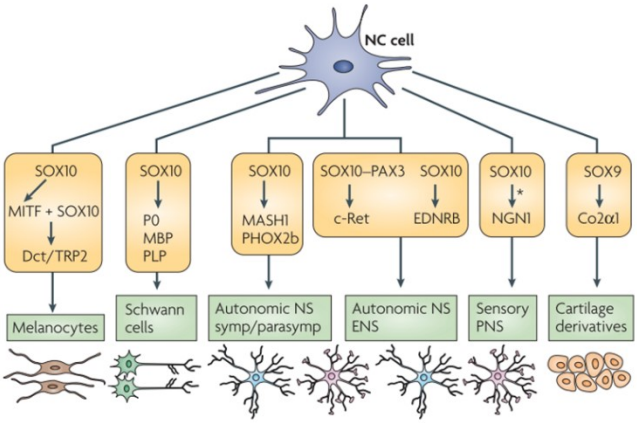

Figure 16: Contribution of SoxE transcription factors in the process of neural crest cells differentiation (adapted from Sauka-Spengler et Bronner-Fraser, 2008). First expression of SoxE genes can be observed during NC specification (pre-migratory specifier - Sox9, Fig.14), then during early delamination and migration (Sox10) of NCCs. Later, the SOX9 is responsible for differentiation of NCC-derived cartilage by binding and activating the collagen type IIα1 promoter (Lefebvre *et al*. 1997)*, meanwhile SOX10 regulates subordinate effector genes in cells of neural system and melanocytes* (Kelsh, 2006)*.*

The study of homeodomain-containing Hox proteins in *Drosophila* revealed that Hox proteins act in concert with other partners, for instance proteins Extradenticle (Exd) and Homothorax (Hth). Vertebrate orthologs of such partners are known as Pbx and Meis, respectively. These partners mutually influence their expression and stability, and control intrinsic specificity of Hox protein in their regulatory activity. Experiments done in the zebrafish suggest the TALE-homeodomain proteins, specifically Meis proteins, bind Hox proteins and contribute to development of proper segmental identity (Fig. 17; Waskiewicz *et al.*, 2001). The Hox proteins bind a rather nonspecific DNA sequence - TAAT (Beachy *et al.*, 1988; Ekker *et al.*, 1991; Catron, Iler *et* Abate, 1993), therefore they require cofactors, increasing their DNA binding

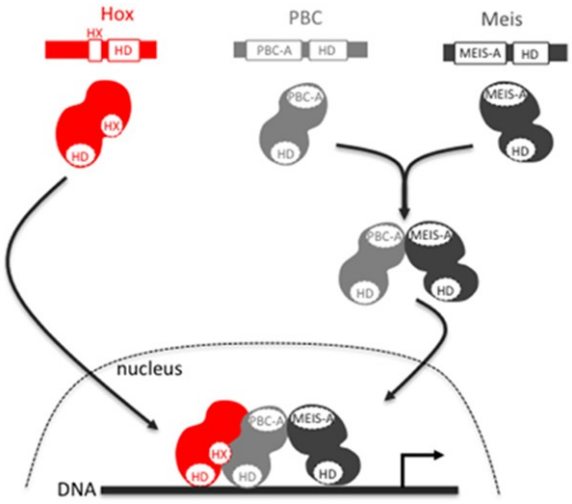

Figure 17: The interaction between Hox and TALE proteins during regulation of gene expression. Hox proteins contain HX (hexapeptide) motif which is essential for binding interacting partners. Meis protein interacts with PBC (Pbx proteins) via MEIS-A and PBC-A domains. This interaction allows translocation of PBC to the nucleus. Final association of Hox/TALE complex and DNA binding occurs in the nucleus (adapted from Merabet et Galliot, 2015) .

specificity. It has been reported that TALE homeodomain proteins are important in development of hindbrain, specifically in identification of rhombomeres 2-4. In the rhombomeres, Meis proteins cooperate with Hox protein and other TALE transcription factors. Together, they form a vast variety of complexes regulating downstream effector genes to identify and determine the fate of specific rhombomere (Salzberg *et al.*, 1999; Dibner, Elias *et* Frank, 2001; Vlachakis, Choe *et* Sagerstrom, 2001; Waskiewicz *et al.*, 2001; Deflorian *et al.*, 2004).

Meis1 transcription factors are not only essential in hindbrain development but they are also involved in other regulatory pathways. They happened to be important in primitive haematopoiesis and regulation of quiescence of hematopoietic stem cells in the mouse (Kocabas *et al*. 2012), proliferation of cardiomyocytes derived from ES cells (Buggisch *et al*. 2007) and development of craniofacial structures derived from NC (Melvin *et al*. 2013). The mouse, lacking Meis1 protein, can suffer from liver hypoplasia (Hisa *et al*. 2004), congenital heart disease (Stankunas *et al*. 2008), impaired haematopoiesis, leukemia and eye defects (Hisa *et al*. 2004). The role of Meis1 protein in context of NC has been partly elucidated by specific mutation of the gene in the mouse, and additionally by knock-down experiments based on morpholinos in the zebrafish. However, a comprehensive view of the Meis1 role in NC development is still missing. In contrast, the developmental function of Meis2 has been more profoundly understood due to phenotype assessment of Meis2 KO mouse (Machon *et al*. 2015) and *Meis2b* KO zebrafish (Guerra *et al*. 2018).

The experiments, studying Meis1 in the zebrafish mentioned above, are often based on knock-down approach which has been proven to be less reliable than gene knock-out done by SSNs (Kok *et al*. 2015). Therefore, it is required to generate knock-out fish and compare its phenotype with morphant phenotype. Furthermore, the zebrafish went through genome duplication during evolution which means the presence of *meis1* paralogues in the genome (Furutani-Seiki *et* Wittbrodt, 2004), therefore their function should be also studied collectively. This thesis focuses on generation of mutant fish with both *meis1* paralogues knocked-out, in order to elucidate regulatory potential of *Meis1* proteins in the zebrafish model.

4 THE GOAL OF THESIS

I. To establish mutant zebrafish lines of *meis1a* and *meis1b* genes using CRISPR technology, in order to study their importance during neural crest cells development.

II. To determine a relationship between meis1 genes in regulation of neural crest cells in the zebrafish by using morpholino based knock down and compare phenotype of morphant and crispant fish.

5 MATERIAL

5.1 Reagents and chemicals

10X Saline sodium citrate (SSC), Sigma-Aldrich (cat.no. 6132-04-3)
1X NEBuffer™ 3.1; NEB
1X T4 DNA Ligase Reaction Buffer, NEB (cat.no. B0202S)
25mM MgCl2, Thermo Fisher Scientific
2X DreamTaq Master Mix, Thermo Fisher Scientific (cat.no. K1081)
4% Paraformaldehyde (PFA), Sigma -Aldrich (cat.no. 30525-89-4)
40% Acrylamide/Bis Solution, 29:1 (3.3% C), Bio Rad (cat.no. 161-0146)
50X TAE (2M Tris Base, 1M Acetic acid, 50mM EDTA)
Absolute ethanol, Penta (cat.no. 64-17-5)
Acetone, Penta (cat.no. 67-64-1)
Alcian Blue Solution (80% Ethanol, 20% Acetic acid, 0,1% Alcian Blue)
Ampicillin, Roche (cat.no. 10835242001)
Anti-DIG alkaline phosphatase, Roche (cat.no. 11093274910)
APS, Ammonium persulfate 10%; Thermo Fisher Scientific (cat.no. 17874)
BamHI restriction endonuclease, NEB (cat.no. R0136)
Bovine serum albumin – BSA, Sigma-Aldrich (cat.no. 9048-46-8)
BsmBI restriction endonuclease, NEB (cat.no. R0580)
Citric acid, Sigma-Aldrich (77-92-9)
DEPC water
Dlx1a probe labelled with DIG
Formamide, Sigma-Aldrich (cat.no. 75-12-7)
FoxD3 probe labelled with DIG
GeneRulerTM 100 bp Plus DNA Ladder
Glycerol, Sigma-Aldrich (cat.no. 56-81-5)
Heparin, Sigma-Aldrich (cat.no. 9041-08-1)
Isopropanol; Penta (cat.no. 67-63-0)
KCl, Serva (cat.no. 7447-40-7)
KOH, Sigma-Aldrich (cat.no. 1310-58-3)
Levamisol, Sigma-Aldrich (cat.no. 16595-80-5)
Lugol solution (10 g KI and 5g I_2 in water)
Luria-Bertani (LB) medium - 1% tryptone, 0,5% yeast extract, 1% NaCl, dH2O
NaCl, Serva (cat.no. 7647-14-5)
NBT/BCIP, Thermo Fisher Scientific (cat.no. 34042)
PBS - Phosphate Buffer Saline (1liter: 80g NaCl, 2 g KCl, 14.4g Na2HPO4, 2.4g KH2PO4, dH2O Ph 7,4)
PBST (1% Triton 100 in 1XPBS)
PBT (0.1% Tween in 1X PBS)
Phenol Red Dye, Sigma-Aldrich (cat.no. 143-74-8)
Phosphotungstic acid – PTA (1%PTA in water)
Primary antibody anti-Meis1a (rabbit) - homemade
Pronase, Roche (cat.no. 10165921001)
Proteinase K and buffer, Roche (cat.no. 3115836001)
pT7-gRNA, Addgene (plasmid no. 46759)
Secondary antibody anti-rabbit IgG (Alexa Fluor® 594), Thermo Fisher Scientific (cat.no. A-21207)
Sheep serum, Merck (cat.no. S3772)
T4 DNA ligase, NEB (cat.no. M0202)
TBE (1M Tris base, 1M boric acid, 0.02M EDTA)

TEMED, Fluka (cat.no. 87689)
Tris-Cl, Sigma (cat.no. 77-86-1)
tRNA, Roche (cat.no. 10109517001)
Tween 20, Sigma-Aldrich (cat.no. 9005-64-5)

Miniprep plasmid DNA isolation:
P1 buffer: 25mM TRIS, 10mM EDTA, 1% glucose
to 500ml - 10ml 0,5M EDTA
- 12,5ml 1M TRIS
- 4,5g glucose
P2 buffer: 0,2M NaOH, 1% SDS
to 200ml - 4ml 10M NaOH
- 20ml 10% SDS
P3 buffer: final conc. 5M Ac
to 500ml - 147,1g KAC
- 75ml HAC

5.1.1 Kits

QIAEX II Gel Extraction Kit, Qiagen (cat.no. 20021)
MEGAscript™ T7 Transcription Kit, Invitrogen (cat.no. AM1334)
Trizol, Thermofisher Scientific (cat.no. 15596026)

5.1.2 Primers, sgRNA and morpholinos (5´->3´)

Meis1aMO- CCAGATCCTCGTACCGTTGCGCCAT
Meis1bMO- TATATCTTCGTACCTCTGCGCCATC
FP1-CATGTCTTTGGACTTTGTGG
RP1-CATTAGCAACTACAGCAGGG
FP2-GCTATTAGTGACCAGGTCC
RP2-CTTACGATCAGGCTGAAATATC
M13 reverse-CAGGAAACAGCTATGAC
Tyrosinase sgRNA- 5´-UGACCUCCUGAAGACCCCCAAAAUCUCGAUCUUUAUCGUUCAAUUUUAUUCC
GAUCAGGCAAUAGUUGAACUUUUUCACCGUGGCUCAGCCACGC-3´

5.2 Equipment

Microinjector (FemtoJet 4i Eppendorf, 5252000013)
Microscope, Olympus SZX9 with camera, Olympus DP72
PCR cycler (Biometra TAdvanced, 2070211)
SKYSCAN 1272 High-Resolution Micro CT
Spectrophotometer, Nanodrop 1000
Zeiss Axiozoom.v16;Apotom 2

5.3 Biological material

Escherichia coli - TOP10 chemically competent cells
Zebrafish, wild-type AB strain

6 METHODS

CRISPR/ Cas9 system was used to generate Meis1a and Meis1b mutant zebrafish. The experiment included design of sgRNAs and their *in vitro* production with T7 RNA polymerase. The sgRNAs were altogether injected into 1-2 cell stage embryo. Injected embryos (F_0 generation) were after 6 weeks genotyped by using PCR and heteroduplex mobility assay (HMA). Selected F_0 fish were crossed to wild type fish to obtain heterozygotes with mutation in the target *locus*. Heterozygotes were crossed to each other to give rise to a generation with mutant fish. The generation containing mutants was genotyped and analysed by staining techniques including whole mount RNA *in situ* hybridization (WISH), Alcian Blue cartilage staining (ABS), immunohistochemical staining (IHC) and scanning with micro computed tomography (microCT). Phenotypes of mutant fish were compared to *meis1a* and *meis1b* morphants phenotypes.

6.1 CRISPR/Cas9 guide RNAs design

Homeobox regions of *meis1a* and *meis1b* have been analysed with online CRISPR target prediction program, CRISPOR (http://crispor.tefor.net/). Program has generated a map of potential single guide RNAs targets by criteria, such as GC content, predicted efficiency, specificity: score (calculated by previously stated criteria)/off-targets and probability of out-of-frame mutation, sgRNAs have been designed.

6.2 Cas9/sgRNA complex preparation and injection of zebrafish embryos

6.2.1 Annealing of complementary singe stranded oligonucleotides, coding for sgRNAs

Oligonucleotide were annealed in the PCR cycler under conditions in Tab.1. Reaction was prepared by mixing 5 µl of each complementary oligonucleotide, concentration of each oligonucleotide solution was 25µM.

Table 1: Complementary single stranded oligonucleotides annealing program.

Temperature	Time
95 °C	5 min
cool down to 25 °C	decrease by 5 °C every 1 minute
4 °C	hold

6.2.2 Cloning of prepared double stranded oligonucleotides into the pT7 vector

Vector pT7 was linearized with restriction endonuclease (RE) BsmBI at conditions described in Tab.2. The reaction was incubated in the cycler for 1 hour at 55 °C, and was stopped by incubation at 80°C for 20 min. The digested vector was purified with agarose gel electrophoresis. The digestion mixture was mixed with 6 µl 6x Loading Dye and pipetted into well, GeneRuler^{TM} 100 bp Plus DNA Ladder was used as a molecular-length size marker. Electrophoretic separation ran in 1% agarose gel with 1xTAE buffer, and lasted 30 min. After separation, a band with digested vector was dissected from the gel. The piece of gel

was melted, and DNA extracted by using *QIAquick Gel Extraction Kit (QIAGEN)*. The ligation reaction of the linearized vector and the annealed oligonucleotides was performed at conditions as shown in Tab.3 and incubated in room temperature (RT) for 1 hour.

Table 2: Reaction mixture for pT7 vector digestion by BsmBI enzyme.

Reagent	Volume [µ]
pT7 vector (0.8 µg/µl)	2
10x NEBuffer™ 3.1	3
BsmBI RE (10 000 U/ml)	1
water (deionized and nuclease free)	24

Table 3: Reaction mixture for cloning of oligonucleotides in pT7 vector.

Reagent	Volume [µl]
pT7 vector (linearized)	1
10x T4 DNA Ligase Reaction Buffer	1
T4 DNA ligase	0,5
Hybridized oligonucleotides	1
water (deionized and nuclease free)	6,5

6.2.3 Transformation of chemically competent bacteria and plasmid DNA isolation

The ligation reaction was used for transformation of bacteria (TOP 10 strain) according to Protocol 1. The vector was isolated from transformed bacteria by Protocol 2.

Protocol 1, Transformation of chemically competent bacteria:

1. Unfreeze a bacteria aliquot on ice.
2. Add whole volume of the ligation reaction to a bacteria suspension and mix with pipette tip.
3. Incubate on ice for 30 min.
4. Do a heat-shock transformation by putting a tube with bacteria suspension in a heat block, warmed up to 42°C for 40 s.
5. Put the tube back on ice, add 200 µl of LB medium and place the tube in a shaking heat block, incubate for 1 hour at 37°C, horizontally shaking (250 rpm).
6. Apply the bacteria suspension on a Petri's dish with agar and antibiotics (Ampicilin/Amp) for cultivation.
7. Cultivate the Petri's dish bottom up, overnight (13-16 h) at 37 °C.
8. Liquid culture: Prepare a cultivation tube and fill it with 2 ml of LB medium with 2 µl antibiotics (Amp,50ng/µl). Pick up a single bacteria colony by a pipette tip and throw the tip into prepared cultivation tube, cultivate at 37°C, for 13-16h, vertically shaking (250 rpm).

The plasmid vector was isolated from the liquid culture by following Protocol 2.

Protocol 2, Isolation of plasmid DNA from bacteria liquid culture:

1. Pipette 1,5ml of liquid culture into 1,5ml tube.
2. Centrifuge for 5 min, 5 000 rpm.
3. Discard supernatant a resuspend pellet in 300µl of P1 solution.

4. Add 300µl of P2 solution and mix by inverting the tube, incubate 5 min at RT, then add P3 solution, mix by inverting the tube and incubate 5 min at RT.
5. Centrifuge for 10 min, 13 000 rpm, at 4 °C.
6. Meanwhile, prepare a new 1,5ml tube for each sample and pipette 600 µl of isopropanol into prepared tubes. Pipette a supernatant from centrifuged samples into tubes with isopropanol and mix by vortexing.
7. Centrifuge for 10 min, use 13 000 rpm at 4 °C.
8. Discard a supernatant and wash a pellet in 75% ethanol.
9. Centrifuge for 3 min with 13 000 rpm, discard the supernatant, and dry the pellet by leaving the tube with pellet at RT for approx. 15 min.
10. Resuspend dried pellet in 20µl of DEPC water.

6.2.4 Verification of the insert presence with sequencing and *in vitro* transcription

The insertion of the oligonucleotides into pT7 vector, coding for gRNAs, was analysed with Sanger sequencing using M13 reverse primer. Sequencing reaction was prepared by requirements of A Eurofins Genomics Company/GATC Biotech (www.eurofinsgenomics.eu). Samples of vector, containing inserts of interest, were linearized with BamHI RE at conditions specified in Tab.4. The reaction was incubated for 2 hours at 37 °C. The product of linearization was purified via electrophoretic separation and subsequent extraction from the gel with *Qiagen Sephadex Gel Extraction Kit*. Next step was *in vitro* transcription of linearized pT7 plasmid at conditions specified in Tab. 5, the reaction was incubated for 2 hours at 37°C. The products of transcription were purified by using *Trizol Reagent* and by following *Trizol Reagent* user guide (Pub. No. MAN0001271).

Table 4: Reaction mixture for selected plasmids linearization.

Reagent	Volume [µl]
BamHI (20 000U/ml)	2
10X NEBuffer™ 3.1	4
pT7 plasmid (1000 ng/ µl)	5
water (deionized and nuclease free)	29

Table 5: Reaction mixture for in vitro transcription of pT7 plasmid.

Reagent	Volume [µl]
T7 enzyme mix	2
10X T7 reaction buffer	2
T7 ATP (75 mM)	2
T7 CTP (75mM)	2
T7 GTP (75 mM)	2
T7 UTP (75 mM)	2
linearized pT7 plasmid (100 ng/µl)	8

6.2.5 Injection of zebrafish egg with gene editing mixture

1-2 cell stage embryos were injected with 5-10nl of CRISPR cocktail (Tab.6), each *meis1* gene was targeted separately. All components of the cocktail are listed in Tab 6. The

mixture was prepared on ice, and then incubated for 3 min at 37°C. As a control was used mixture with sgRNA targeting gene, coding for tyrosinase (Materials, 5.1.2), an enzyme essential for pigment biosynthesis, to assess the Cas9 activity.

Table 6: Components of injection mixture editing meis1a and meis1b genes.

Reagent	Volume [µl]
Cas9 (1000 ng/µl)	2
sgRNA (500 ng/µl)	0.6
KCl (2M)	0.5
10X NEBuffer™ 3.1	0.5
Phenol Red Dye	0.5
water (deionized nuclease/RNase free)	0.9

6.3 F_0 and F_1 generation genotyping and analysis of mutant phenotype

At the age of 6 weeks, injected (F_0) fish were genotyped by using PCR and set of primers FP1, RP1 (*meis1a* locus) and FP2 and RP2 (*meis1b* locus), each locus was amplified separately. PCR products were analysed with heteroduplex mobility assay (HMA). Potential founder fish were selected and crossed to wild type fish to generate F1 generation. F1 heterozygotes were analysed with PCR, using the same set of primers as previously, native PAGE and sequenced by A Eurofins Genomics Company. Heterozygous fish with frame shifting mutation in *meis1* loci, were crossed to each other to give rise to homozygotes. Phenotype of *meis1* mutants was assessed with WISH, ABS, IHC and microCT imaging.

6.3.1 Genotyping of a F_0 and F_1 generation

A part of tail fin of 6 weeks old fish was cut and processed by proteinase K. Produced lysate was used as DNA template for amplification. PCR reaction was prepared and set by Tab.7 and Tab.8, respectively. PCR product separation was performed in polyacrylamide gel (40% acrylamide/bis-acrylamide, 29:1), in 1X TBE buffer for 1 hour at 80V. Three fish and one wt fish from F0 generation, and all found heterozygotes were sequenced. The result of sequencing was analysed with CRISP-ID, online open-access software that is able to detect indels in raw sequencing data.

Table 7: Reaction mixture for genotyping PCR.

Reagent	Volume [µl]
2X DreamTaq PCR Master Mix	10
DNA template	2
FP1(meis1a) or FP2(meis1b)	1
RP1(meis1a) or RP2(meis1b	1
water (deionized and nuclease free)	6

Table 8: Genotyping PCR program profile of meis1a and meis1b loci amplification.

Temperature	Time	
95°C	5:00	
95°C	1:00	35X
61.2°C (*meis1a*)/60°C (*meis1b*)	0:30	
72°C	0:30	
72°C	5:00	
12°C	∞	

6.3.2 *In vitro* fertilization

Due to health problems and inability to reproduce of one F_1 mutant fish, with large deletion in exon 8 of *meis1a* gene (fish 27), *in vitro* fertilization (IVF) had to be performed. The procedure was done by following protocols from manual available on zebrafish.org, ZIRC E400/RMMB SPERM CRYOPRESERVATION & IVF PROTOCOL by J. Matthews, J. Murphy, C. Carmichael and Z. Varga (v.1.2, 07/01/2017 JLM) protocols 1.8 (Protocol for Collecting Sperm by Testis Dissection) and 4 (Introduction to Sperm Thawing and *In Vitro* Fertilization)

6.3.3 Analysis of mutant and morphant phenotype

To analyse mutant and morphant phenotype four techniques were used: whole mount *in situ* RNA hybridization of NCC specifiers (Protocol 3, adapted from https://wiki.zfin.org/display/prot/Thisse+Lab+-+In+Situ+Hybridization+Protocol+-+2010+update), Alcian Blue Staining for craniofacial cartilage (Protocol 4), Immunohistochemical staining (Protocol 5) and MicroCT imaging to prove whether the technique can be apply to assess morphological changes in mutant fish.

Protocol 3, Whole mount in situ mRNA hybridization:

1) Dechorionation: Place 24 hpf embryos in Petri´s dish and remove water. Pour 50 µl Pronase (warmed to 28 °C) into the dish and incubate for 5 min. Gently wash eggs 3 times with E3 water and remove digested chorions. Then, incubate embryos in the Petri´s dish at 28,5 °C until desired developmental stage.
2) Fixation: Fix dechorionated embryos in 4% (wt/vol) paraformaldehyde with 1X PBS overnight at 4°C.

Day 1

3) Dehydration of the embryos:

   PBS …2 x 5 min

   25% MeOH/PBS …5 min

   50% MeOH/PBS …5 min

   75% MeOH/PBS …5 min

   100% MeOH/PBS…5 min

4) Rehydration:

   75% MeOH/PBS …5 min

50% MeOH/PBS …5 min

25% MeOH/PBS …5 min

PBS …4 x 5 min

5) Proteinase treatment: Pipette 500 µl of proteinase K solution (Proteinase K in PBT,1:1000), 24hpf embryos incubate for 10 min.

6) Refix samples in 4% PFA, 800µl/sample, for 20 min at RT, then wash the samples in PBT 5 times for 5 min at RT.

7) Prehybridization: Prepare Hybe$^+$ solution by Tab. 9. Do not mix Hybe$^+$ at once, take 8 ml of Hybe$^-$ solution and mix it with 8µl Heparin and 400 µl tRNA. Use 500 µl of the prepared Hybe$^+$ per sample and prehybridize samples at 70°C, for 2 hours, do not shake.

Table 9: The composition of Hybe$^+$ solution.

Reagents	Volume [ml]	Final solution
Formamide	25	50% formamide
20X SSC	12.5	5X SSC
Herparin (100 ng/ml)	0.5	50 µg/ml
tRNA (10 mg/ml)	0.5	500 µg/ml
Tween 20 (20%)	0.25	0.1%
Citric acid (1M, pH 6)	0.46	pH 6
H_2O	to 50 ml	

Note: Hybe$^-$: Hybe$^+$ without tRNA and heparin

8) Hybridization: Denaturate probe in a PCR cycler at 80°C for 5 min and then place the probe on ice. Dilute probe 1:250 in pre-heated Hybe$^+$ at 70°C and apply 500 µl of hybridization solution on samples. Incubate hybridization reaction over night at 70°C.

Day 2

9) Wash:
   a) 1x quickly in Hybe$^-$ 70°C
   b) 75% Hybe$^-$ /25% 2X SSC … 15 min/70°C
   c) 50% Hybe$^-$ /50% 2X SSC … 15 min/70°C
   d) 25% Hybe$^-$ /75% 2X SSC … 15 min/70°C
   e) 100% 2X SSC … 15 min/70°C
   f) 100% 0.2X SSC … 2 x 30 min/70°C
   g) 75% 0.2X SSC/25% PBT … 10 min/RT
   h) 50% 0.2X SSC/50% PBT … 10 min/RT
   i) 25% 0.2X SSC/75% PBT … 10 min/RT
   j) PBT (PBS + Tween)

10) Blocking: Mix a blocking solution by Tab. 10. Use 500 µl of blocking solution per sample and incubate for 3 hours at RT with agitation.

Table 10: The composition of blocking solution.

Reagent	Volume [µl]
Sheep serum (50X)	20
BSA (100mg/ml,50X)	20
Levamisol (1M, 1000X)	1
PBT	959
Total volume	1 ml

11) Dilute anti-DIG Alkaline Phosphatase in blocking solution (1:3000) and treat samples with the solution and incubate O/N at 4°C agitating.

Day 3

12) Wash the samples in PBT 6 times for 15 min.

13) Staining: Prepare AP buffer according to Tab. 11. Wash the samples in 1 ml of AP buffer 3 times for 5 min. After 2nd wash transfer samples into 12-well plate and do 3rd wash. Then, remove AP buffer and add NBT/BCIP solution (50X stock), 600 µl per sample and incubate in dark at RT. Check every approx. 15 min if the samples are stained enough.

Table 11: The composition of AP buffer.

Reagent	Volume [ml]	Final concentration
Tris HCl (1M, pH 9.5)	10	100 mM
$MgCl_2$ (1M)	5	50 mM
NaCl (5M)	2	100 mM
Tween 20 (20%)	0.5	0,1%
H_2O	to 100	-

14) Wash: Prepare stop solution by mixing 1X PBS and EDTA (1mM) and wash the samples by 1 ml of stop solution twice for 5 min. Place the samples to 100% MetOH or 4% PFA for few minutes to clear out background and rinse the samples in methylcellulose. High density of methylcellulose enables better manipulation with the samples while analysing the result of staining.

Protocol 4, Alcian Blue cartilage staining:

1) Fixing embryos (5 dpf) with 96% ethanol for 1 day.
2) Staining: Completely immerse the sample in a solution of 0.1% Alcian Blue (7:3 absolute ethanol: acid acetic anhydride) O/N.
3) Rehydration: Place the sample in the bath 95% ethanol, twice for 15 min. After, place each sample in gradually decreasing baths 75%, 40% and 15% ethanol, 5 min for each solution.
4) Wash: Immerse the sample in several changes of distilled water 3 times for 5 min.
5) Depigmentation: Place samples in solution of 1% H_2O_2 and 1% KOH until the pigment is bleached.
6) Clearing: Leave the samples in 1% potassium hydroxide until the skeletal system of the embryo is exposed.
7) Treat the samples with ascending series of glycerol in 1% potassium hydroxide, 15 min for each step (first step is 1% KOH and 25% glycerol). The ascending series: 1%KOH; 1% and 25% glycerol; 1% KOH and 50% glycerol; 1% KOH and 75% glycerol; 100% glycerol (storage).
8) Place the sample in pure glycerol for permanent storage.

Fish generated by crossing F2 heterozygous fish were immunohistochemically stained with rabbit antibody (Ab) to the mouse Meis1 protein (Ab binds first 16 aa of mouse Meis1 protein) and Goat polyclonal Secondary antibody anti-rabbit IgG (Alexa Fluor® 594). Images were taken with Zeiss Axiozoom v.16 with Apotom 2 analysed by ZEN program.

Protocol 5: The zebrafish whole mount immunohistochemistry

1. Dechorionate embryos by using Pronase, 5 min at 28 °C and fix 24 hpf embryos in 4% PFA.
2. Place approximately 25 embryos in a micro tube and rock 1,5 hours at RT.
3. Rinse embryos 3 X in 1 ml PBST at RT for 5 min shaking. Remove 1X PBST.

4. Add 1 ml methanol, invert to mix and let embryos settle to the bottom. Remove methanol and replace with fresh methanol, incubate O/N at -20 °C.
5. Store in methanol at -20 °C until ready to use or rehydrate in gradual MeOH/1X PBST progression: 95% MeOH, 75% MeOH, 50% MeOH, and 25% MeOH in 1X PBST.
6. Wash 4 X 5 min in 1 ml 1X PBST.
7. Permeabilize embryos in 1 ml ice-cold acetone (-20 °C) for 8 min.
8. Wash 4 X 5 min in 1 ml 1X PBST.
9. Incubate embryos in 1 ml block (10% BSA/PBS) for 3-4 hours.
10. Remove block and add primary antibody in block solution (1:500).
11. Incubate O/N with gentle rocking at 4 °C.
12. Wash embryos 5 X 5 min in 1ml block solution at RT.
13. Add secondary fluorescent antibody (1:750).
14. Wrap in foil and incubate for 2,5 hours at RT with gentle rocking.
15. Wash embryos 5 X 5 min in 1 ml 1X PBST.

6.4 Morpholino based knock-down of *meis1a* and *meis1b* genes

Zebrafish eggs were injected with morpholinos targeting start codon of *meis1* mRNAs. Each *meis1* (*meis1a* and *meis1b*) gene was knocked down (KD) separately. Injection mixture was prepared by Tab. 12. Generated phenotypes were evaluated by using WISH of NCC specifiers (*foxD3* and *dlx1a*; Protocol 3), and Alcian Blue staining for cartilage (Protocol 4).

Table 12: The composition of morpholino cocktail for single gene knock-down.

Reagent	Volume [µl]
Morpholino oligonucleotide (100 mM)	1
Phenol Red (0.5%)	1
water (deionized and nuclease free)	8

6.5 Sample preparation for Microcomputed Tomography Imaging

The microCT imaging was mediated by Czech Center for Phenogenomics, IMG. Wild type and mutant fish were fixed for 5 days in 4% PFA, then rinsed for 14 days in 1% PTA and then for 2 days in 25% Lugol solution. Then fish were embedded in agarose gel and scanned with SKYSCAN 1272 High-Resolution Micro CT, Bruker.

7 RESULTS

7.1 Designed guide RNAs and their synthesis

The most optimal target sequence for editing with Cas9 protein were found (Tab.13 and Tab.14). To navigate Cas9 protein to target *loci* specific sgRNAs were designed (Tab.15). Oligonucleotides coding for sgRNAs (sgDNA) were ordered, inserted into pT7 vector and transcribed. The preparation of vector with specific insert included linearization of the vector (Fig.19), insertion of sgDNA and linearization before *in vitro* transcription (Fig.22), the oligonucleotides are shown at Tab. 16. The single guide RNA consists of unique 20 ribonucleotides (crRNA, Tab. 15) at the 5´end and universal downstream part, tracrRNA that serves for the formation of optimal secondary RNA structure to interact with Cas9 protein. The target sequences are in the exon 8 of both *meis1* genes, in both cases the exon 8 is a part of gene, coding for DNA binding domain (Fig. 18), therefore this part was picked to abrogate the ability of transcription factor to bind DNA. All used sequences were found in the zebrafish genome (alignment GRCz11) and annotated according to *ensembl.org*.

The complementary sgDNA oligonucleotides were hybridized and cloned in pT7-sgRNA vector. Sanger sequencing proved an insertion of oligonucleotides into the vector (Fig.20 and 21). After, the presence of needed insert in the vector was proven, the vector was used for *in vitro* transcription. Agarose gel electrophoresis of sgRNAs showed a good quality of transcribed sgRNAs, but also showed a formation of sgRNAs dimers (Fig.23) therefore sgRNAs had to be denaturate and slowly renaturated to form only monomers.

Table 13: meis1a target sequences of splice variants 201 and 204.

No.	Target sequence (5´->3´)
8a	CAGAGACGTGTTTTACCGTGAGG
9a	CAGCCATGCTCTCATGATATTGG
10a	CAACCAATATCATGAGAGCATGG

PAM sequence in red

Table 14: meis1b target sequences of splice variants 201 and 203.

No.	Target sequence (5´->3´)
1b	ACGCGGAATCTTTCCTAAAGTGG
2b	AGATGATGACGACCCTGACAAGG
3b	AGTGTGGCATCACCTAGCACAGG

PAM sequence in red

Table 15: sgRNAs navigating Cas9 to homeobox sequence of meis1a and meis1b gene.

No.	guide RNA (5´->3´)
8a	CAGAGACGUGUUUUACCGUG*
9a	CAGCCAUGCUCUCAUGAUAU*
10a	CAACCAAUAUCAUGAGAGCA*
1b	ACGCGGAAUCUUUCCUAAAG*
2b	AGATGATGACGACCCTGACA*
3b	AGTGTGGCATCACCTAGCAC*

*tracrRNA–5´ AAATCTCGATCTTTATCGTTCAATTTTATTCCGATCAGGCAATAGTTGAACTTTTTCACCGTGGCTCAGCCACGCCTAG

Table 16: Complementary oligonucleotides coding for sgRNA targeted on meis1a and meis1b genes.

No.	Forward	Reverse
8a	TAGGCAGAGACGTGTTTTACCGTG	AAACCACGGTAAAACACGTCTCTG
9a	TAGGCAGCCATGCTCTCATGATAT	AAACATATCATGAGAGCATGGCTG
10a	TAGGCAACCAATATCATGAGAGCA	AAACTGCTCTCATGATATTGGTTG
1b	TAGGACGCGGAATCTTTCCTAAAG	AAACCTTTAGGAAAGATTCCGCGT
2b	TAGGAGATGATGACGACCCTGACA	AAACTGTCAGGGTCGTCATCATCT
3b	TAGGAGTGTGGCATCACCTAGCAC	AAACGTGCTAGGTGATGCCACACT

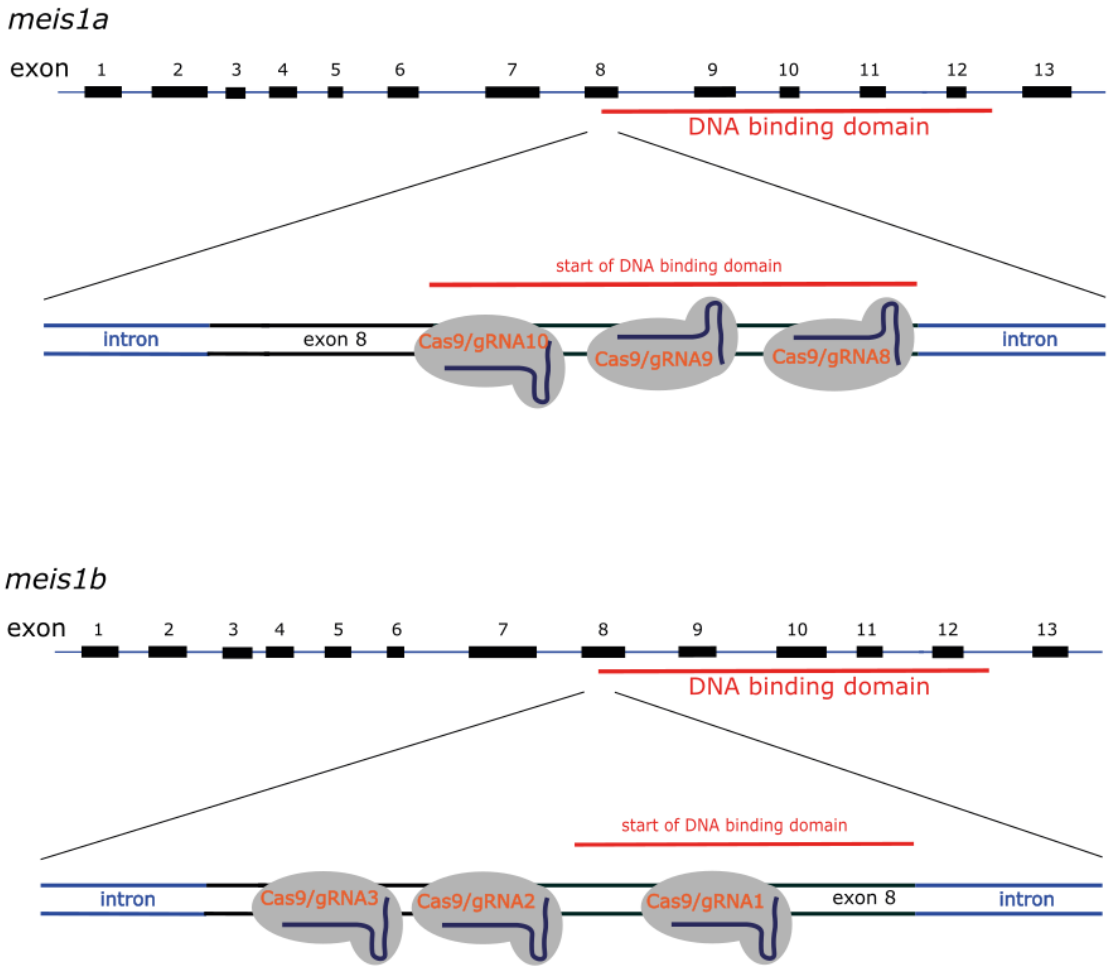

Figure 18: Binding of Cas9/sgRNA complexes in exon 8 of meis1 genes. meis1a (splice variant 201), orientation of target sequences in meis1a gene that are common for splice variants 201 and 204; meis1b (splice variant 201), orientation of target sequences in meis1b gene that are common for splice variants 201 and 203. Cas9/gRNA complexes 9 and 8 interact with meis1 gene coding strand, and complexes 10, 3, 2 and 1 with non-coding strand.

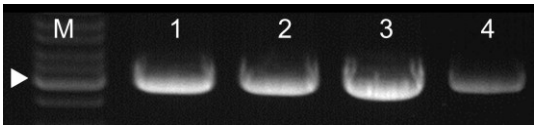

Figure 19: Agarose gel electrophoretogram linearized pT7 plasmid with BsmBI restriction endonuclease. Four clones of pT7 plasmid linearized with BsmBI. Arrow marks 3000 bp long DNA fragment of the marker.

Figure 20: Chromatograms showing the results of the pT7 vector sequencing to check a presence of needed insert

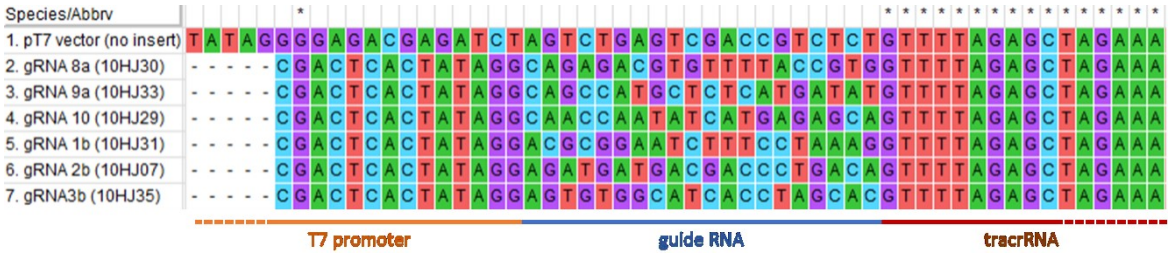

Figure 21: Alignment of the sequences generated by Sanger sequencing of pT7 vector

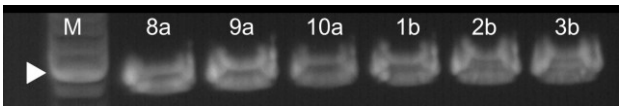

Figure 22: Agarose gel electrophoretogram pT7 plasmid, containing sgDNA insert, linearized with BamHI restriction endonuclease. Arrow marks 3000 bp long DNA fragment of the marker.

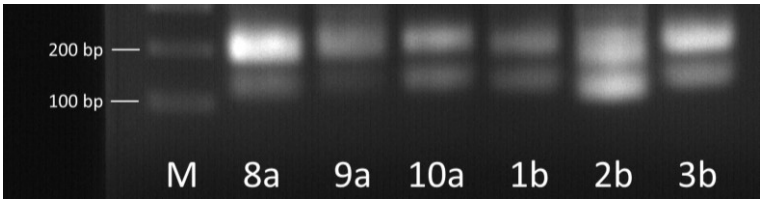

Figure 23: Agarose gel electrophoretogram showing the separation of transcribed sgRNAs

7.2 Genotype of F_0 and F_1 generation

Genotyping of F_0 generation revealed that almost a half of injected fish with editing complexes targeting *meis1a* and *meis1b* genes, were mosaics (Tab.17, Fig. 24 and 26). The fish whose sample showed presence of heteroduplexes was selected for following crossing to wild type fish. Some heteroduplex-positive samples were picked for sequencing to analyse occurrence of mutation in *locus* of interest (Fig. 25). The sequence analysis of *meis1a* locus showed that the most active Cas9/sgRNA complex is complex with sgRNA 8a (Fig.25).

The comparison of uninjected fish (wt), injected fish with Cas9/sgRNA complex targeting *meis1a* locus (meis1a mut) and complex cleaving the tyrosinase gene showed change in pigmentation pattern of the fish injected with tyrosinase gene editing cocktail. The test of Cas9 activity confirmed ability of Cas9 to form complex with sgRNA, cleave sequence of interest and generate and potentially introduce frame shifting mutation to the locus, causing change in phenotype as shown in Fig. 27. The pigmentation pattern of F_0 *meis1b* mutant fish was not changed (not shown).

Crossing of F_0 fish (*meis1a* and *meis1b* mutants) to wild type fish gave a rise to F_1 generation. Among the F_1 generation, several heterozygotes were identified in both studied *loci* with native PAGE as shown in Fig. 28 and Fig. 29. Potentially heterozygous samples were sequenced and analysed with CRISP-ID software. The results of sequencing are listed in Fig. 30A and 30B. In *meis1a* locus, analysed sequences were mostly changed with small deletions (3-10 bp) but also large deletions were detected (Fig. 30A). Despite the low number of heterozygous fish bearing mutation in *meis1b* locus, most of mutation were large (Fig. 30B) and frame shifting (Fig. 31D). For further work two fish with different and easily to genotype mutation were picked to establish mutant lines.

In case of *meis1a* mutants, fish 9, 10, 12 and 27 (Fig. 30A) were selected for establishment of mutant lines. For the same purpose, fish 26 and 54 were used for *meis1b* mutant line (Fig. 30B). As shown in electrophoretogram in Fig. 32 establishment of *meis1a* mutant line with 37 bp deletion was successful. The only complication while establishing second mutant line with 270 bp deletion was inability of fish 27 (Fig. 30A) to reproduce on its own due to health problems. The reproduction was mediated by using IVF. The obtained generation, involving 32 fish, has not been genotyped yet due to small size of the fish. In contrast, *meis1b* mutants had no difficulty with reproduction, therefore two heterozygous mutant lines were established (Fig. 33 and 34).

Efficiency of mutagenesis and frequency of mutation transfer to the subsequent generation was quantified in Tab.17. The data shows that 37.6% of injected meis1a F0 mutant and 52.8% *meis1b* F0 fish were mutated but number of transferred mutations to the next generation did not exceed ten in both studied genes. The sequence analysis of F1 meis1a mutant revealed that only 7 out of 10 analysed fish have some frame shifting mutation, despite the low number of F1 *meis1b* mutants all mutated fish had frame shifting mutation in the *locus*.

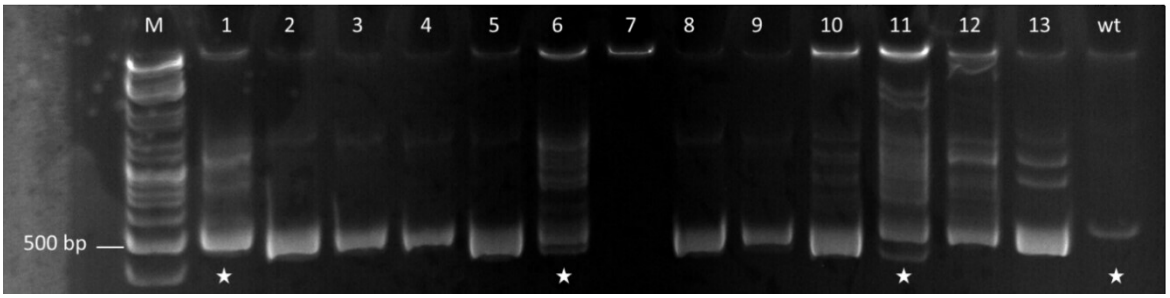

Figure 24: Genotyping F_0 generation with heteroduplex mobility assay of meis1a locus. Heteroduplexes were detected in samples 1, 2, 4, 6, 7, 9, 10 and 11. The results indicate that analysed fish are mosaics. These fish were chosen for following crossing. Samples marked with asterisk were sequenced, analysed sequences are shown in Fig.12

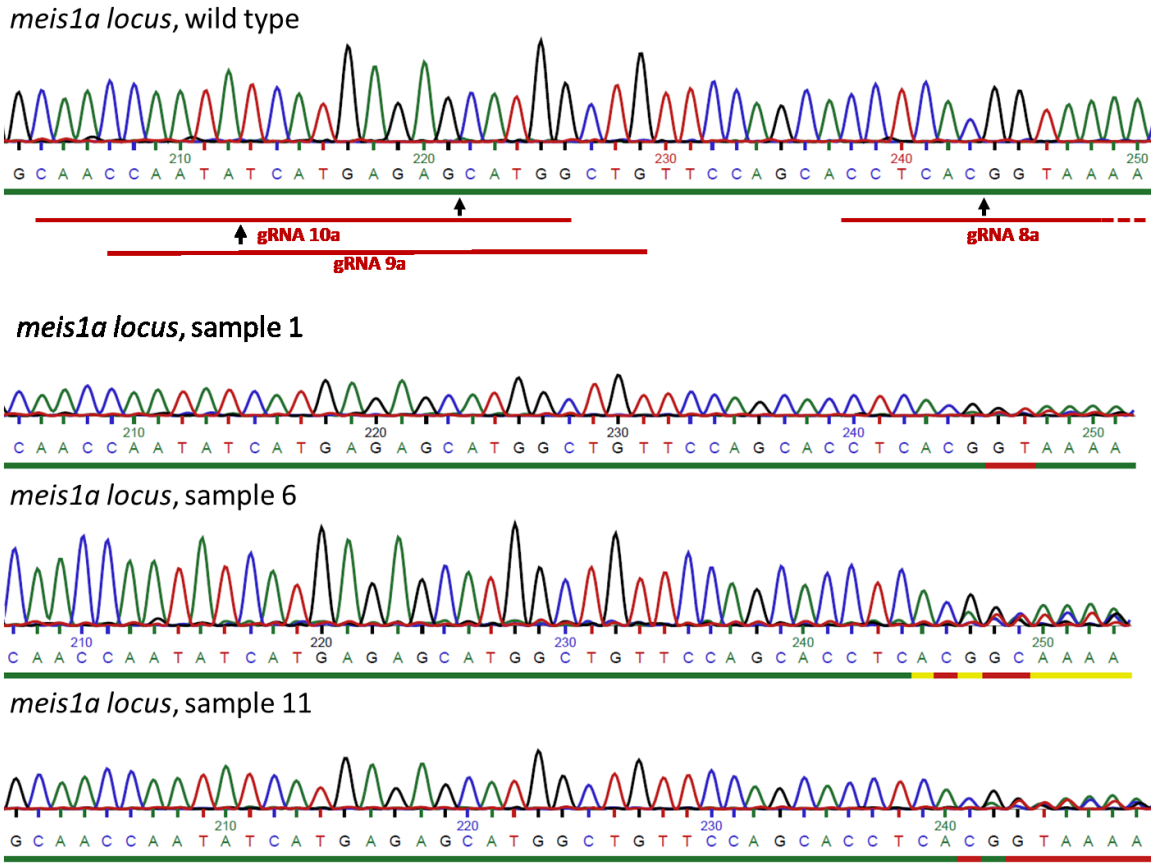

Figure 25: The results of sequence analysis of meis1a locus in selected samples. The only active Cas9/sgRNA complex appears to be Cas9/sgRNA 8a complex. Red line shows the position in which given Cas9/sgRNA complex interacts with DNA, arrows mark the site of perspective DSB. The line below sequences indicates the quality of sequence reading, red = low quality; yellow = medium quality, green = high quality.

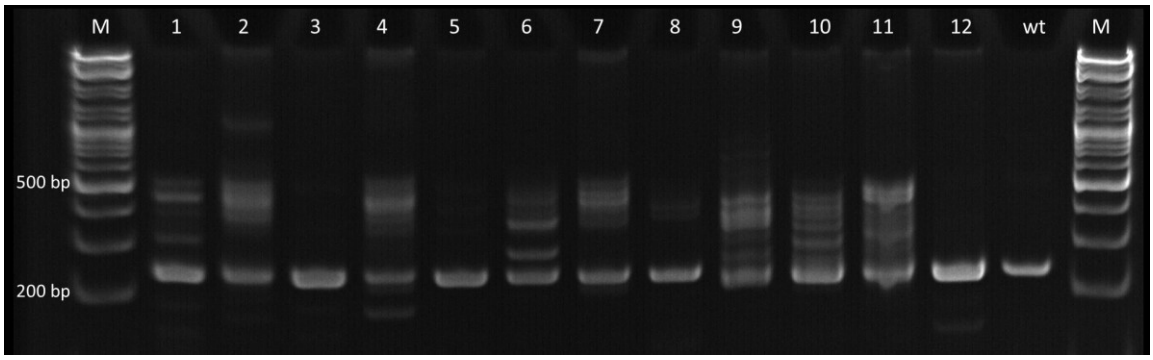

Figure 26: Genotyping F_0 generation with heteroduplex mobility assay of meis1b locus. Heteroduplexes were detected in samples 1, 6, 10, 11, 12 and 13. The results indicate that analysed fish are mosaics. These fish were chosen for following crossing. F_0 meis1b mutants were not sequenced.

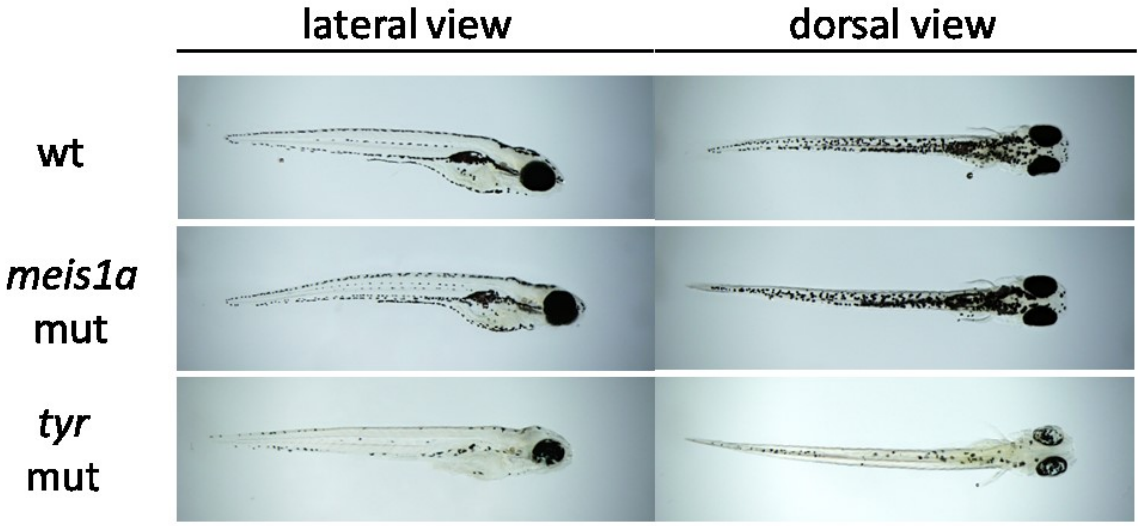

Figure 27: Injected fish with meis1a and tyrosinase gene editing mixture, and uninjected wild type control. (wt) wild type, (meis1a mut) meis1a fish showed no change in pigmentation pattern or morphology. In contrast, the fish injected with Cas9 and sgRNA targeting tyrosinase gene (tyr mut) showed a significant change in pigmentation.

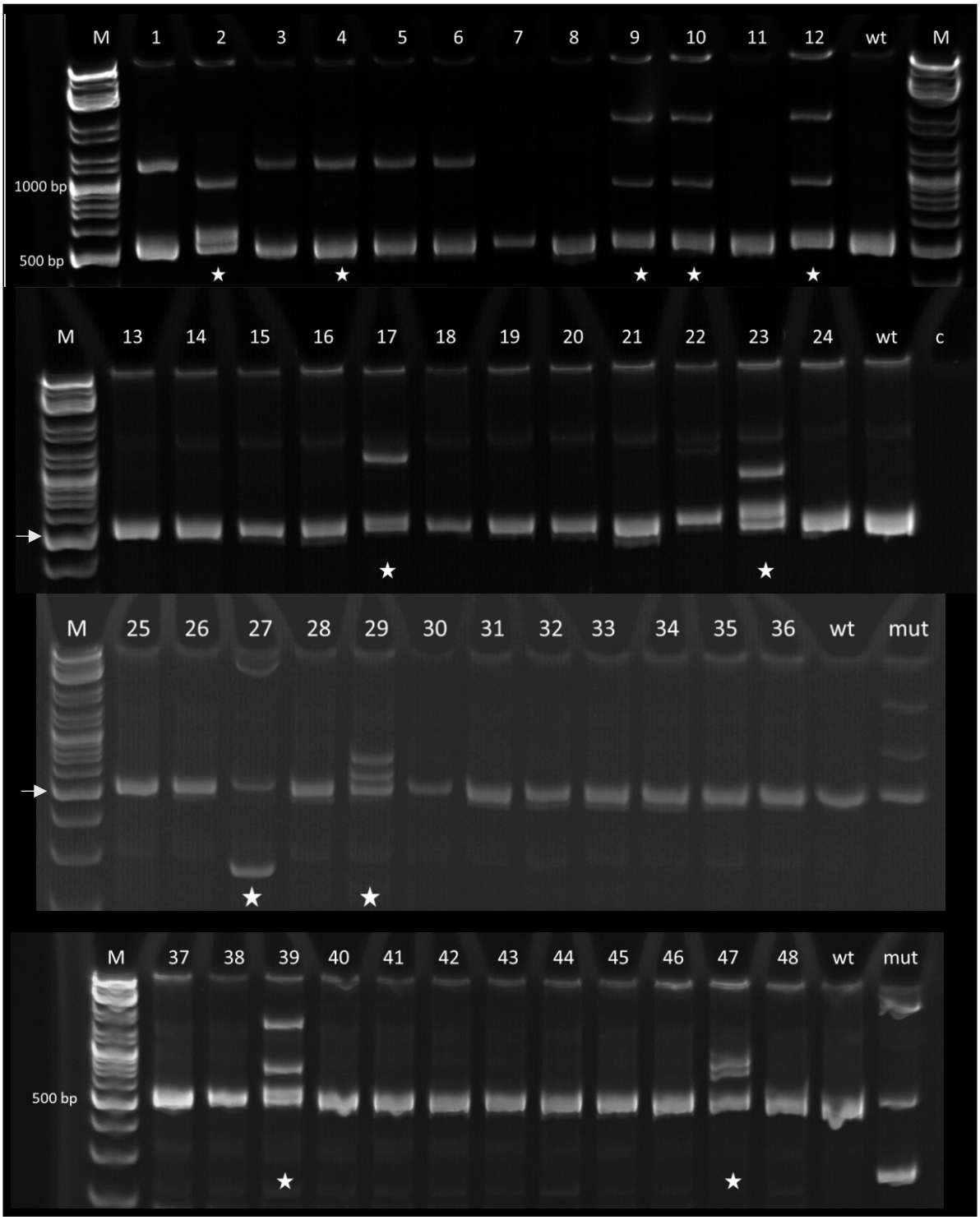

Figure 28: Polyacrylamide gel electrophoresis analysis of meis1a locus and detected heterozygotes in F_1 generation. Only 10 heterozygous fish were found. Fish with distinct mutations were selected for sequencing. Asterisk marks sequenced sample, the sequence is listed in the Fig. 30A, the arrow corresponds to 500 bp long DNA fragment of the marker (M).

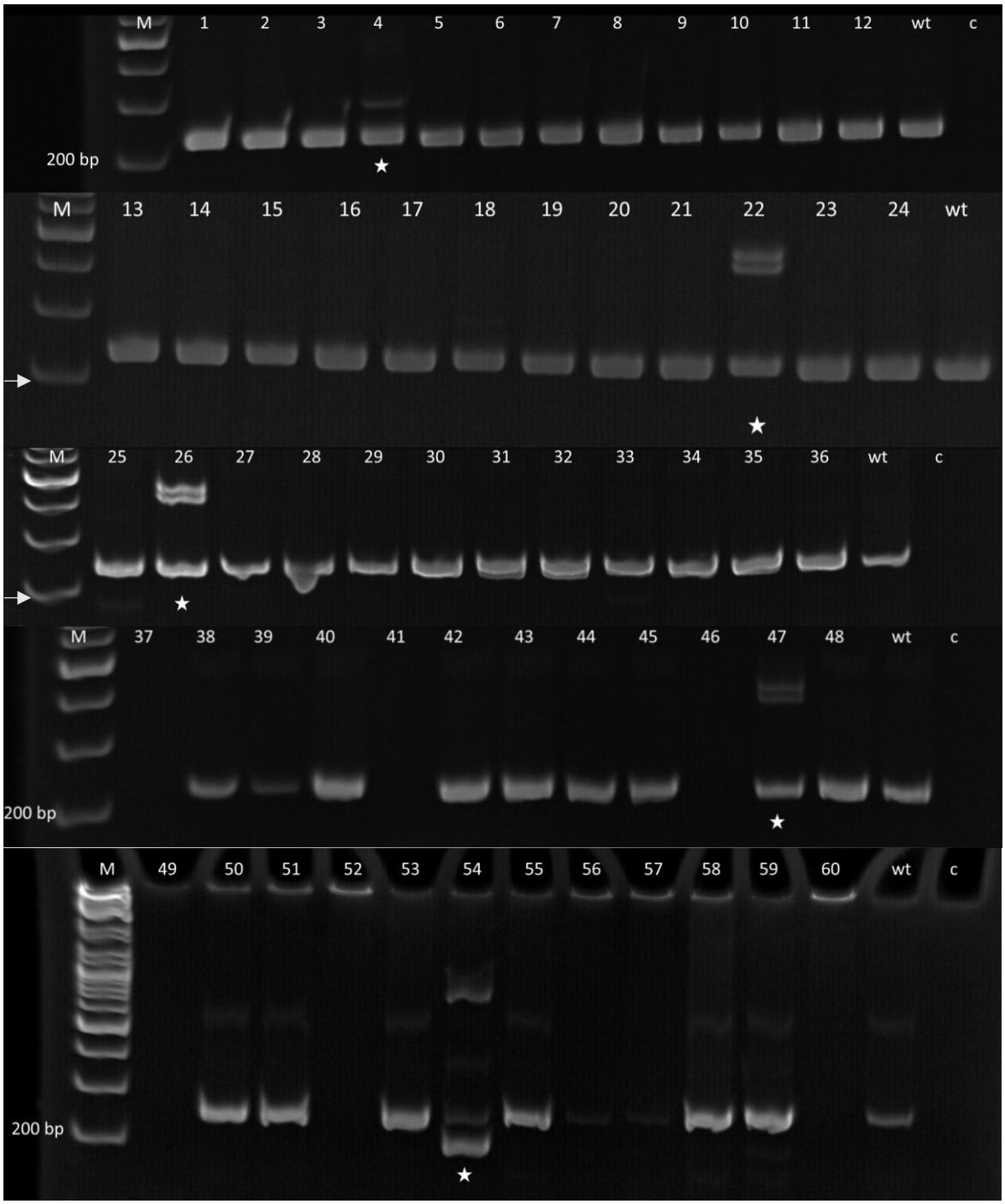

Figure 29: Polyacrylamide gel electrophoresis analysis of meis1b locus and detected heterozygotes in F_1 generation. Four heterozygotes were found and each one of them was sequenced. Asterisk marks sequenced sample, the sequence is listed in the Fig. 30B, the arrow corresponds to 200 bp long DNA fragment of the marker (M).

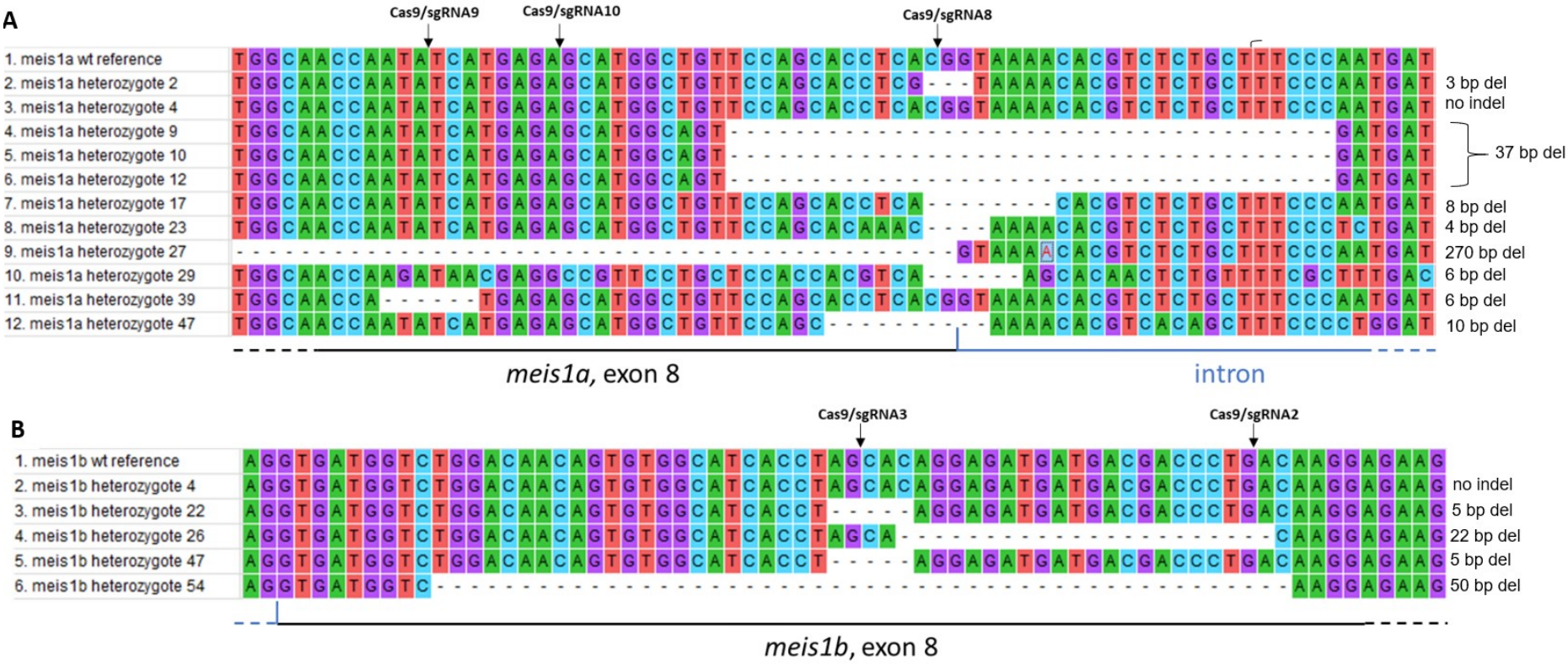

Figure 30: Mutated alleles of heterozygotes and wild type (reference) sequence alignment. Listed sequences represent mutated alleles of heterozygotes marked with asterisk in Fig.28 and 29. (A) meis1a locus: 7 out of 10 analysed alleles contained a frame shifting mutation, fish with 37 bp (samples 9, 10, 12) and 270 bp (missing whole exon 8) deletion were picked for further crossing. (B) meis1b locus: All analysed heterozygotes contained a frame shifting mutation, but only fish with 22 bp (sample 26) and 50 bp (sample 54) deletions were picked for further crossing. A dash symbolizes missing base, a black line marks exon region, a blue line marks intron region, arrows mark expected sites of cleavage.

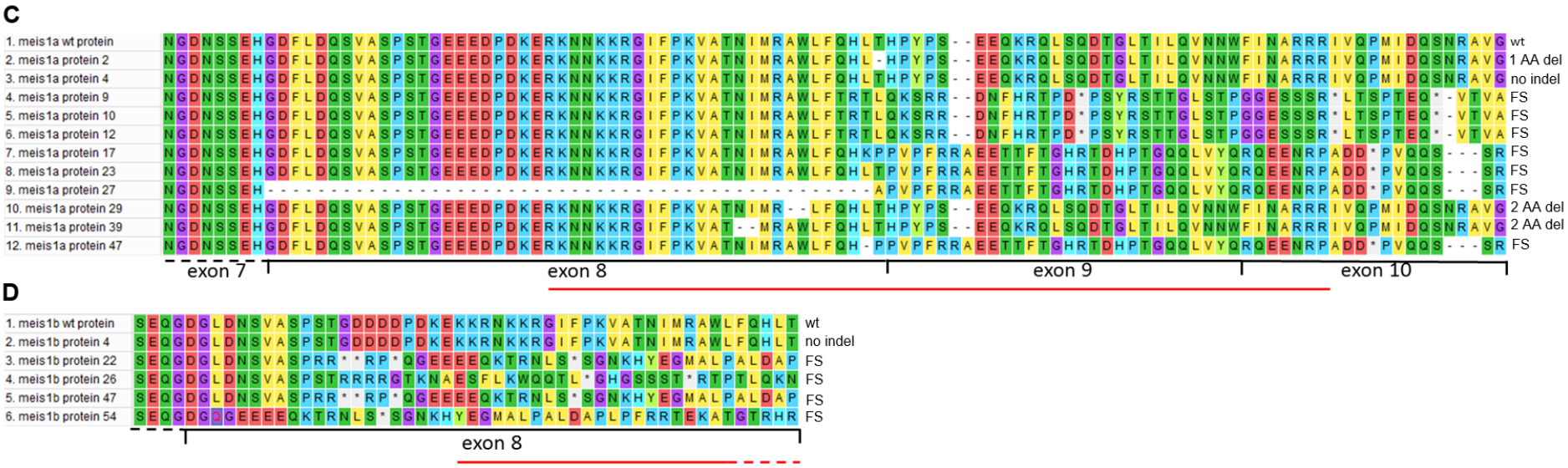

Figure 31: Alignment of protein sequences encoded by mutated alleles in homozygotes and wild type fish. Listed sequences represent products of mutated alleles listed in Fig.30,(C) Meis1a protein: alignment of predicted products of the mutated gene, DNA sequences predict production of impaired proteins of samples 9, 10, 12 , 17, 23, 27 and 47. (D) Meis1b protein: alignment of predicted products of the mutated gene DNA sequences predict production of impaired proteins of samples 22, 26, 47 and 54. A dash symbolizes missing amino acid, asterisk stands for a stop codon, the black line marks exon region and the red line marks homeodomain, FS = frame shift, del = deletion, indel = insertion/deletion

Table 17: Quantification of genotyping and evaluation of mutagenesis.

Gene	Total number of genotyped F_0 fish	Number of F_0 mutants	Mutagenesis efficiency [%]	Total number of genotyped F_1 fish	Number of F_1 mutants	Number of F_1 fish with frame shifting mutation
meis1a	117	44	37.6	108	10	7
meis1b	53	28	52.8	137	4	4

7.3 Genotyping of F_2 generation

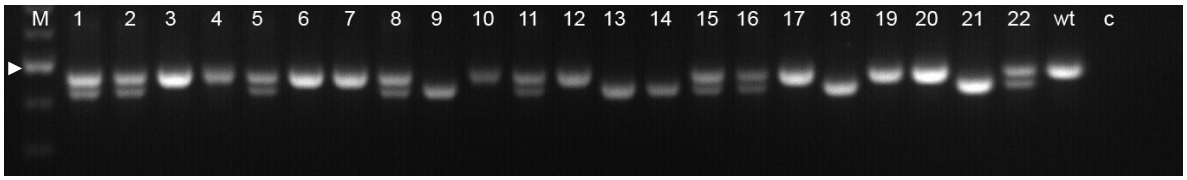

Figure 32: Genotyping of F_2 generation after crossing two heterozygotes (9 and 12) with 37 bp deletion in meis1a homeobox locus. The electrophoretogram confirms presence of homozygotes in the F_2 generation, wells: 9, 13, 14, 18, 21. The arrow points at 500 bp long DNA fragment of the ladder.

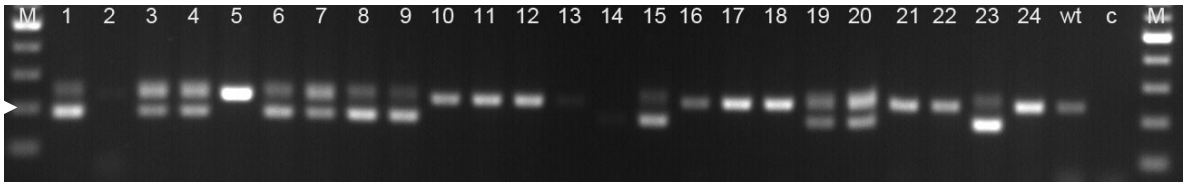

Figure 33: Genotyping of F_2 generation after crossing heterozygote (54) with 50 bp deletion in meis1b homeobox locus and wild type fish. The electrophoretogram confirms presence of heterozygotes in the F_2. The arrow points at 200 bp long DNA fragment of the ladder.

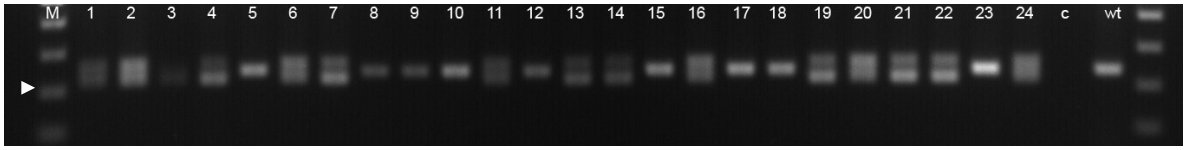

Figure 34: Agarose gel electrophoresis analysis of F_2 generation after crossing heterozygote (26) with 22 bp deletion in meis1b homeobox locus and wild type fish. The electrophoretogram confirms presence of heterozygotes in the F_2. The arrow points at 200 bp long DNA fragment of the ladder. The arrow points at 200 bp long DNA fragment of the ladder.

7.4 Phenotype analysis of *meis1a* and *meis1b* mutant and morphant fish

7.4.1 Whole-mount *in situ* RNA hybridization and cartilage staining

The morpholino based knock-down was performed to determine whether a relationship between *meis1* genes is complementary or only one of the studied genes plays dominant role in development. The WISH of neural crest cells specifiers was performed. Specifiers, such as *dlx1a*, marker for craniofacial structures derived from NCC and *foxD3*, neural plate border marker, expressed during neurulation in neural crest cells and located

along the neural plate. According to the results of WISH meis*1b* is dominant gene playing a significant role in NCC development in both studied locations, in craniofacial structures as well as in neural plate border (Fig. 35E). No changes were seen in phenotype of *meis1a* morphant, and additionally no phenotype was seen in *meis1a* mutant as well. However, more NCC specifiers must be examined.

Also, cartilage staining confirmed the importance of *meis1b* gene in craniofacial cartilage development. Craniofacial cartilage in all *meis1b* morphants was highly underdeveloped (Fig. 35G). Similar effect but with less severity was observed in *meis1b* mutant with mutated homeodomain (*meis1bΔHD*). However, *meis1a* morphants showed a moderate phenotype in mandible structures such as Meckel´s, ceratohyal and palatoquadrate cartilage. Nevertheless, none of those structures were changed or underdeveloped in *meis1a* mutants (Fig. 35G).

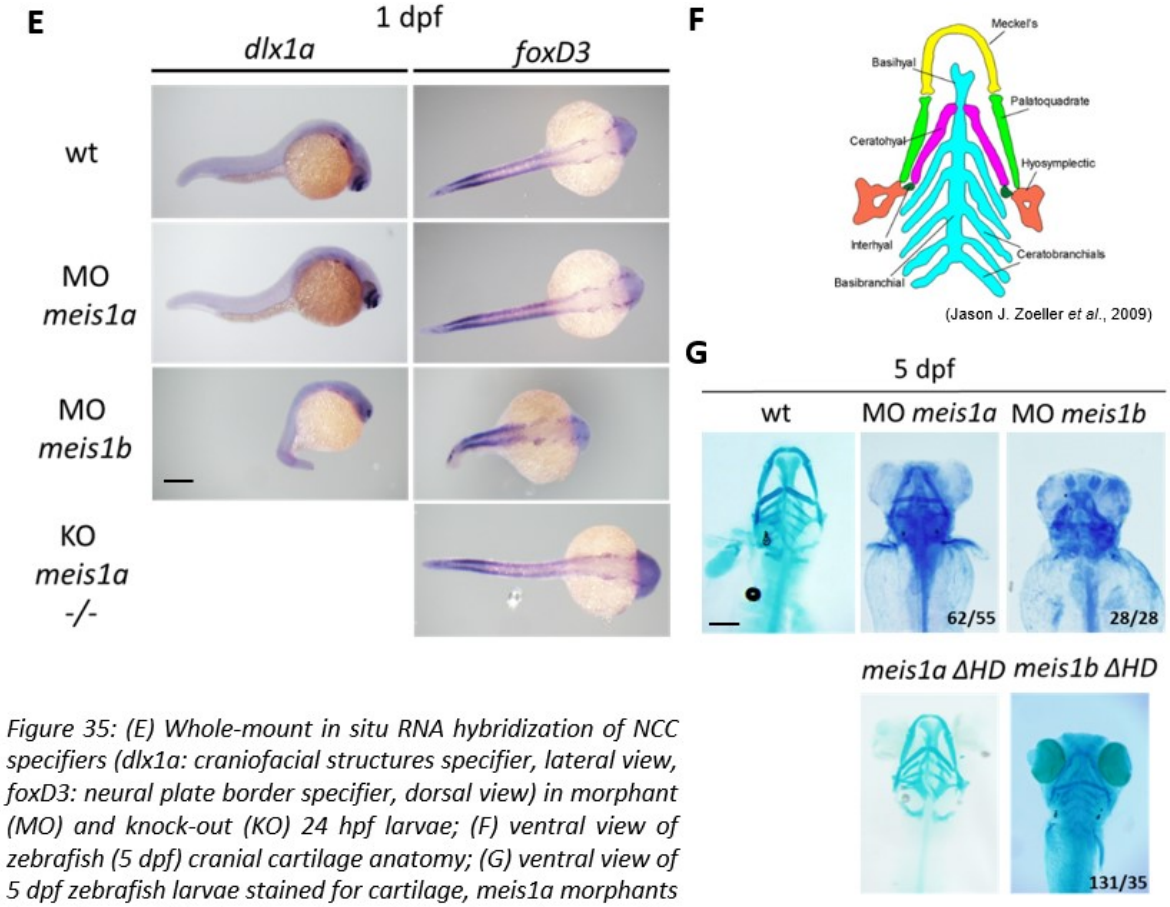

Figure 35: (E) Whole-mount in situ RNA hybridization of NCC specifiers (dlx1a: craniofacial structures specifier, lateral view, foxD3: neural plate border specifier, dorsal view) in morphant (MO) and knock-out (KO) 24 hpf larvae; (F) ventral view of zebrafish (5 dpf) cranial cartilage anatomy; (G) ventral view of 5 dpf zebrafish larvae stained for cartilage, meis1a morphants have shown mild phenotype in craniofacial structures. meis1b morphant shows impaired expression pattern of NCC specifiers that suggests its importance in processes, such as neural plate border specification and development of craniofacial structures. Importance of meis1b was also proven by cartilage staining. meis1b morphant showed highly underdeveloped craniofacial cartilage, 28 out of 28 fish showed the same phenotype. Less severe phenotype was also observed in meis1b mutants. Those mutant were generated by crossing heterozygotes. 35 out of 131 analysed fish showed underdeveloped Meckel´s cartilage, shorten palatoquadrates and flattened ceratohyals. Listed structures are mostly formed from NC. Left scale bar = 250 µm, right scale bar = 500 µm.

7.4.2 Immunohistochemical staining

The imaging of immunohistochemical staining has shown the efficiency of used antibody to bind *Meis1* proteins in fish, further it determined specific location of studied proteins in 24 hpf fish. A strong immunofluorescent signal of *Meis1* proteins was detected in circulating hematopoietic cells in the posterior cardinal veins. The studied generation of zebrafish was composed of wild type fish, homozygotes and heterozygotes, with mutated homeobox of *meis1a* (Fig.36) or *meis1b* (Fig.37) genes. In all groups (*Meis1a*, *Meis1b* and wt fish) was observed a change in signal intensity. Therefore, groups were divided to two sub-groups, a sub-group showing high intensity signal and a sub-group with low intensity signal. Five samples of each sub-group were taken and genotyped. The intensity of signal was assessed by signal histogram (Fig.36, shown below the figure). The histograms show distribution of pixels in the interval of intensity from black to white colour, more intense signal higher the count of more white pixels, thus wider scale. The intensity range of low intensity group was often smaller by half than high intensity group. Genotyping revealed that intensity of fluorescent signal does not correlate with genotype of the fish in *Meis1a* mutants. Interestingly. 4 out of 5 Meis1b animals with low histogram intensity were genotyped to be mutants. These results suggest that mouse antibody is able to bind zebrafish *Meis1* proteins and, in case of *Meis1b*, whole mount immunofluorescent staining revealed a decrease of *Meis1b* in circulating blood of 1-day old embryo.

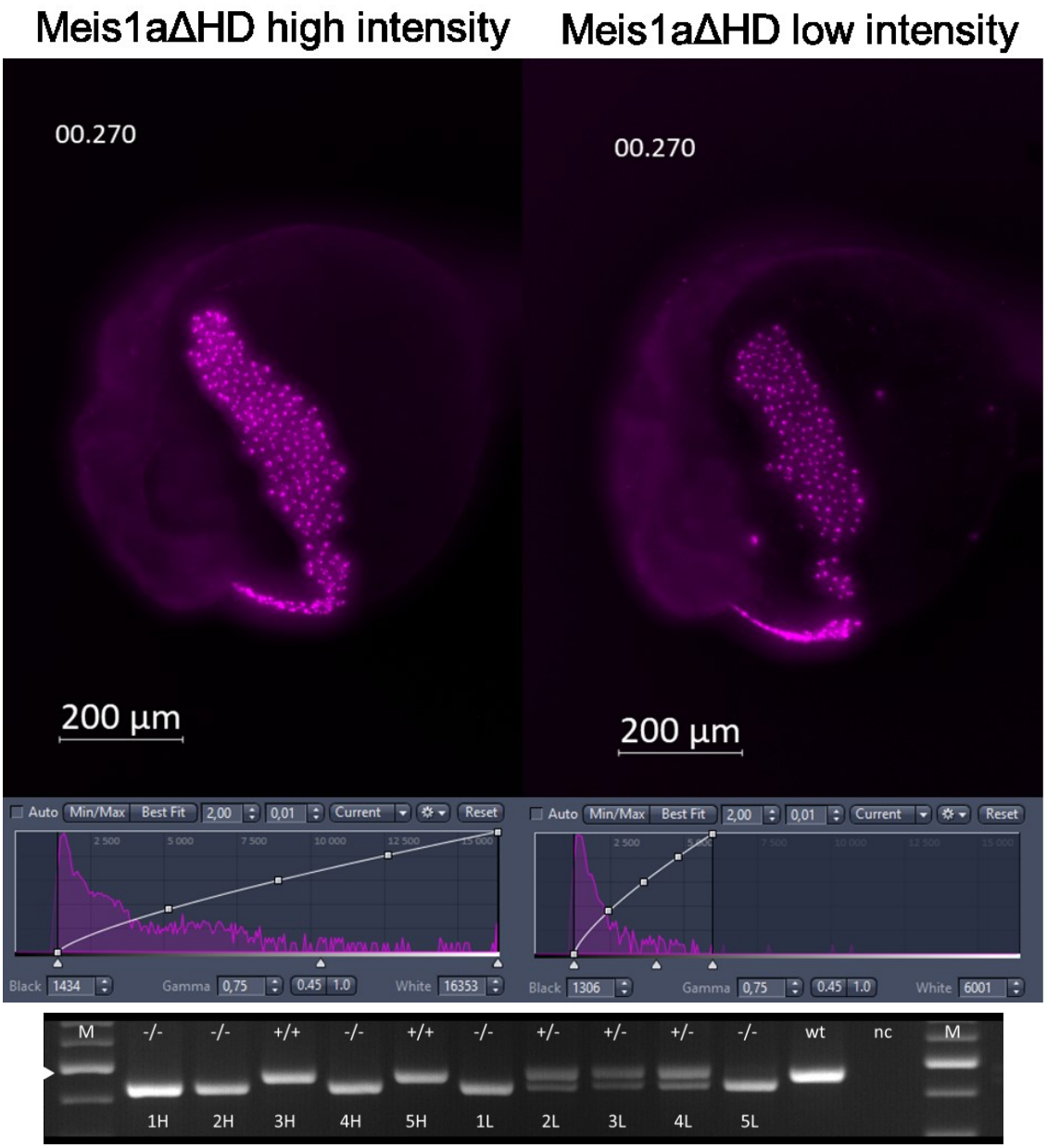

Figure 36: Immunohistochemical staining and genotyping of meis1aΔHD mutants. Representatives of each sub-group high and low intensity signal. The genotyping proves that low intensity of signal does not correlate with homozygous genotype of the fish. High intensity fish corresponds to 1H sample which is homozygote (-/-). Low intensity fish corresponds to 1L sample which is also homozygote (-/-). Number in the left corner show time of exposure in seconds, histograms show quantitative representation of signal, electrophoretogram: arrowhead marks 500 bp long fragment of the marker, nc = negative control, wt = wild type.

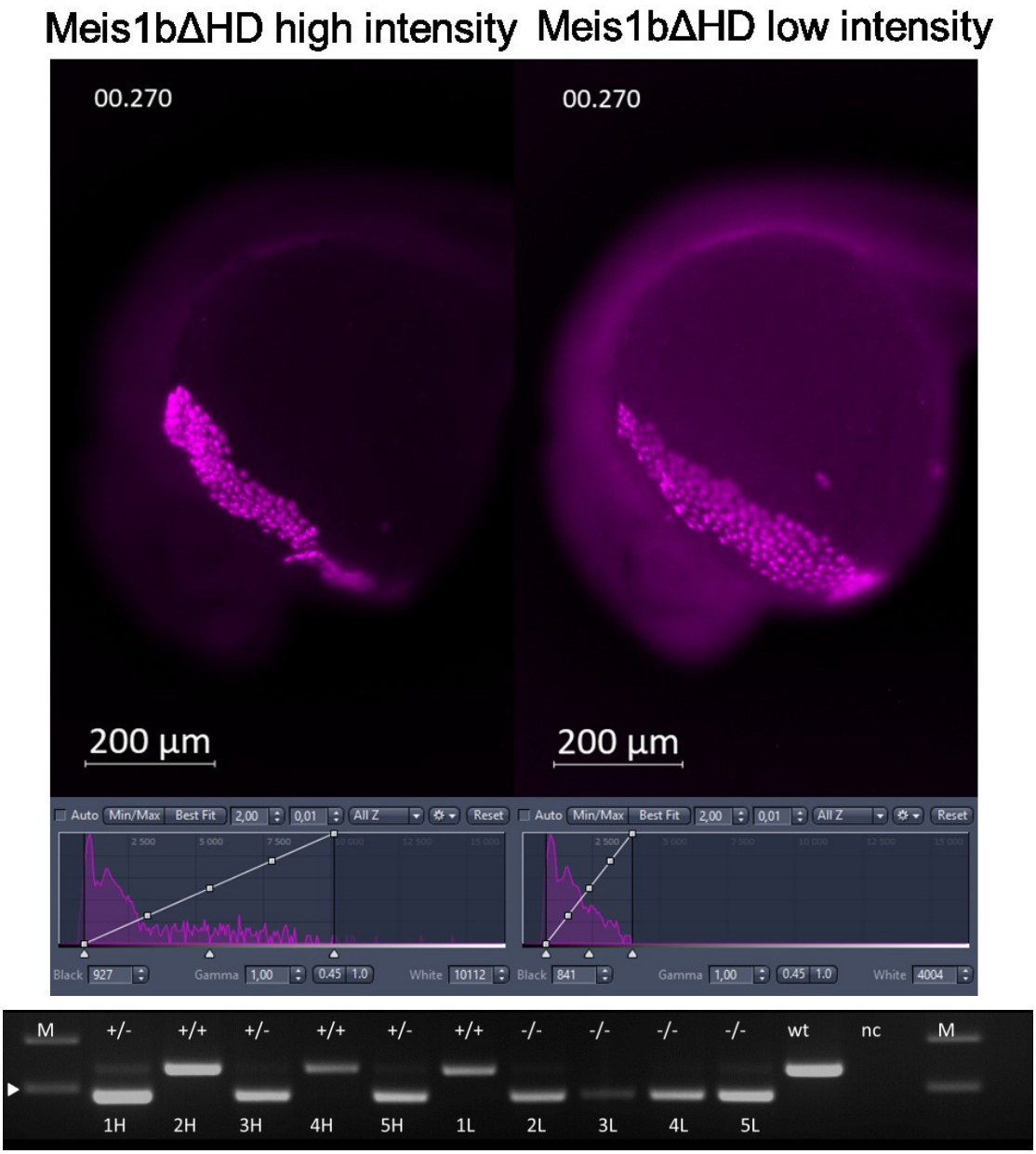

Figure 37: Immunohistochemical staining and genotyping of meis1bΔHD mutants. Representatives of each sub-group high and low intensity signal. The genotyping proves that low intensity of signal may correlate with homozygous genotype of the fish. High intensity fish corresponds to 1H sample, which is heterozygote (+/-). Low intensity fish corresponds to 2L sample which is homozygote (-/-). Number in the left corner shows time of exposure in seconds, histograms show quantitative representation of signal, electrophoretogram: arrowhead marks 500 bp long fragment of the marker, nc = negative control, wt = wild type.

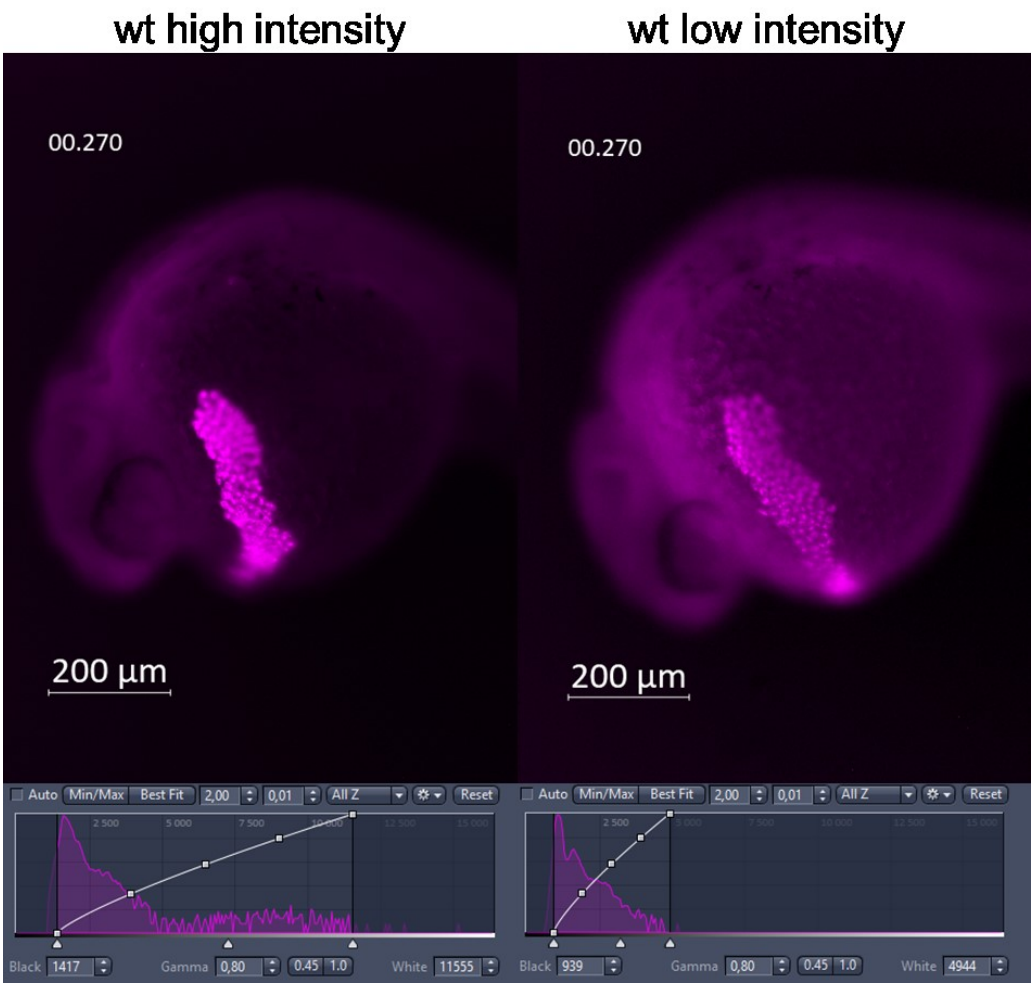

Figure 38: Immunohistochemical staining of wild type fish. Representatives of each sub-group high and low intensity signal. The imaging showed that division of stained fish to two sub-groups by signal intensity was observed even in wild type group. Number in the left corner shows time of exposure in seconds, histograms show quantitative representation of signal.

7.4.3 Microcomputed Tomography (MicroCT) Imaging

In F_2 generation were found viable adult mutants with both *meis1a* alleles mutated to *meis1aΔHD* (37 bp deletion). MicroCT imaging allowed to look at structures that might be changed due to the mutation. Figures below show specific sections of adult fish where a morphological change is expected. However, the structures derived or influenced by neural crest cells involving craniofacial structures, such as palatoquadrate (Fig. 39 and 41), basihyal (Fig. 39), interhyal (Fig. 39), dentary (Fig. 40), bones of olfactory apparatus (Fig. 39 and 41), and eye (Fig. 39) and heart (Fig. 40) did not show significant changes, therefore ablated homeodomain of *meis1a* had no impact on regulation of morphogenesis of NC derivatives.

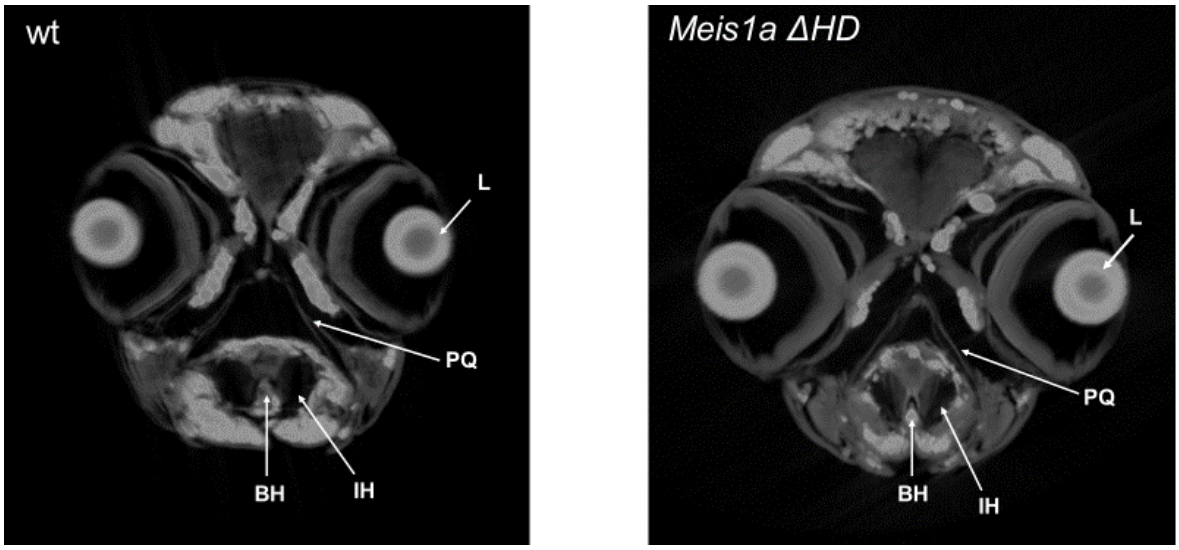

Figure 39: Transverse section of zebrafish head of wild type fish (WT) and mutant fish with mutated homeodomain of meis1a (meis1a ΔHD). Fish were 2 months old (2mpf). Arrows mark structures, such as PQ-palatoquadrate, L-lens, BH-basihyal, IH-interhyal. No significant morphological difference between wild type fish and mutant were observed.

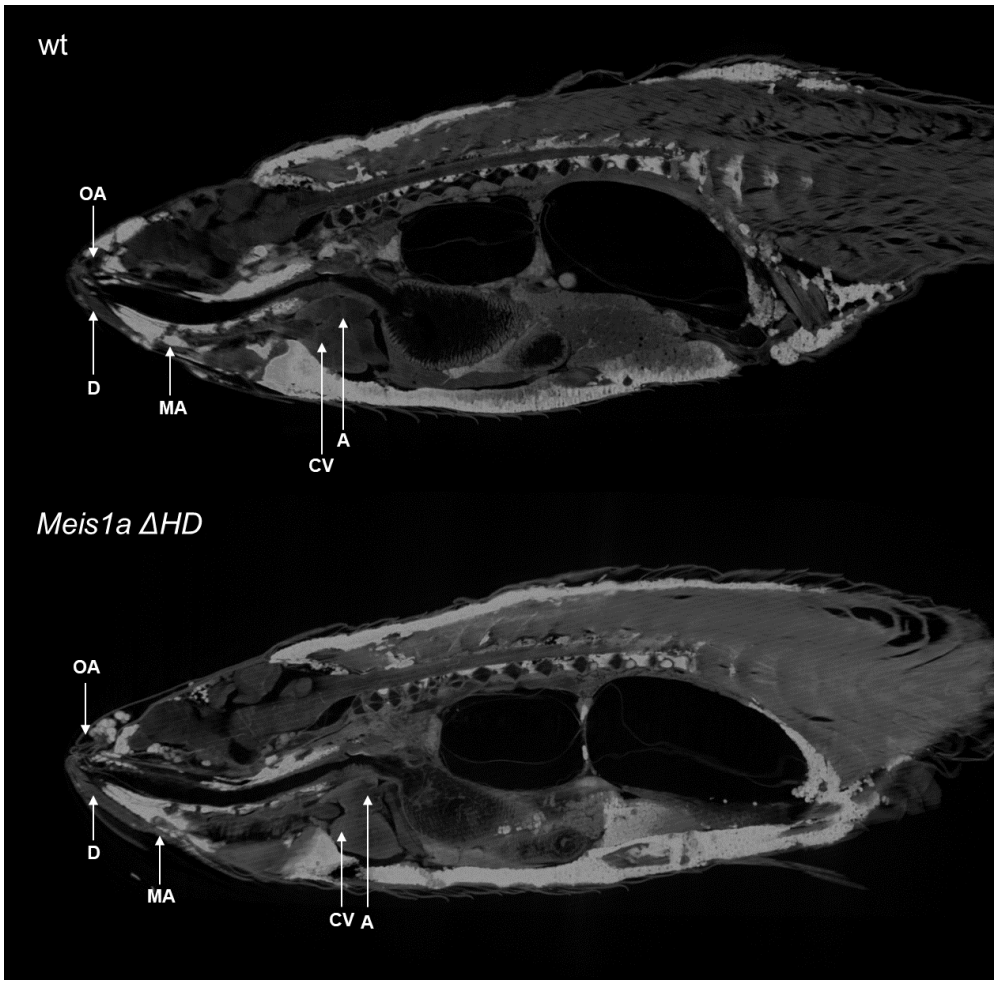

Figure 40: Sagittal section of zebrafish (2mpf) of wild type fish (WT) and mutant fish with mutated homeodomain of meis1a (meis1a ΔHD). Arrows mark structures, such as: MA-maxilla, OA-bones of olfactory apparatus, A-atrium, CV-cardiac ventricle, D-dentary. No significant morphological difference between wild type fish and mutant were observed.

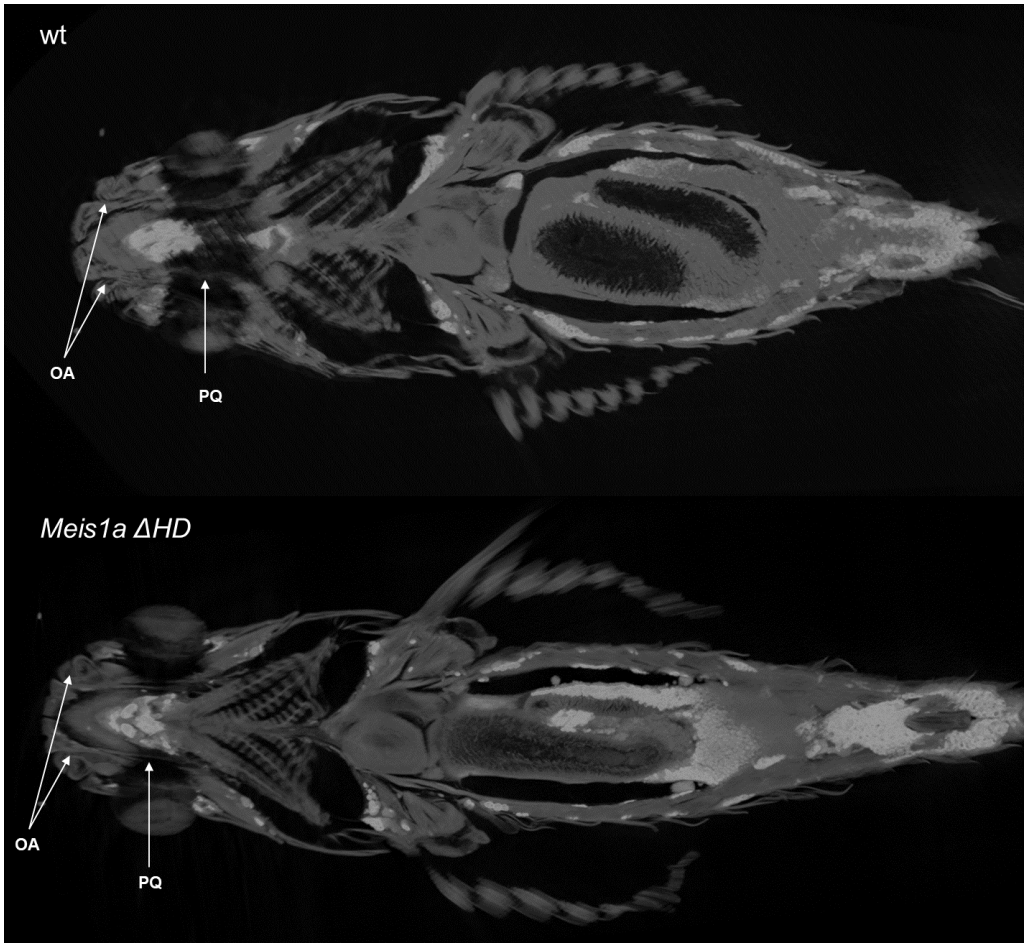

Figure 41: Coronal section of zebrafish (2mpf) of wild type fish (WT) and mutant fish with mutated homeodomain of meis1a (meis1a ΔHD). Arrows mark structures, such as: OA-bones of olfactory apparatus PQ-palatoquadrate. No significant morphological difference between wild type fish and mutant were observed.

8 DISCUSSION

The neural crest is often referred to as the fourth germ layer due to its multipotency, migratory behaviour and ability to give rise to plethora of cell types. This transient population of cells is unique for vertebrates which suggest its complexity in terms regulation. Any disruptions of neural crest integrity can negatively influence development of essential organs or functional structures of the body.

Although, the model of main regulatory network of neural crest developmental involving stages, such as NC specification, segregation, epithelial to mesenchymal transition, delamination, migration and differentiation, is understood (Sauka-Spengler *et* Bronner-Fraser, 2008), not all factors, playing crucial parts, are included in the model. One group of potential non-included factors are TALE homeodomain transcription factors, and specifically Meis protein. It has been reported in the mouse and zebrafish models that impaired expression of Meis genes during neural crest development leads to developmental defects and malformations (Machon *et al.*, 2015). However, the specific role of Meis transcription factors in regulatory hierarchy remains unrevealed. The main goal of this thesis is to contribute to the research of Meis proteins and attempt to elucidate their function in the zebrafish.

Most functional researches done in the zebrafish model are based on knock-down approach, using morpholino oligonucleotides. However, fish phenotypes, generated by employing this RNA targeting approach, often did not correlate with phenotypes achieved by DNA editing with site-specific nucleases (Kok *et al*. 2015). Therefore, this theses aims for using the CRISPR/Cas9 system as a tool to disrupt gene of interest, because it has been proven to be more reliable approach of studying the gene function (Kok *et al*. 2015). Nonetheless, morpholino mediated gene knock-down was used in this work, in order to determine the relationship between two studied paralogous genes.

The main interest of the thesis was *meis1* genes which are present in zebrafish genome as two paralogues, *meis1a* and *meis1b*, where each of them can be during mRNA processing alternatively spliced and produce distinct splice variants. Zebrafish *meis1a* have four known splice variants and *meis1b* tree. Human and mouse possess only one *MEIS1,* but RNA of the gene can be alternatively spliced and give rise to 17 and 9 splice variant, respectively. The question is, whether the duplication of zebrafish genome caused only functional division of meis1 genes (sub-functionalization) or also development of a novel different function (neo-functionalization). Other question might be, whether the function of each single splice variants of *MEIS1* in human or mouse is complementary to *meis1* splice variants in zebrafish. It is relevant to study *Meis1* proteins importance in zebrafish development to find congeniality in development of regulatory systems in higher vertebrates, mouse and human. In addition, the zebrafish is an appropriate model for studying development of any cell population *in vivo,* due to small size, external and fast development, transparency, high fecundity and a rich toolkit of genome editing systems.

Meis1 proteins are transcription factors, thus they contain DNA binding domain – homeodomain, which is essential not only for recognition and binding to specific DNA sequence but also for interaction with other proteins. It has been shown that homeodomain might mediated the interaction with Hox proteins and any disruption in this domain can lead to abrogation of ability to bind DNA. To study a functional significance of homeodomain the CRISPR/Cas9 technology was used to edit the region of Meis1 genes, coding for homeodomain was targeted, and by that generate functional knock-out.

Two knock-out zebrafish lines of each *meis1* gene were generated by injecting 1-2 cells stage embryos with SpCas9 protein and mixture of sgRNAs, targeting meis1a and meis1b homeobox locus. Mutated fish were repeatedly crossed to obtain fish with both mutated alleles of the gene. Consecutively, phenotypes of mutant and fish treated with morpholinos were examined with multiple staining techniques, including WISH, ABS, IHC and adult *meis1aΔHD* mutants were scanned with MicroCT imaging system. The results of knock-down experiment showed that meis1b is a dominant gene, contributing the most to early specification of NC and formation of craniofacial structures. In contrast, *meis1a* does not contributes to early specification nor craniofacial cartilage formation. Cartilage staining (ABS) of mutant fish also suggests that *meis1b* plays more significant role in development of craniofacial structures despite the phenotype of *meis1b* mutant was less severe than in *meis1b* morphant.

Immunohistochemical staining was performed to determine affinity of used antibody and therefore its specificity, and to observe whether expression of mutated genes is changed or not. This analysis of mutants did not confirm decreased amount of the *Meis1a* protein, but we observed a strong correlation between *Meis1b* protein intensity and respective genotype. We also confirmed the ability of anti-mouse Meis1 antibody to bind zebrafish *Meis1* proteins which means the antibody can be used for future experiments, such as Western blotting.

Microcomputed tomography was employed to evaluate this technique as a substitute for histology analysis of male adult fish and to investigate morphology of 2 months old mutant fish. Even though, the mutant fish *meis1a* had no visible malformations of craniofacial structure in early stages of life. The microCT imaging was used to see whether the fish developed growth anomalies equivalent to cleft palate, impaired septation of heart or optical defects, basically malformation of structures derived from NCC. The scanning of the adult *meis1aΔHD* mutant did not reveal any significant morphological deviations but it has proven to be decent alternative to histological sectioning.

In conclusion, the main goal of this thesis was accomplished. Two mutant zebrafish lines were generated, with mutations abrogating function of DNA binding domain of meis1a and meis1b genes. Secondly, the dominant *meis1* gene, contributing to development of NCC derivatives, was determined as *meis1b* by using morpholino based knock-down approach. Additional phenotype assessment of generated mutants confirms

dominancy *meis1b* gene in NCC development in zebrafish model. However, more experiments need to be done to verify total abrogation of homeodomain function in both studied genes and to affirm the hypothesis that homeodomain is essential for regulatory function of the protein.

Following chapters are dedicated to discussion of the results with literature and proposes the hypothesis that illustrates the importance of *meis1* genes in NCC development.

8.1 Design and synthesis of sgRNAs

SgRNAs were designed to navigate Cas9 protein to 5´end of homeobox region of *meis1a* and *meis1b* genes (Fig.18). Homeobox region codes for homeodomain, DNA-binding domain. This region was targeted due to the function of homeodomain mediate the interaction with DNA and through that interaction stabilize MEIS/PREP-PBX complex or form complexes with Hox proteins, as stated Longobardi *et al*., 2014, and Merabet *et* Galliot, 2015, respectively.

Target sequences within homeobox region analysed with CRISPOR online software and selected by algorithm based on Moreno-Mateos and collective, 2017 high-throughput screens. Other criteria for selection were specificity score, number of potential off-target cleavages and probability of introduction of frame shifting deletion. In the Tab. 18 (suppl. data) are listed features of used sgRNAs. The Moreno-Mateos algorithm, also called CrisprScan, is predicated on linear regression model, trained on data from 1000 guides targeting about 100 genes, from zebrafish 1-cell stage embryos injected with Cas9 mRNA and single guide RNAs transcribed in-vitro with T7 RNA polymerase an it is rated form 0 (lowest) to 100 (highest). Specificity column shows the uniqueness of the target within the genome (The higher the specificity score, the lower are off-target effects in the genome). Probability of out-of-frame mutation shows a percentage of clones that will carry out-of-frame deletions, based on the micro-homology in the sequence flanking the target site. This prediction is adapted from Bae et al. 2014. Off-targets column shows all potential target sites within the zebrafish genome (GRCz11). The CRISPRscan algorithm was used due to similar approach, on which the algorithm was based, to conditions of experiments conducted in this work.

The presence and integrity of sgRNAs after transcription were assessed by separation in agarose gel (Fig.23, results). The electrophoretogram showed formation of sgRNA dimers which is common phenomena after purification of sgRNA with phenol-chloroform (Low, Kutny *et* Wiles, 2016).

8.2 Genotype of F_0 and F_1 generation

Genotyping of F_0 revealed the efficiency of used Cas9/sgRNA complex, targeting *meis1a* locus, was below predicted efficiency. The number was close to predicted efficiency of Cas9/sgRNA10a complex (Tab.18), however, sequencing data of *meis1a* locus imply that the most active was the complex targeting 3´ end of exon 8, Cas9/sgRNA8a (Fig.25 and

30A). The claim, Cas9/sgRNA8a complex, being the most efficient, confirms the character of transferred mutation in *meis1a* locus to next generation. In case of *meis1b* locus, the efficiency of sgRNAs was than average of predicted efficiency. Especially, sgRNA2b and sgRNA3b in complex with Cas9 protein introduced most of mutation to the locus according to analysed alleles of F_1 generation listed in Fig. 30B.

Nonetheless, this efficiency evaluation is only illustrative due to combinatorial use of sgRNAs. All three sgRNA, targeting one of *meis1* genes were injected into embryo together, therefore their activity or efficiency is dependent on many factors preventing an objective evaluation. Factors, such as preparation of injection mixture. The mixture is prepared by mixing microliter volumes which is prone to pipetting error. It can lead to unbalanced concentration ratio of sgRNA in the mixture. Other factor might affinity of Cas9/sgRNA complex to DNA. The composition of spacer sequence can influence activity of Cas9/sgRNA complex (Moreno-Mateos *et al*. 2015; Doench *et al*. 2014). Eventually, the overlap of sgRNA target sites can negatively influence activity of both involved complexes as in the case of sgRNA9a and sgRNA10a, although in literature, such association often enhances the mutagenesis (Fig.25; Jang *et al.*, 2018).

The results of sequence analysis of mutated alleles in Fig.30 were translated to protein sequences listed in Fig. 31. Mere translation to protein sequence does not provide an evidence that *in silico* predicted protein is expressed in the cell. Therefore, other protein analysing techniques need to be used, specifically Western blotting or whole-mount immunohistochemical staining.

8.3 Genotyping of F2

Heterozygous fish selected by occurrence of frame shifting mutation were crossed to each other or to wild type fish. Heterozygous and homozygous progeny of the crossing was kept as a mutant line. Genotyping of the second *meis1a* mutant line (progeny of fish 27 with 270 bp deletion) is not shown due to health problem of the fish. To generate such mutant line *in vitro* fertilization was performed. The fertilization was successful, but progeny fish were not grown enough for genotyping on publishing date of this thesis. All generated heterozygotes were subsequently crossed to each other to give rise homozygotes (meis1aΔ -/- and meis1bΔ -/-) and double-heterozygotes (meis1aΔ +/-, meis1bΔ +/-). Phenotype of double heterozygote was not assessed due to small size of fish on publishing date of the thesis.

8.4 *meis1b* is dominant gene in development of NCCs and NC derivatives

The knock-down of *meis1* genes revealed dominant contribution to development of neural crest and its derivatives Fig. 35E and G. This contribution, specifically in craniofacial morphogenesis, was also confirmed in mutant fish. The possible explanations of difference between morphant and mutant phenotype are following: morpholino, targeting *meis1b* mRNA also targets mRNA of *meis1a* because of it has a certain level of homology to the start codon region of *meis1a*, which is the level of homology for some interaction as stated

in (Moulton, 2006). The combinatorial activity affecting both meis1 genes expression can lead to development of sever phenotype, such as in *meis1b* morphant. Other possible explanation of phenotype discrepancy is the fact that *meis1b* morpholino targets start codon of mRNA and both translated splice variants of the gene are affected by the morpholino, therefore expression of the protein is highly reduced. In case of *meis1bΔHD* mutant the expression is not reduced the protein is translated but it is missing homeodomain. Although, it has been proven that homeodomain is important for DNA-protein and interaction with other partners (Longobardi *et al*. 2014), it has been also demonstrated the role of N-terminus of meis1 proteins, particularly interaction domains, as a part of regulatory complexes independent of DNA binding (Singh *et* Kango-Singh, 2013). The N-terminus fragment can remain some regulatory function, reducing severity of the phenotype.

Whole mount RNA in situ hybridization of NCC specifiers, dlx1a and foxD3, detected no change of their expression pattern in *meis1a* morphants nor in mutants. This absence of changed phenotype may have several explanations: *meis1a* does not participate in the process of NC specification and determination of cranial NCCs. *meis1a* targeting morpholino binds the start codon region of the larges *meis1a* splice variant 201 (380 aa) but meis1a gene has two more splice variant (203, 204; suppl. data-Fig.42) that do not share the start codon region with splice variant 201. Therefore, shorter splice variants can compensate lack of variant 201 and rescue the phenotype.

Morphological abnormalities of craniofacial structures in meis1a morphants can be apparent due to the importance of *meis1a* gene, specifically splice variant 201, during late development of craniofacial cartilage. Furthermore, *meis1a* morpholinos can partially affect *meis1b* mRNA in late stages of craniofacial development. Nonetheless, phenotype of *meis1aΔHD* fish suggest that homeodomain is not essential part of the protein contributing to regulation of NCCs in the region, or *Meis1a* protein is not involved in regulation of craniofacial development.

However, to make solid hypothesis of regulatory function of *meis1* genes more NCCs specifiers need to be analysed to elucidate the position of *meis1* gene in regulatory hierarchy. Also, function of homeodomain in NCCs regulation needs to be tested. Broader analysis of NCCs specifiers can be performed with WISH in mutant fish or with IHC staining of *meis1a* splice variant products in fish, lacking some of those variant and observe with combinatorial IHC staining changes in patterns or signal.

8.5 IHC did not confirm reduced expression of *meis1* genes

The mutation in homeobox region of *meis1* genes did not influenced expression their product nor behaviour of the *Meis1* expressing cells. *Meis1* protein shown their expression in hematopoietic progenitors around the yolk (Fig. 36-38) and along the neural tube (not shown; Murayama *et al.*, 2006). Among all groups of analyse fish were observed a difference in intensity of signal, therefore every group of mutant and wild type fish was

divided to sub-groups according to intensity of signal and genotyped. Genotyping showed no correlation between intensity of signal and genotype of the fish in *Meis1aΔHD* fish. Although, in case of *Meis1bΔHD* correlation was observable.

The experiment was conducted to test the antibody against mouse MEIS1 and its ability to bind zebrafish *Meis1* epitope, which consist of first 16 aa on the N-terminus. The antibody binds both zebrafish *Meis1*, therefore the expression pattern in Fig. 36-38 belongs to *Meis1a* as well as *Meis1b* proteins. This experiment would be more quantitatively and qualitatively informative, if it was done with antibody binding any epitope on the C-terminus. Because the C-terminus supposed to be disrupted, thus the antibody would not be able to bind it and fluorescent signal would be less intense or absent. This would also decrease a probability of binding gene splice variants lacking homeodomain. The most optimal option would be the usage of *Meis1a* or *Meis1b* specific antibody, binding C-terminal epitope. This approach would prevent false positive signal caused by compensation mediated by the paralogue. The compensation process has been reported in Blasi *et al.*, 2017. However, the applicated mouse Meis1 antibody is convenient to be used for Western blotting to test a presence of Meis1 protein with missing homeodomain in the fish.

The quantitative assessment based on number of pixels with specific intensity from black to white, as shown in Fig.36 and 37, might have a higher significance if the number of samples was higher and the data were more statistically processed.

8.6 No morphological abnormalities were observed in an adult *meis1aΔHD* fish

Two months old *Meis1aΔHD* fish and wild-type fish were scanned (Fig.39-41). Morphological analysis did not reveal any abnormalities of craniofacial structures, heart or eyes. No structural changes can be evidence of: meis1a does not contribute to development of any studied structures. Meis1a can fulfil its regulatory function in homeodomain independent manner. Furthermore, *Meis1b* protein compensates for impaired *Meis1a*, a similar phenomenon was observed between MEIS1 and MEIS2 in myeloid leukemia cells (Lai *et al*. 2017). Eventually, the 37 bp long deletion in exon 8 of meis1a, involving exon-intron junction, does not causes reading frame shift. Therefore, the mutant fish from second *meis1a* mutant line, with 270 bp deletion (Fig.30A27), should be used to test this hypothesis.

8.7 Summary

To conclude, *Meis1aΔHD* and *Meis1bΔHD* mutant lines were generated by using CRISPR technology and mutations were confirmed at the level of DNA by sequencing. However, expression of mutated protein can be tested with other protein analysing techniques to prove production of aberrant protein, e.g. Western blotting. Collected data, compared with literature, suggest that *meis1b* plays dominant role in development of NC derivatives and requires DNA-domain for proper function in this process. In case of *meis1a*,

the contribution of the gene to NCCs development remains unclear due to possible functional compensation by *meis1b* or by its splice variants. Other explanation could be unnecessity of homeodomain in *meis1a* regulatory function. Rational future steps would be phenotype assessment of double-mutant line (*Meis1aΔHD/Meis1bΔHD)* or generation and phenotyping of *meis1a and meis1b* null knockout lines.

9 CONCLUSION

This work was dedicated to study of TALE transcription factors, specifically *Meis1a* and *Meis1b*, and their significance during development of neural crest cells in the zebrafish model. The neural crest is figuratively called fourth germ layer due to its potency to participate in production of a broad range of cell types. *Meis1* transcription factors are known as regulators or co-regulators involved in development of hindbrain, eye, heart and other structures. The main goal of the work was to establish zebrafish mutant lines of *Meis1a* and *Meis1b* with deleted DNA-binding domain – homeodomain and outline their regulatory function in neural crest cells by assessment of mutant phenotypes.

Mutant zebrafish lines were generated by using CRISPR technology and potential relationship between studied transcription factors was determined via morpholinos based knock-down. Analysis of mutant and morphant phenotypes revealed significant contribution of *meis1b* to regulation of craniofacial morphogenesis. In contrast, *meis1a* mutant and morphant phenotypes have not disclosed any participation in regulatory network of NCC development.

Nevertheless, more experiments are needed to be performed for detailed understanding of the function of these transcription factors. Experiment, such as generation of double mutant fish to prevent functional compensation which is a common phenomenon in this class transcription factors or complete knock-out of *meis1a* and *meis1b* genes, optionally combinatorial knock-out of both *meis1* genes.

11 REFERENCE

Abudayyeh, Omar O., Jonathan S. Gootenberg, Patrick Essletzbichler, Shuo Han, Julia Joung, Joseph J. Belanto, Vanessa Verdine, et al. 2017. "RNA Targeting with CRISPR–Cas13." *Nature* 550 (7675): 280–84. https://doi.org/10.1038/nature24049.

Adli, Mazhar. 2018. "The CRISPR Tool Kit for Genome Editing and Beyond." *Nature Communications 2018 9:1* 9 (1): 1911. https://doi.org/10.1038/s41467-018-04252-2.

Bae, Sangsu, Jiyeon Kweon, Heon Seok Kim, and Jin-Soo Kim. 2014. "Microhomology-Based Choice of Cas9 Nuclease Target Sites." *Nature Methods* 11 (7): 705–6. https://doi.org/10.1038/nmeth.3015.

Barrangou, Rodolphe. 2015. "The Roles of CRISPR–Cas Systems in Adaptive Immunity and Beyond." *Current Opinion in Immunology* 32 (February): 36–41. https://doi.org/10.1016/J.COI.2014.12.008.

Bassett, D. I., and P. D. Currie. 2003. "The Zebrafish as a Model for Muscular Dystrophy and Congenital Myopathy." *Human Molecular Genetics* 12 (suppl 2): R265–70. https://doi.org/10.1093/hmg/ddg279.

Beachy, P A, M A Krasnow, E R Gavis, and D S Hogness. 1988. "An Ultrabithorax Protein Binds Sequences near Its Own and the Antennapedia P1 Promoters." *Cell* 55 (6): 1069–81. http://www.ncbi.nlm.nih.gov/pubmed/2904838.

Bellmeyer, Amy, Jessica Krase, Julie Lindgren, and Carole LaBonne. 2003. "The Protooncogene C-Myc Is an Essential Regulator of Neural Crest Formation in Xenopus." *Developmental Cell* 4 (6): 827–39. https://doi.org/10.1016/S1534-5807(03)00160-6.

Bertrand, E, P Chartrand, M Schaefer, S M Shenoy, R H Singer, and R M Long. 1998. "Localization of ASH1 MRNA Particles in Living Yeast." *Molecular Cell* 2 (4): 437–45. http://www.ncbi.nlm.nih.gov/pubmed/9809065.

Best, J D, and Wendy K Alderton. 2008. "Zebrafish: An in Vivo Model for the Study of Neurological Diseases." *Neuropsychiatric Disease and Treatment* 4 (3): 567–76. http://www.ncbi.nlm.nih.gov/pubmed/18830398.

Blasi, Francesco, Chiara Bruckmann, Dmitry Penkov, and Leila Dardaei. n.d. "A Tale of TALE, PREP1, PBX1, and MEIS1: Interconnections and Competition in Cancer; A Tale of TALE, PREP1, PBX1, and MEIS1: Interconnections and Competition in Cancer." Accessed April 22, 2019. https://doi.org/10.1002/bies.201600245.

Bolukbasi, Mehmet Fatih, Ankit Gupta, Sarah Oikemus, Alan G Derr, Manuel Garber, Michael H Brodsky, Lihua Julie Zhu, and Scot A Wolfe. 2015. "DNA-Binding-Domain Fusions Enhance the Targeting Range and Precision of Cas9." *Nature Methods* 12 (12): 1150–56. https://doi.org/10.1038/nmeth.3624.

Briner, Alexandra E, Paul D Donohoue, Ahmed A Gomaa, Kurt Selle, Euan M Slorach, Christopher H Nye, Rachel E Haurwitz, Chase L Beisel, Andrew P May, and Rodolphe Barrangou. 2014. "Molecular Cell Short Article Guide RNA Functional Modules Direct Cas9 Activity and Orthogonality." *Molecular Cell* 56: 333–39. https://doi.org/10.1016/j.molcel.2014.09.019.

Bronner, Marianne E., and Nicole M. LeDouarin. 2012. "Development and Evolution of the Neural Crest: An Overview." *Developmental Biology* 366 (1): 2–9. https://doi.org/10.1016/j.ydbio.2011.12.042.

Buggisch, M., B. Ateghang, C. Ruhe, C. Strobel, S. Lange, M. Wartenberg, and H. Sauer. 2007. "Stimulation of ES-Cell-Derived Cardiomyogenesis and Neonatal Cardiac Cell Proliferation by Reactive Oxygen Species and NADPH Oxidase." *Journal of Cell Science* 120 (5): 885–94. https://doi.org/10.1242/jcs.03386.

Catron, K M, N Iler, and C Abate. 1993. "Nucleotides Flanking a Conserved TAAT Core Dictate the DNA Binding Specificity of Three Murine Homeodomain Proteins." *Molecular and Cellular Biology* 13 (4): 2354–65. http://www.ncbi.nlm.nih.gov/pubmed/8096059.

Chavez, Alejandro, Jonathan Scheiman, Suhani Vora, Benjamin W Pruitt, Marcelle Tuttle, Eswar P R Iyer,

Shuailiang Lin, et al. 2015. “Highly Efficient Cas9-Mediated Transcriptional Programming.” *Nature Methods* 12 (4): 326–28. https://doi.org/10.1038/nmeth.3312.

Chen, Baohui, Luke A. Gilbert, Beth A. Cimini, Joerg Schnitzbauer, Wei Zhang, Gene-Wei Li, Jason Park, et al. 2013. “Dynamic Imaging of Genomic Loci in Living Human Cells by an Optimized CRISPR/Cas System.” *Cell* 155 (7): 1479–91. https://doi.org/10.1016/j.cell.2013.12.001.

Cheung, Martin, Marie-Christine Chaboissier, Anita Mynett, Elizabeth Hirst, Andreas Schedl, and James Briscoe. 2005. “The Transcriptional Control of Trunk Neural Crest Induction, Survival, and Delamination.” *Developmental Cell* 8 (2): 179–92. https://doi.org/10.1016/j.devcel.2004.12.010.

Choe, C. P., and J. G. Crump. 2014. “Tbx1 Controls the Morphogenesis of Pharyngeal Pouch Epithelia through Mesodermal Wnt11r and Fgf8a.” *Development*. https://doi.org/10.1242/dev.111740.

Choe, S-k, N Vlachakis, and C G Sagerström. n.d. “Hox Co-Factors in Hindbrain Development.”

Christian, Michelle, Tomas Cermak, Erin L Doyle, Clarice Schmidt, Feng Zhang, Aaron Hummel, Adam J Bogdanove, and Daniel F Voytas. 2010. “Targeting DNA Double-Strand Breaks with TAL Effector Nucleases.” *Genetics* 186 (2): 757–61. https://doi.org/10.1534/genetics.110.120717.

Colon, Nadja C., and Dai H. Chung. 2011. “Neuroblastoma.” *Advances in Pediatrics* 58 (1): 297. https://doi.org/10.1016/J.YAPD.2011.03.011.

Corey, David R, and John M Abrams. 2001. “Morpholino Antisense Oligonucleotides: Tools for Investigating Vertebrate Development.” *Genome Biology* 2 (5): reviews1015.1. https://doi.org/10.1186/gb-2001-2-5-reviews1015.

Cvejic, Ana, Jovana Serbanovic-Canic, Derek L. Stemple, and Willem H. Ouwehand. 2011. “The Role of Meis1 in Primitive and Definitive Hematopoiesis during Zebrafish Development.” *Haematologica*. https://doi.org/10.3324/haematol.2010.027698.

Dahlman, James E, Omar O Abudayyeh, Julia Joung, Jonathan S Gootenberg, Feng Zhang, and Silvana Konermann. 2015. “Orthogonal Gene Knockout and Activation with a Catalytically Active Cas9 Nuclease.” *Nature Biotechnology* 33 (11): 1159–61. https://doi.org/10.1038/nbt.3390.

Dardaei, Leila, Elena Longobardi, and Francesco Blasi. n.d. “Prep1 and Meis1 Competition for Pbx1 Binding Regulates Protein Stability and Tumorigenesis.” Accessed December 14, 2018. https://doi.org/10.1073/pnas.1321200111.

Deflorian, G., Natascia Tiso, Elisabetta Ferretti, Dirk Meyer, Francesco Blasi, Marino Bortolussi, and Francesco Argenton. 2004. “Prep1.1 Has Essential Genetic Functions in Hindbrain Development and Cranial Neural Crest Cell Differentiation.” *Development* 131 (3): 613–27. https://doi.org/10.1242/dev.00948.

Dibner, Charna, Sarah Elias, and Dale Frank. 2001. “XMeis3 Protein Activity Is Required for Proper Hindbrain Patterning in Xenopus Laevis Embryos.” *Development* 128 (18).

Doench, John G, Ella Hartenian, Daniel B Graham, Zuzana Tothova, Mudra Hegde, Ian Smith, Meagan Sullender, Benjamin L Ebert, Ramnik J Xavier, and David E Root. 2014. “Rational Design of Highly Active SgRNAs for CRISPR-Cas9–mediated Gene Inactivation.” *Nature Biotechnology* 32 (12): 1262–67. https://doi.org/10.1038/nbt.3026.

Douarin, N M Le, and M A Teillet. 1974. “Experimental Analysis of the Migration and Differentiation of Neuroblasts of the Autonomic Nervous System and of Neurectodermal Mesenchymal Derivatives, Using a Biological Cell Marking Technique.” *Developmental Biology* 41 (1): 162–84. http://www.ncbi.nlm.nih.gov/pubmed/4140118.

Doyon, Yannick, Thuy D Vo, Matthew C Mendel, Shon G Greenberg, Jianbin Wang, Danny F Xia, Jeffrey C Miller, Fyodor D Urnov, Philip D Gregory, and Michael C Holmes. 2011. “Enhancing Zinc-Finger-Nuclease Activity with Improved Obligate Heterodimeric Architectures.” *Nature Methods* 8 (1): 74–79. https://doi.org/10.1038/nmeth.1539.

Dupé, V, and A Lumsden. 2001. “Retinoic Acid and Hindbrain Patterning.” http://dev.biologists.org/content/develop/128/12/2199.full.pdf.

Dupin, Elisabeth, and Lukas Sommer. 2012. “Neural Crest Progenitors and Stem Cells: From Early Development to Adulthood.” *Developmental Biology* 366 (1): 83–95. https://doi.org/10.1016/j.ydbio.2012.02.035.

Eisen, Judith S, and James C Smith. 2008. “Controlling Morpholino Experiments: Don’t Stop Making Antisense.” *Development (Cambridge, England)* 135 (10): 1735–43. https://doi.org/10.1242/dev.001115.

Ekker, S C, K E Young, D P von Kessler, and P A Beachy. 1991. “Optimal DNA Sequence Recognition by the Ultrabithorax Homeodomain of Drosophila.” *The EMBO Journal* 10 (5): 1179–86. http://www.ncbi.nlm.nih.gov/pubmed/1673656.

Esvelt, Kevin M, Prashant Mali, Jonathan L Braff, Mark Moosburner, Stephanie J Yaung, and George M Church. 2013. “Orthogonal Cas9 Proteins for RNA-Guided Gene Regulation and Editing.” *Nature Methods* 10 (11): 1116–21. https://doi.org/10.1038/nmeth.2681.

Friedland, Ari E., Reshica Baral, Pankhuri Singhal, Katherine Loveluck, Shen Shen, Minerva Sanchez, Eugenio Marco, et al. 2015. “Characterization of Staphylococcus Aureus Cas9: A Smaller Cas9 for All-in-One Adeno-Associated Virus Delivery and Paired Nickase Applications.” *Genome Biology* 16 (1): 257. https://doi.org/10.1186/s13059-015-0817-8.

Fu, Yanfang, Jeffry D Sander, Deepak Reyon, Vincent M Cascio, and J Keith Joung. 2014. “Improving CRISPR-Cas Nuclease Specificity Using Truncated Guide RNAs.” *Nature Biotechnology* 32 (3): 279–84. https://doi.org/10.1038/nbt.2808.

Furutani-Seiki, Makoto, and Joachim Wittbrodt. 2004. “Medaka and Zebrafish, an Evolutionary Twin Study.” *Mechanisms of Development* 121 (7–8): 629–37. https://doi.org/10.1016/J.MOD.2004.05.010.

Gaj, Thomas, Jing Guo, Yoshio Kato, Shannon J Sirk, and Carlos F Barbas. 2012. “Targeted Gene Knockout by Direct Delivery of Zinc-Finger Nuclease Proteins.” *Nature Methods* 9 (8): 805–7. https://doi.org/10.1038/nmeth.2030.

Gasiunas, G., R. Barrangou, P. Horvath, and V. Siksnys. 2012. “Cas9-CrRNA Ribonucleoprotein Complex Mediates Specific DNA Cleavage for Adaptive Immunity in Bacteria.” *Proceedings of the National Academy of Sciences* 109 (39): E2579–86. https://doi.org/10.1073/pnas.1208507109.

Gerlai, R, M Lahav, S Guo, and A Rosenthal. 2000. “Drinks like a Fish: Zebra Fish (Danio Rerio) as a Behavior Genetic Model to Study Alcohol Effects.” *Pharmacology, Biochemistry, and Behavior* 67 (4): 773–82. http://www.ncbi.nlm.nih.gov/pubmed/11166068.

Gersbach, Charles A., Thomas Gaj, and Carlos F. Barbas. 2014. “Synthetic Zinc Finger Proteins: The Advent of Targeted Gene Regulation and Genome Modification Technologies.” *Accounts of Chemical Research* 47 (8): 2309–18. https://doi.org/10.1021/ar500039w.

Gilbert, Scott F. 2000. “The Neural Crest.” https://www.ncbi.nlm.nih.gov/books/NBK10065/#.

Górecka, Karolina M, Weronika Komorowska, and Marcin Nowotny. 2013. “Crystal Structure of RuvC Resolvase in Complex with Holliday Junction Substrate.” *Nucleic Acids Research* 41 (21): 9945–55. https://doi.org/10.1093/nar/gkt769.

Govindan, Ganesan, and Sivaprakash Ramalingam. 2016. “Programmable Site-Specific Nucleases for Targeted Genome Engineering in Higher Eukaryotes.” *Journal of Cellular Physiology* 231 (11): 2380–92. https://doi.org/10.1002/jcp.25367.

Groner, Anna C., Sylvain Meylan, Angela Ciuffi, Nadine Zangger, Giovanna Ambrosini, Nicolas Dénervaud, Philipp Bucher, and Didier Trono. 2010. “KRAB–Zinc Finger Proteins and KAP1 Can Mediate Long-Range Transcriptional Repression through Heterochromatin Spreading.” Edited by Hiten D. Madhani. *PLoS*

Genetics 6 (3): e1000869. https://doi.org/10.1371/journal.pgen.1000869.

Guerra, Almary, Raoul FV Germano, Oliver Stone, Rima Arnaout, Stefan Guenther, Suchit Ahuja, Verónica Uribe, Benoit Vanhollebeke, Didier YR Stainier, and Sven Reischauer. 2018. "Distinct Myocardial Lineages Break Atrial Symmetry during Cardiogenesis in Zebrafish." *ELife* 7 (May). https://doi.org/10.7554/eLife.32833.

Guilinger, John P, David B Thompson, and David R Liu. 2014. "Fusion of Catalytically Inactive Cas9 to FokI Nuclease Improves the Specificity of Genome Modification." *Nature Biotechnology* 32 (6): 577–82. https://doi.org/10.1038/nbt.2909.

Hadeball, Beate, Annette Borchers, and Doris Wedlich. 1998. "Xenopus Cadherin-11 (Xcadherin-11) Expression Requires the Wg/Wnt Signal." *Mechanisms of Development* 72 (1–2): 101–13. https://doi.org/10.1016/S0925-4773(98)00022-7.

Hardy, Serge, Vincent Legagneux, Yann Audic, and Luc Paillard. 2010. "Reverse Genetics in Eukaryotes." *Biology of the Cell* 102 (10): 561–80. https://doi.org/10.1042/BC20100038.

Hirano, Hisato, Jonathan S. Gootenberg, Takuro Horii, Omar O. Abudayyeh, Mika Kimura, Patrick D. Hsu, Takanori Nakane, et al. 2016. "Structure and Engineering of Francisella Novicida Cas9." *Cell* 164 (5): 950–61. https://doi.org/10.1016/j.cell.2016.01.039.

Hisa, Tomoyuki, Sally E Spence, Rivka A Rachel, Masami Fujita, Takuro Nakamura, Jerrold M Ward, Deborah E Devor-Henneman, et al. 2004. "Hematopoietic, Angiogenic and Eye Defects in Meis1 Mutant Animals." *The EMBO Journal* 23 (2): 450–59. https://doi.org/10.1038/sj.emboj.7600038.

Hisano, Yu, Tetsushi Sakuma, Shota Nakade, Rie Ohga, Satoshi Ota, Hitoshi Okamoto, Takashi Yamamoto, and Atsuo Kawahara. 2015. "Precise In-Frame Integration of Exogenous DNA Mediated by CRISPR/Cas9 System in Zebrafish." *Scientific Reports*. https://doi.org/10.1038/srep08841.

Hou, Zhonggang, Yan Zhang, Nicholas E Propson, Sara E Howden, Li-Fang Chu, Erik J Sontheimer, and James A Thomson. 2013a. "Efficient Genome Engineering in Human Pluripotent Stem Cells Using Cas9 from Neisseria Meningitidis." *Proceedings of the National Academy of Sciences of the United States of America* 110 (39): 15644–49. https://doi.org/10.1073/pnas.1313587110.

Howden, Sara E., Bradley McColl, Astrid Glaser, Jim Vadolas, Steven Petrou, Melissa H. Little, Andrew G. Elefanty, and Edouard G. Stanley. 2016. "A Cas9 Variant for Efficient Generation of Indel-Free Knockin or Gene-Corrected Human Pluripotent Stem Cells." *Stem Cell Reports* 7 (3): 508–17. https://doi.org/10.1016/J.STEMCR.2016.07.001.

Howe, Kerstin, Matthew D. Clark, Carlos F. Torroja, James Torrance, Camille Berthelot, Matthieu Muffato, John E. Collins, et al. 2013. "The Zebrafish Reference Genome Sequence and Its Relationship to the Human Genome." *Nature*. https://doi.org/10.1038/nature12111.

Hsu, Patrick D, David A Scott, Joshua A Weinstein, F Ann Ran, Silvana Konermann, Vineeta Agarwala, Yinqing Li, et al. 2013. "DNA Targeting Specificity of RNA-Guided Cas9 Nucleases." *Nature Biotechnology* 31 (9): 827–32. https://doi.org/10.1038/nbt.2647.

Huang, Xiao, and Jean-Pierre Saint-Jeannet. 2004. "Induction of the Neural Crest and the Opportunities of Life on the Edge." *Developmental Biology* 275 (1): 1–11. https://doi.org/10.1016/J.YDBIO.2004.07.033.

Hwang, Woong Y, Yanfang Fu, Deepak Reyon, Morgan L Maeder, Shengdar Q Tsai, Jeffry D Sander, Randall T Peterson, J-R Joanna Yeh, and J Keith Joung. 2013. "Efficient Genome Editing in Zebrafish Using a CRISPR-Cas System." *Nature Biotechnology* 31 (3): 227–29. https://doi.org/10.1038/nbt.2501.

Inoue, Jun, Yukuto Sato, Robert Sinclair, Katsumi Tsukamoto, and Mutsumi Nishida. 2015. "Rapid Genome Reshaping by Multiple-Gene Loss after Whole-Genome Duplication in Teleost Fish Suggested by Mathematical Modeling." *Proceedings of the National Academy of Sciences of the United States of America* 112 (48): 14918–23. https://doi.org/10.1073/pnas.1507669112.

Jang, Da Eun, Jae Young Lee, Jae Hoon Lee, Ok Jae Koo, Hee Sook Bae, Min Hee Jung, Ji Hyun Bae, et al. 2018. "Multiple SgRNAs with Overlapping Sequences Enhance CRISPR/Cas9-Mediated Knock-in Efficiency." *Experimental & Molecular Medicine* 50 (4): 16. https://doi.org/10.1038/s12276-018-0037-x.

Jinek, M., K. Chylinski, I. Fonfara, M. Hauer, J. A. Doudna, and E. Charpentier. 2012a. "A Programmable Dual-RNA-Guided DNA Endonuclease in Adaptive Bacterial Immunity." *Science* 337 (6096): 816–21. https://doi.org/10.1126/science.1225829.

Jinek, M., F. Jiang, D. W. Taylor, S. H. Sternberg, E. Kaya, E. Ma, C. Anders, et al. 2014. "Structures of Cas9 Endonucleases Reveal RNA-Mediated Conformational Activation." *Science* 343 (6176): 1247997–1247997. https://doi.org/10.1126/science.1247997.

Julian Pampel. 2016. "A Quick Introduction to CRISPR." 2016. https://www.genomics-online.com/resources/16/5014/a-quick-introduction-to-crispr/.

Kelsh, Robert N. 2006. "Sorting OutSox10 Functions in Neural Crest Development." *BioEssays* 28 (8): 788–98. https://doi.org/10.1002/bies.20445.

Kiani, Samira, Jacob Beal, Mohammad R Ebrahimkhani, Jin Huh, Richard N Hall, Zhen Xie, Yinqing Li, and Ron Weiss. 2014. "CRISPR Transcriptional Repression Devices and Layered Circuits in Mammalian Cells." *Nature Methods* 11 (7): 723–26. https://doi.org/10.1038/nmeth.2969.

Kiani, Samira, Alejandro Chavez, Marcelle Tuttle, Richard N Hall, Raj Chari, Dmitry Ter-Ovanesyan, Jason Qian, et al. 2015. "Cas9 GRNA Engineering for Genome Editing, Activation and Repression." *Nature Methods* 12 (11): 1051–54. https://doi.org/10.1038/nmeth.3580.

Kiecker, C, and C Niehrs. 2001. "AP Neural Patterning by a Wnt Gradient." http://dev.biologists.org/content/develop/128/21/4189.full.pdf.

Kim, Eunji, Taeyoung Koo, Sung Wook Park, Daesik Kim, Kyoungmi Kim, Hee-Yeon Cho, Dong Woo Song, et al. 2017. "In Vivo Genome Editing with a Small Cas9 Orthologue Derived from Campylobacter Jejuni." *Nature Communications* 8 (February): 14500. https://doi.org/10.1038/ncomms14500.

Kim, Sojung, Daesik Kim, Seung Woo Cho, Jungeun Kim, and Jin-Soo Kim. 2014. "Highly Efficient RNA-Guided Genome Editing in Human Cells via Delivery of Purified Cas9 Ribonucleoproteins." *Genome Research* 24 (6): 1012–19. https://doi.org/10.1101/gr.171322.113.

Kim, Yang-Gyun, Jooyeun Cha, and Srinivasan Chandrasegaran. 1996. "Hybrid Restriction Enzymes: Zinc Finger Fusions to Fok I Cleavage Domain (Flavobacterium Okeanokoites/Chimeric Restriction Endonuclease/Protein Engineering/Recognition and Cleavage Domains)." Vol. 93. https://www.ncbi.nlm.nih.gov/pmc/articles/PMC40048/pdf/pnas01507-0203.pdf.

Kimura, Yukiko, Yu Hisano, Atsuo Kawahara, and Shin Ichi Higashijima. 2014. "Efficient Generation of Knock-in Transgenic Zebrafish Carrying Reporter/Driver Genes by CRISPR/Cas9-Mediated Genome Engineering." *Scientific Reports*. https://doi.org/10.1038/srep06545.

Kirby, M L, and K L Waldo. 1990. "Role of Neural Crest in Congenital Heart Disease." *Circulation* 82 (2): 332–40. http://www.ncbi.nlm.nih.gov/pubmed/2197017.

Kirby, Margaret L., and Mary R. Hutson. 2010. "Factors Controlling Cardiac Neural Crest Cell Migration." *Cell Adhesion & Migration* 4 (4): 609–21. https://doi.org/10.4161/cam.4.4.13489.

Kleinstiver, Benjamin P., Michelle S. Prew, Shengdar Q. Tsai, Ved V. Topkar, Nhu T. Nguyen, Zongli Zheng, Andrew P. W. Gonzales, et al. 2015a. "Engineered CRISPR-Cas9 Nucleases with Altered PAM Specificities." *Nature* 523 (7561): 481–85. https://doi.org/10.1038/nature14592.

Kocabas, Fatih, Junke Zheng, Suwannee Thet, Neal G Copeland, Nancy A Jenkins, Ralph J DeBerardinis, Chengcheng Zhang, and Hesham A Sadek. 2012. "Meis1 Regulates the Metabolic Phenotype and Oxidant Defense of Hematopoietic Stem Cells." *Blood* 120 (25): 4963–72. https://doi.org/10.1182/blood-2012-05-432260.

Kok, Fatma O., Masahiro Shin, Chih Wen Ni, Ankit Gupta, Ann S. Grosse, Andreas vanImpel, Bettina C. Kirchmaier, et al. 2015. “Reverse Genetic Screening Reveals Poor Correlation between Morpholino-Induced and Mutant Phenotypes in Zebrafish.” *Developmental Cell*. https://doi.org/10.1016/j.devcel.2014.11.018.

Komor, Alexis C., Yongjoo B. Kim, Michael S. Packer, John A. Zuris, and David R. Liu. 2016. “Programmable Editing of a Target Base in Genomic DNA without Double-Stranded DNA Cleavage.” *Nature* 533 (7603): 420–24. https://doi.org/10.1038/nature17946.

Konermann, Silvana, Mark D. Brigham, Alexandro E. Trevino, Julia Joung, Omar O. Abudayyeh, Clea Barcena, Patrick D. Hsu, et al. 2015. “Genome-Scale Transcriptional Activation by an Engineered CRISPR-Cas9 Complex.” *Nature* 517 (7536): 583–88. https://doi.org/10.1038/nature14136.

Lai, C K, G L Norddahl, T Maetzig, P Rosten, T Lohr, L Sanchez Milde, N von Krosigk, et al. 2017. “Meis2 as a Critical Player in MN1-Induced Leukemia.” *Blood Cancer Journal* 7 (9): e613. https://doi.org/10.1038/bcj.2017.86.

Lefebvre, V, W Huang, V R Harley, P N Goodfellow, and B de Crombrugghe. 1997. “SOX9 Is a Potent Activator of the Chondrocyte-Specific Enhancer of the pro Alpha1(II) Collagen Gene.” *Molecular and Cellular Biology* 17 (4): 2336–46. http://www.ncbi.nlm.nih.gov/pubmed/9121483.

Lieschke, Graham J., and Peter D. Currie. 2007. “Animal Models of Human Disease: Zebrafish Swim into View.” *Nature Reviews Genetics* 8 (5): 353–67. https://doi.org/10.1038/nrg2091.

Lièvre, C S Le, and N M Le Douarin. 1975. “Mesenchymal Derivatives of the Neural Crest: Analysis of Chimaeric Quail and Chick Embryos.” *Journal of Embryology and Experimental Morphology* 34 (1): 125–54. http://www.ncbi.nlm.nih.gov/pubmed/1185098.

Lin, Chien-Jung, Chieh-Yu Lin, Chen-Hao Chen, Bin Zhou, and Ching-Pin Chang. 2012. “Partitioning the Heart: Mechanisms of Cardiac Septation and Valve Development.” *Development (Cambridge, England)* 139 (18): 3277–99. https://doi.org/10.1242/dev.063495.

Liu, Jia, Thomas Gaj, Mark C Wallen, and Carlos F Barbas. 2015. “Improved Cell-Penetrating Zinc-Finger Nuclease Proteins for Precision Genome Engineering.” *Molecular Therapy - Nucleic Acids* 4 (January): e232. https://doi.org/10.1038/MTNA.2015.6.

Liu, Jia, and Sai lan Shui. 2016. “Delivery Methods for Site-Specific Nucleases: Achieving the Full Potential of Therapeutic Gene Editing.” *Journal of Controlled Release* 244: 83–97. https://doi.org/10.1016/j.jconrel.2016.11.014.

Longobardi, E., D. Penkov, D. Mateos, G. De Florian, M. Torres, and Francesco Blasi. 2014. “Biochemistry of the Tale Transcription Factors PREP, MEIS, and PBX in Vertebrates.” *Developmental Dynamics*. https://doi.org/10.1002/dvdy.24016.

Louw, Jacoba J., Anniek Corveleyn, Yaojuan Jia, Greet Hens, Marc Gewillig, and Koenraad Devriendt. 2015. “*MEIS2* Involvement in Cardiac Development, Cleft Palate, and Intellectual Disability.” *American Journal of Medical Genetics Part A* 167 (5): 1142–46. https://doi.org/10.1002/ajmg.a.36989.

Low, Benjamin E, Peter M Kutny, and Michael V Wiles. 2016. *Chapter 2 Simple , Effi Cient CRISPR-Cas9-Mediated Gene Editing in Mice : Strategies and Methods*. Vol. 1438. https://doi.org/10.1007/978-1-4939-3661-8.

Lu, Jia, Chen Zhao, Yingze Zhao, Jingfang Zhang, Yue Zhang, Li Chen, Qiyuan Han, et al. 2017. “Multimode Drug Inducible CRISPR/Cas9 Devices for Transcriptional Activation and Genome Editing.” *Nucleic Acids Research* 46 (5): 25. https://doi.org/10.1093/nar/gkx1222.

Lumsden, A., N. Sprawson, and A. Graham. 1991. “Segmental Origin and Migration of Neural Crest Cells in the Hindbrain Region of the Chick Embryo.” *Development* 113 (4).

Lumsden, A, and R Krumlauf. 1996. “Patterning the Vertebrate Neuraxis.” *Science (New York, N.Y.)* 274 (5290):

1109–15. https://doi.org/10.1126/SCIENCE.274.5290.1109.

Ma, Hanhui, Li-Chun Tu, Ardalan Naseri, Maximiliaan Huisman, Shaojie Zhang, David Grunwald, and Thoru Pederson. 2016. “Multiplexed Labeling of Genomic Loci with DCas9 and Engineered SgRNAs Using CRISPRainbow.” *Nature Biotechnology* 34 (5): 528–30. https://doi.org/10.1038/nbt.3526.

Machon, Ondrej, Jan Masek, Olga Machonova, Stefan Krauss, and Zbynek Kozmik. 2015. “Meis2 Is Essential for Cranial and Cardiac Neural Crest Development.” *BMC Developmental Biology* 15 (1): 40. https://doi.org/10.1186/s12861-015-0093-6.

Maeda, Ryu, Kathleen Mood, Teri L Jones, Jun Aruga, Arthur M Buchberg, and Ira O Daar. 2001. “Xmeis1, a Protooncogene Involved in Specifying Neural Crest Cell Fate in Xenopus Embryos.” *Oncogene* 20 (11): 1329–42. https://doi.org/10.1038/sj.onc.1204250.

Mali, Prashant, John Aach, P Benjamin Stranges, Kevin M Esvelt, Mark Moosburner, Sriram Kosuri, Luhan Yang, and George M Church. 2013. “CAS9 Transcriptional Activators for Target Specificity Screening and Paired Nickases for Cooperative Genome Engineering.” *Nature Biotechnology* 31 (9): 833–38. https://doi.org/10.1038/nbt.2675.

Marraffini, Luciano A. 2015. “CRISPR-Cas Immunity in Prokaryotes.” *Nature* 526 (7571): 55–61. https://doi.org/10.1038/nature15386.

Melvin, Vida Senkus, Weiguo Feng, Laura Hernandez-Lagunas, Kristin Bruk Artinger, and Trevor Williams. 2013. “A Morpholino-Based Screen to Identify Novel Genes Involved in Craniofacial Morphogenesis.” *Developmental Dynamics*. https://doi.org/10.1002/dvdy.23969.

Merabet, Samir, and Brigitte Galliot. 2015. “The TALE Face of Hox Proteins in Animal Evolution.” *Frontiers in Genetics* 6 (Aug). https://doi.org/10.3389/fgene.2015.00267.

Miller, Jeffrey C, Michael C Holmes, Jianbin Wang, Dmitry Y Guschin, Ya-Li Lee, Igor Rupniewski, Christian M Beausejour, et al. 2007. “An Improved Zinc-Finger Nuclease Architecture for Highly Specific Genome Editing.” *Nature Biotechnology* 25 (7): 778–85. https://doi.org/10.1038/nbt1319.

Moreno-Mateos, Miguel A., Juan P. Fernandez, Romain Rouet, Charles E. Vejnar, Maura A. Lane, Emily Mis, Mustafa K. Khokha, Jennifer A. Doudna, and Antonio J. Giraldez. 2017. “CRISPR-Cpf1 Mediates Efficient Homology-Directed Repair and Temperature-Controlled Genome Editing.” *Nature Communications* 8 (1). https://doi.org/10.1038/s41467-017-01836-2.

Moreno-Mateos, Miguel A, Charles E Vejnar, Jean-Denis Beaudoin, Juan P Fernandez, Emily K Mis, Mustafa K Khokha, and Antonio J Giraldez. 2015. “CRISPRscan: Designing Highly Efficient SgRNAs for CRISPR-Cas9 Targeting in Vivo.” *Nature Methods* 12 (10): 982–88. https://doi.org/10.1038/nmeth.3543.

Morgan, Stefanie L., Natasha C. Mariano, Abel Bermudez, Nicole L. Arruda, Fangting Wu, Yunhai Luo, Gautam Shankar, et al. 2017. “Manipulation of Nuclear Architecture through CRISPR-Mediated Chromosomal Looping.” *Nature Communications* 8 (July): 15993. https://doi.org/10.1038/ncomms15993.

Morpholinos, Antisense. n.d. “Using Morpholinos to Control Gene.” *Read*, no. 2006: 1–24.

Moskow, J J, F Bullrich, K Huebner, I O Daar, and A M Buchberg. 1995. “Meis1, a PBX1-Related Homeobox Gene Involved in Myeloid Leukemia in BXH-2 Mice.” *Molecular and Cellular Biology* 15 (10): 5434–43. http://www.ncbi.nlm.nih.gov/pubmed/7565694.

Murayama, Emi, Karima Kissa, Agustin Zapata, Elodie Mordelet, Valérie Briolat, Hui-Feng Lin, Robert I Handin, and Philippe Herbomel. 2006. “Tracing Hematopoietic Precursor Migration to Successive Hematopoietic Organs during Zebrafish Development.” *Immunity* 25 (6): 963–75. https://doi.org/10.1016/j.immuni.2006.10.015.

Mussolino, Claudio, Jamal Alzubi, Eli J. Fine, Robert Morbitzer, Thomas J. Cradick, Thomas Lahaye, Gang Bao, and Toni Cathomen. 2014. “TALENs Facilitate Targeted Genome Editing in Human Cells with High Specificity and Low Cytotoxicity.” *Nucleic Acids Research* 42 (10): 6762–73.

https://doi.org/10.1093/nar/gku305.

Nakagawa, S, and M Takeichi. 1995. “Neural Crest Cell-Cell Adhesion Controlled by Sequential and Subpopulation-Specific Expression of Novel Cadherins.” *Development (Cambridge, England)* 121 (5): 1321–32. http://www.ncbi.nlm.nih.gov/pubmed/7540531.

Nakagawa, S, and M Takeichi. 1998. “ Neural crest emigration from the neural tube depends on regulated cadherin expression" Development 125-15. http://dev.biologists.org/content/develop/125/15/2963.full.pdf.

Nishimasu, Hiroshi, F. Ann Ran, Patrick D. Hsu, Silvana Konermann, Soraya I. Shehata, Naoshi Dohmae, Ryuichiro Ishitani, Feng Zhang, and Osamu Nureki. 2014. “Crystal Structure of Cas9 in Complex with Guide RNA and Target DNA.” *Cell* 156 (5): 935–49. https://doi.org/10.1016/j.cell.2014.02.001.

Nowak, Chance M, Seth Lawson, Megan Zerez, and Leonidas Bleris. 2016. “SURVEY AND SUMMARY Guide RNA Engineering for Versatile Cas9 Functionality.” *Nucleic Acids Research* 44: 9555–64. https://doi.org/10.1093/nar/gkw908.

Paige, Sharon L., Sean Thomas, Cristi L. Stoick-Cooper, Hao Wang, Lisa Maves, Richard Sandstrom, Lil Pabon, et al. 2012. “A Temporal Chromatin Signature in Human Embryonic Stem Cells Identifies Regulators of Cardiac Development.” *Cell*. https://doi.org/10.1016/j.cell.2012.08.027.

Peabody, D S. 1993. “The RNA Binding Site of Bacteriophage MS2 Coat Protein.” *The EMBO Journal* 12 (2): 595–600. http://www.ncbi.nlm.nih.gov/pubmed/8440248.

Pennonen, Jana, and Jaakko T. Leinonen. 2017. “Characterization of Human Pubertal Timing Gene VGLL3 in Zebrafish Development.” https://www.semanticscholar.org/paper/Characterization-of-Human-Pubertal-Timing-Gene-in-Pennonen-Leinonen/d153b43dc130a3f2c8df09d0cfc6836a7b43a784.

Pomeranz, H D, T P Rothman, and M D Gershon. 1991. “Colonization of the Post-Umbilical Bowel by Cells Derived from the Sacral Neural Crest: Direct Tracing of Cell Migration Using an Intercalating Probe and a Replication-Deficient Retrovirus.” *Development (Cambridge, England)* 111 (3): 647–55. http://www.ncbi.nlm.nih.gov/pubmed/1879333.

Qin, Peiwu, Mahmut Parlak, Cem Kuscu, Jigar Bandaria, Mustafa Mir, Karol Szlachta, Ritambhara Singh, Xavier Darzacq, Ahmet Yildiz, and Mazhar Adli. 2017. “Live Cell Imaging of Low- and Non-Repetitive Chromosome Loci Using CRISPR-Cas9.” *Nature Communications* 8 (March): 14725. https://doi.org/10.1038/ncomms14725.

Ran, F. Ann, Le Cong, Winston X. Yan, David A. Scott, Jonathan S. Gootenberg, Andrea J. Kriz, Bernd Zetsche, et al. 2015a. “In Vivo Genome Editing Using Staphylococcus Aureus Cas9.” *Nature* 520 (7546): 186–91. https://doi.org/10.1038/nature14299.

Rijli, F M, A Gavalas, and P Chambon. 1998. “Segmentation and Specification in the Branchial Region of the Head: The Role of the Hox Selector Genes.” *The International Journal of Developmental Biology* 42 (3): 393–401. http://www.ncbi.nlm.nih.gov/pubmed/9654024.

Rossi, Andrea, Zacharias Kontarakis, Claudia Gerri, Hendrik Nolte, Soraya Hölper, Marcus Krüger, and Didier Y. R. Stainier. 2015. “Genetic Compensation Induced by Deleterious Mutations but Not Gene Knockdowns.” *Nature* 524 (7564): 230–33. https://doi.org/10.1038/nature14580.

Salzberg, A, S Elias, N Nachaliel, L Bonstein, C Henig, and D Frank. 1999. “A Meis Family Protein Caudalizes Neural Cell Fates in Xenopus.” *Mechanisms of Development* 80 (1): 3–13. http://www.ncbi.nlm.nih.gov/pubmed/10096059.

Sauka-Spengler, Tatjana, and Marianne Bronner-Fraser. 2008. “A Gene Regulatory Network Orchestrates Neural Crest Formation.” *Nature Reviews Molecular Cell Biology* 9 (7): 557–68. https://doi.org/10.1038/nrm2428.

Schneider-Maunoury, S, P Gilardi-Hebenstreit, and P Charnay. 1998. “How to Build a Vertebrate Hindbrain.

Lessons from Genetics." *Comptes Rendus de l'Academie Des Sciences. Serie III, Sciences de La Vie* 321 (10): 819–34. https://doi.org/10.1016/S0764-4469(99)80022-5.

Sechrist, J., G.N. Serbedzija, T. Scherson, S.E. Fraser, and M. Bronner-Fraser. 1993. "Segmental Migration of the Hindbrain Neural Crest Does Not Arise from Its Segmental Generation." *Development* 118 (3).

Serbedzija, G.N., M. Bronner-Fraser, and S.E. Fraser. 1992. "Vital Dye Analysis of Cranial Neural Crest Cell Migration in the Mouse Embryo." *Development* 116 (2).

Shao, Shipeng, Weiwei Zhang, Huan Hu, Boxin Xue, Jinshan Qin, Chaoying Sun, Yuao Sun, Wensheng Wei, and Yujie Sun. 2016. "Long-Term Dual-Color Tracking of Genomic Loci by Modified SgRNAs of the CRISPR/Cas9 System." *Nucleic Acids Research* 44 (9): e86–e86. https://doi.org/10.1093/nar/gkw066.

Simoes-Costa, M., and M. E. Bronner. 2015. "Establishing Neural Crest Identity: A Gene Regulatory Recipe." *Development*. https://doi.org/10.1242/dev.105445.

Singh, Amit, and Madhuri Kango-Singh. 2013. *Molecular Genetics of Axial Patterning, Growth and Disease in the Drosophila Eye*. *Molecular Genetics of Axial Patterning, Growth and Disease in the Drosophila Eye*. https://doi.org/10.1007/978-1-4614-8232-1.

Spence, Rowena, Gabriele Gerlach, Christian Lawrence, and Carl Smith. 2007. "The Behaviour and Ecology of the Zebrafish, Danio Rerio." *Biological Reviews* 83 (1): 13–34. https://doi.org/10.1111/j.1469-185X.2007.00030.x.

Stankunas, Kryn, Ching Shang, Karen Y. Twu, Shih-Chu Kao, Nancy A. Jenkins, Neal G. Copeland, Mrinmoy Sanyal, Licia Selleri, Michael L. Cleary, and Ching-Pin Chang. 2008. "Pbx/Meis Deficiencies Demonstrate Multigenetic Origins of Congenital Heart Disease." *Circulation Research* 103 (7): 702–9. https://doi.org/10.1161/CIRCRESAHA.108.175489.

Stedman, Aline, Virginie Lecaudey, Emmanuelle Havis, Isabelle Anselme, Michel Wassef, Pascale Gilardi-Hebenstreit, and Sylvie Schneider-Maunoury. 2009. "A Functional Interaction between Irx and Meis Patterns the Anterior Hindbrain and Activates Krox20 Expression in Rhombomere 3." *Developmental Biology*. https://doi.org/10.1016/j.ydbio.2008.12.018.

Stern, Howard M., and Leonard I. Zon. 2003. "Cancer Genetics and Drug Discovery in the Zebrafish." *Nature Reviews Cancer* 3 (7): 533–39. https://doi.org/10.1038/nrc1126.

Sternberg, Samuel H., Sy Redding, Martin Jinek, Eric C. Greene, and Jennifer A. Doudna. 2014. "DNA Interrogation by the CRISPR RNA-Guided Endonuclease Cas9." *Nature* 507 (7490): 62–67. https://doi.org/10.1038/nature13011.

Sullivan, P B. 1996. "Hirschprung's Disease." *Archives of Disease in Childhood* 74 (1): 5–7. http://www.ncbi.nlm.nih.gov/pubmed/8660047.

Tanenbaum, Marvin E., Luke A. Gilbert, Lei S. Qi, Jonathan S. Weissman, and Ronald D. Vale. 2014. "A Protein-Tagging System for Signal Amplification in Gene Expression and Fluorescence Imaging." *Cell* 159 (3): 635–46. https://doi.org/10.1016/j.cell.2014.09.039.

Thakore, Pratiksha I, Anthony M D'Ippolito, Lingyun Song, Alexias Safi, Nishkala K Shivakumar, Ami M Kabadi, Timothy E Reddy, Gregory E Crawford, and Charles A Gersbach. 2015. "Highly Specific Epigenome Editing by CRISPR-Cas9 Repressors for Silencing of Distal Regulatory Elements." *Nature Methods* 12 (12): 1143–49. https://doi.org/10.1038/nmeth.3630.

Trainor, Paul A. 2010. "Craniofacial Birth Defects: The Role of Neural Crest Cells in the Etiology and Pathogenesis of Treacher Collins Syndrome and the Potential for Prevention." *American Journal of Medical Genetics. Part A* 152A (12): 2984–94. https://doi.org/10.1002/ajmg.a.33454.

Vlachakis, N., S.K. Choe, and C.G. Sagerstrom. 2001. "Meis3 Synergizes with Pbx4 and Hoxb1b in Promoting Hindbrain Fates in the Zebrafish." *Development* 128 (8).

Waskiewicz, A J. n.d. “Zebrafish Meis Regulates Hindbrain Pattern.”

Waskiewicz, A J, H A Rikhof, R E Hernandez, and C B Moens. 2001. “Zebrafish Meis Functions to Stabilize Pbx Proteins and Regulate Hindbrain Patterning.” *Development (Cambridge, England)* 128 (21): 4139–51. http://www.ncbi.nlm.nih.gov/pubmed/11684652.

Williams, Antionette L., and Brenda L. Bohnsack. 2015. “Neural Crest Derivatives in Ocular Development: Discerning the Eye of the Storm.” *Birth Defects Research Part C: Embryo Today: Reviews* 105 (2): 87–95. https://doi.org/10.1002/bdrc.21095.

Wixon, Jo. 2000. “Danio Rerio, the Zebrafish.” *Yeast* 1 (3): 225–31. https://doi.org/10.1002/1097-0061(20000930)17:3<225::AID-YEA34>3.0.CO;2-5.

Wu, Xuebing, David A Scott, Andrea J Kriz, Anthony C Chiu, Patrick D Hsu, Daniel B Dadon, Albert W Cheng, et al. 2014. “Genome-Wide Binding of the CRISPR Endonuclease Cas9 in Mammalian Cells.” *Nature Biotechnology* 32 (7): 670–76. https://doi.org/10.1038/nbt.2889.

Xu, Xingxing, Yonghui Tao, Xiaobo Gao, Lei Zhang, Xufang Li, Weiguo Zou, Kangcheng Ruan, Feng Wang, Guo-liang Xu, and Ronggui Hu. 2016. “A CRISPR-Based Approach for Targeted DNA Demethylation.” *Cell Discovery* 2 (1): 16009. https://doi.org/10.1038/celldisc.2016.9.

Yang, Hui, Haoyi Wang, Chikdu S Shivalila, Albert W Cheng, Linyu Shi, and Rudolf Jaenisch. 2013. “One-Step Generation of Mice Carrying Reporter and Conditional Alleles by CRISPR/Cas-Mediated Genome Engineering.” *Cell* 154 (6): 1370–79. https://doi.org/10.1016/j.cell.2013.08.022.

Yoshimi, Kazuto, Yayoi Kunihiro, Takehito Kaneko, Hitoshi Nagahora, Birger Voigt, and Tomoji Mashimo. 2016. “SsODN-Mediated Knock-in with CRISPR-Cas for Large Genomic Regions in Zygotes.” *Nature Communications* 7 (1): 10431. https://doi.org/10.1038/ncomms10431.

Yuan, Xuejun, and Thomas Braun. 2013. “An Unexpected Switch.” *Circulation Research* 113 (3): 245–48. https://doi.org/10.1161/CIRCRESAHA.113.302023.

Zalatan, Jesse G., Michael E. Lee, Ricardo Almeida, Luke A. Gilbert, Evan H. Whitehead, Marie La Russa, Jordan C. Tsai, et al. 2015. “Engineering Complex Synthetic Transcriptional Programs with CRISPR RNA Scaffolds.” *Cell* 160 (1–2): 339–50. https://doi.org/10.1016/j.cell.2014.11.052.

Zetsche, Bernd, Sara E Volz, and Feng Zhang. 2015. “A Split-Cas9 Architecture for Inducible Genome Editing and Transcription Modulation.” *Nature Biotechnology* 33 (2): 139–42. https://doi.org/10.1038/nbt.3149.

10 SUPPLEMENTARY DATA

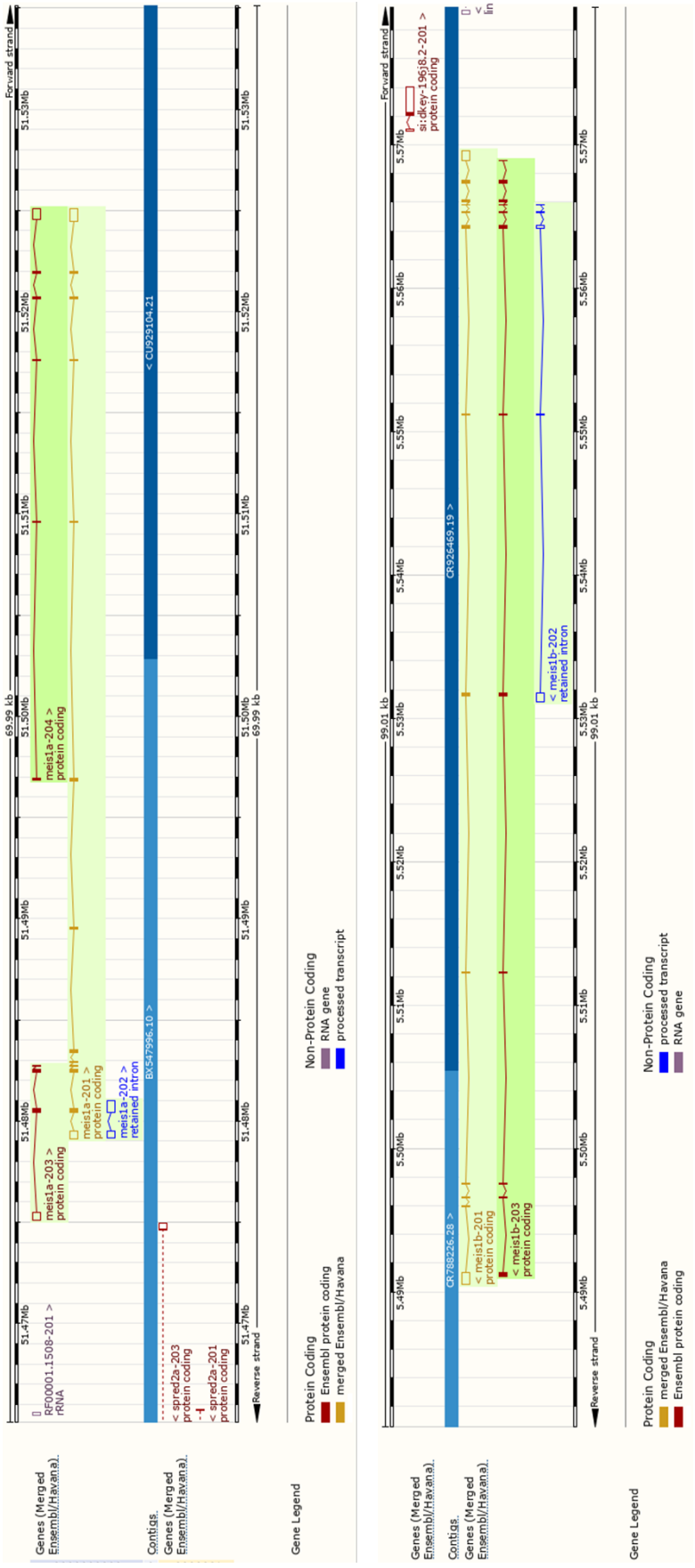

Figure 42: Location of meis1a and meis1b genes and their splice variant in the zebrafish genome (source: ensembl.org)

Table 18: Feature profile of designed and selected single guide RNAs by CRISPRscan.

Single-guide RNA	Specificity score	Predicted efficiency	Probability of out-of-frame mutation [%]	Off-targets
sgRNA8a	92	71	74	0-0-0-5-32
sgRNA9a	91	59	65	0-0-0-8-43
sgRNA10a	87	38	80	0-0-0-2-49
sgRNA1b	99	53	74	0-0-0-0-6
sgRNA2b	94	26	75	0-0-1-2-45
sgRNA3b	96	38	70	0-0-0-2-24

Off-targets: 1-2-3-4-5 means 1 off-target with 0 mismatches, 2 off-targets with 1 mismatch, 3 off-targets with 2 mismatches and so on.